Università degli Studi di Roma "La Sapienza"

Anno Accademico 2009-2010

Facoltà di Scienze Matematiche Fisiche e Naturali

Dottorato di Ricerca in Matematica–XXII Ciclo

Some results on the dynamics of conservative and dissipative systems with applications to Celestial Mechanics

Relatore
Professoressa
Alessandra Celletti

Candidato
Sara Di Ruzza
Matricola: 692381 (11118040)

Contents

Introduction

This thesis concerns the study of some Dynamical Systems which are related to interesting problems in Celestial Mechanics. For example, a really fascinating subject of Celestial Mechanics is the occurrence of resonances in the solar system, which are particular configurations of celestial bodies, that recur periodically in the time. In particular, we will be interested in the so–called *spin–orbit resonances*, which can be studied through the analysis of the dynamics of the *dissipative standard map*, a discrete system strictly related to the *spin–orbit problem.* The existence of periodic solutions of the dissipative standard map as well as the presence of invariant tori and cantori can be very useful to understand the real physical phenomena occurring in the solar system and, more generally, in the Universe. The existence of periodic orbits can be proved within their Arnold's tongues, which are particular structures involving the parameters which define the dissipative standard map; the existence of cantori is proved by means of the Aubry–Mather theory for twist maps. In this thesis we deal also with the Sitnikov's problem, which is a particular case of restricted three–body problem where two massive bodies (primaries) move in Keplerian orbits around a common barycenter, while a third body moves perpendicularly to the plane of the primaries. The motion of the third body strictly depends on the eccentricity of the Keplerian ellipses in which the primaries move; it is of great interest the study of the dynamics as the eccentricity varies. KAM and Nekhoroshev's theory can be suitably applied in order to analyze the dynamics of this model.

In the following, we start with a short background of Dynamical Systems and a description of the most important problems of Celestial Mechanics; then, we explain in detail the content of the thesis.

0.1. Background and notation

A dynamical system can be described by a real function $H = H(I, \phi, t)$ called *Hamiltonian*, where the variables $(I, \phi) \in \mathbb{R}^n \times \mathbb{T}^n$ represent the *action–angle variables* which are related, through a symplectic transformation, to the position and the velocity of the system. If the Hamiltonian depends only on the action variables I, namely $H(I, \phi, t) = H(I)$, the system is *integrable* and the solution can be written explicitly. Thus, the motion of an integrable system is completely known. The $2n$–dimensional phase–space is fibrated by invariant tori, namely n–dimensional surfaces invariant with respect to the motion: if the initial condition is on such surface, the motion will remain on it for all times.

The motion of integrable systems is fully characterized by periodic and quasi–periodic motions. We have a *periodic* motion when there exists a quantity T, such that the system at time $t = T$ is again in the same configuration in which it was at time $t = 0$. This kind of motion occurs when the frequency of the motion, given by $\omega = \partial H/\partial I$, is rationally dependent, i.e. $\omega \cdot k = 0$ for some $k \in \mathbb{Z}^n \setminus \{0\}$, where the dot stands for the scalar product. In this case, the trajectories are closed. On the contrary, we have a *quasi–periodic* motion when the frequency ω is rationally independent, namely when $\omega \cdot k = 0$ implies $k = 0$ with $k \in \mathbb{Z}^n$. In this case the trajectory on an invariant torus is not closed, but it fills densely the whole torus and any point never comes back to itself.

Let us see what happens when we modify an integrable system by adding a small perturbation. The system, eventually, becomes *non–integrable*, but it is close to an integrable one. We refer to these systems as *nearly–integrable* systems. The Hamiltonian of a nearly–integrable system can be written as:

$$H(I, \phi, t) = H_0(I) + \varepsilon H(I, \phi, t) \ , \tag{0.1}$$

meaning that, the Hamiltonian can be split into two parts, one depending only on the action variables I and another part, which is in norm very small, depending also on the angle variables ϕ and, eventually, also on the time t. The quantity ε represents a small real parameter greater than zero, which measures the size of the perturbation.

The dynamics of a nearly–integrable system changes a lot from the dynamics of an integrable system, but starting from the latter, we can deduce many properties of the former. The dynamics of a nearly–integrable system is described by regular and bounded motions as in the case of an integrable system; in addition we can find *chaotic* motions, showing a deep sensitivity to the initial conditions. Nearly–integrable systems show also *cantori*, which are totally disconnected invariant sets and they are graphs of a Cantor set. A cantorus arises from the break–down of a KAM torus. Let us explain better this concept. If we consider an integrable system, the phase–space is foliated by invariant tori on which periodic and quasi–periodic motions take place. When the system is perturbed, some of the quasi–periodic tori do not persist under the perturbation and they give rise to cantori. The determination of cantori is far from be trivial as well as the proof of their existence. Most important theories, as KAM, Aubry–Mather or Nekhoroshev's theory, concern the study of the behavior of the dynamics when, in a nearly–integrable system, the tori deform and break–down as the perturbing parameter ε increases.

Let us also remark that Dynamical Systems can be conservative or dissipative. A system is *conservative* if the total energy is preserved. A system is *dissipative* if it exchanges and disperses energy. A conservative system is characterized by a set of equations which preserve the volume of the phase–space, and it is said to be *area–preserving*. In a conservative system, the determinant of the Jacobian of the equations of motion must be equal to one. On the contrary in a dissipative system the volume of the phase–space is not preserved and the determinant of the Jacobian of the equations of motion turns out to be different from one; in particular, it can be less than one (*contractive system*) or greater than one (*expansive system*). We will see that the dissipation plays a very important role in the explanation of models describing real phenomena.

0.2. Some problems of Celestial Mechanics

We describe three important problems of Celestial Mechanics, in particular the *three–body problem*, the *spin–orbit problem*, and the *Sitnikov's problem*, which is a special case of the restricted 3–body problem.

The 3–body–problem will allows us to define the orbital resonances of Chapter 1; the spin–orbit problem will provide a physical motivation of the dissipative standard map studied in Chapter 3; the Sitnikov's problem will be extensively analyzed in Chapter 4.

0.2.1. Three–body–problem. One of the most important problems of Celestial Mechanics is the *three–body problem* or, more generally, the *n–body problem*. Let us take two bodies (for example the Sun and a planet, or a planet and a satellite) interacting by the gravitational law; it is well known that such problem is integrable and it admits an explicit solution provided by Kepler's laws, which fully describe the motion of the two bodies. Let us add a third body interacting gravitationally with the first two. Let us consider, for example, the model Sun–Earth and the interaction with Jupiter, which has a mass much bigger than the mass of the Earth. The system formed by the three bodies is non–integrable. In 1889, H. Poincaré proved that the three–body problem, and more generally the n–body problem, does not admit a formal mathematical solution. This model is a nearly–integrable system (since the mass of Jupiter is small compared to that of the Sun) and the Hamiltonian describing the model can be split into two parts: the first part is integrable and the other part represents the perturbation due to Jupiter. The integrable part is the Keplerian interaction between the two bodies (Sun–Earth); the non–integrable part is a perturbation and it represents the interaction with the third body (Jupiter); the perturbing parameter, measuring the size of the perturbation, is the ratio between the two primaries' mass. In the Sun–Earth–Jupiter system, the perturbing parameter is given by m_G/m_S, where m_G is the mass of Jupiter, m_S is the mass of the Sun; such ratio amounts approximatively to 10^{-3}. Since the three–body–problem is non–integrable, the dynamics of such model is very difficult to predict. In fact, we can have regular motions, like periodic and quasi–periodic motions, as well as chaotic motions.

The model turns out to be more realistic if we add some dissipations as the *radiation pressure* (which is exerted on any surface subject to electromagnetic radiation), or the *solar wind* which is caused by charged particles originating from the Sun, or the *Poynting–Robertson effect* due to the absorption and re–emission of the solar radiation. The dissipation is very useful in the study of the formation and the evolution of the Solar System. For example, if we consider a protoplanetary disk, the motion of a particle orbiting around the Sun can be well described by the three–body–problem with dissipation (compare with [**2**], [**3**]).

0.2.2. Spin–orbit problem. We introduce an important model of interest in Celestial Mechanics, which goes under the name of *spin–orbit problem*. Let us consider two bodies (a planet and a satellite) interacting by the gravitational law; let us introduce the following hypotheses: (*i*) the satellite is a triaxial body (it is an ellipsoid), orbiting on a Keplerian ellipse around the planet (we neglect the perturbations due to other bodies); (*ii*) the direction of the spin–axis coincides with that of the smallest physical axis of the ellipsoid; *iii*) the spin–axis is perpendicular to the orbital plane; *iv*) dissipative effects are neglected (in the case of the conservative model). This is a nearly–integrable system, where the perturbation is due to the equatorial oblateness of the satellite. In the Earth–Moon system, the perturbing parameter is about equal to 10^{-4}. In this model, we can consider a dissipation if the hypothesis *iv*) is removed; for example we can introduce a dissipative force, like the tidal torque due to the non-rigidity of planets and satellites. Also in this case, the dissipation plays a very important role in the formation of the Solar System; in particular, the capture into a spin–orbit resonance increases as the dissipation gets stronger, thus suggesting that the dissipative contribution allowed for a selection of the resonances during the formation of the Solar System (compare with [**18**]).

0.2.3. Sitnikov's problem. A very simple but not trivial example of three–body–problem, is provided by the *Sitnikov's problem*. It is an example in which we can find oscillatory motions, quasi–periodic motions as well as chaotic motions. Two bodies (the *primaries*) orbit in the same plane and move on Keplerian orbits in an antisymmetric way. A third body with negligible mass moves perpendicularly to the primaries through their common barycenter. The study concerns the motion of the third body under the influence of the primaries. It could be thought as a model describing the motion of a small body interacting with a pair of binary stars.

0.3. Content of the thesis

The present thesis is formed by four Chapters. Chapter 1 concerns a review of orbital and spin–orbit resonances occurring in the Solar System; the content of this Chapter is part of a review paper written in collaboration with A. Celletti (see [**16**]). In Chapter 2 we review the Aubry–Mather theory with special emphasis to the dissipative setting. In Chapter 3, the dissipative standard map is described; some new results about the existence of periodic orbits and about the relation between periodic and quasi–periodic orbits are presented. The new results are provided in an original paper written in collaboration with A. Celletti (see [**15**]). Chapter 4 concerns the Sitnikov's problem. A new formulation of the problem and new results about the stability of the system are presented. The content of this Chapter is contained in an original paper written in collaboration with C. Lhotka (see [**29**]).

0.3.1. Resonances. In the first Chapter of the thesis, we introduce the resonances which can be observed in many objects of the Solar System. Let us consider some quantities characterizing the motion of two or more celestial bodies; a *resonance* in Celestial Mechanics occurs when the relation between these quantities is the ratio of two small integers. In particular, a celestial body has two fundamental motions: the revolution around a central body and the rotation around its spin–axis; thus, we find two important resonances in our Solar System: the orbital resonances and the spin–orbit resonances. The first is related to the three–body–problem and concerns the motion of two bodies orbiting around the Sun (for example two planets). We consider the two periods of revolution T_1 and T_2 of the two bodies around the Sun. If their ratio is a rational number which can be written as the ratio of two small integers, then we will say that the two bodies are in an *orbital resonance*. The second resonance concerns the motion of the two bodies (for example a satellite orbiting around the host planet). Let T_{rev} and T_{rot} be, respectively, the period of revolution of the satellite around the planet, and the period of rotation of the satellite around itself. Then, we will say that a *spin–orbit resonance* occurs if the ratio between T_{rev} and T_{rot} can be written as the ratio of two small integers.

There is an important link between the resonances and the models described before. Let us consider the equations of motion of the three–body–problem and of the spin–orbit model; then, it is easy to show that periodic solutions of these models correspond to the orbital and spin–orbit resonances, respectively. Periodic orbits play a fundamental role in the explanation of real phenomena appearing in the Solar System. In fact, resonances are periodic configurations that recur in time, placing the celestial bodies involved always in the same location. Periodic solutions of the equations of motion describe exactly these events.

0.3.2. Aubry–Mather theory. In the last decades, many theories about non–integrable systems have been developed. In the second Chapter, a detailed description of the Aubry–Mather theory is presented. It provides many information about the sets appearing in the phase–space. Let us consider an invariant torus on which the dynamics of an unperturbed system takes place. If we introduce a perturbation, KAM theory ensures that, under suitable conditions on the system, the torus persists provided the perturbing parameter is sufficiently small.

If the size of the perturbation is greater than a critical value, then the torus breaks-down and Aubry–Mather theory ensures that in conservative systems, the torus is replaced by a cantorus. As we have already said, this set is totally disconnected and it provides an important property of the dynamics, allowing diffusion of the trajectories.

Periodic orbits are very important in the study of quasi–periodic motions. In fact, given an irrational frequency ω, we can find a sequence $\{p_n/q_n\}$ of rational numbers converging to ω as n goes to infinity. Thus, if we know the periodic solutions of periods p_n/q_n, we can write the approximate solution of the quasi–periodic orbit with frequency ω and in the same way we can approximate a cantorus. Periodic orbits are, therefore, a very interesting object of study, since, through them, we can obtain information about the whole dynamics.

The Aubry–Mather theory is well known in the conservative setting, but in dissipative systems the existence of cantori is not obvious and it is quite difficult to extend it. In Chapter 2, we review many results about the Aubry–Mather theory for dissipative twist maps, like the works by A. Katok (see [**44**]) and M. Casdagli (see [**9**]). We collect these results in order to have a global view on the state–of–art about the existence of cantori in dissipative systems.

0.3.3. The dissipative standard map. An interesting model within the class of discrete nearly–integrable systems with dissipation is the so–called *dissipative standard map.* The study of attractors of such map is particularly relevant in Celestial Mechanics, since the dissipative standard map is the Poincaré map of a suitable integration of the spin–orbit problem with dissipation. The equations defining the mapping can be written as

$$\begin{cases} y_{n+1} = by_n + c + \varepsilon \sin x_n \\ x_{n+1} = x_n + y_{n+1} \ , \end{cases} \tag{0.2}$$

where $x_n \in \mathbb{T} = \mathbb{R}/(2\pi\mathbb{Z})$, $y_n \in \mathbb{R}$, $\varepsilon > 0$ is the *perturbing parameter*, $0 < b < 1$ is the *dissipative parameter* and $c > 0$ is a *drift parameter*. The dynamics of the dissipative standard map admits periodic, quasi–periodic and chaotic motions. We study the dynamics with great emphasis to the existence of periodic orbits. To this end, we develop a suitable parameterization for periodic orbits apt to provide an analytical approximation of invariant attractors.

We see that the drift c plays a very important role for the existence of periodic orbits. A quasi–periodic orbit with frequency ω exists for a specific value of the drift, namely $c = c(\omega)$. On the contrary, the existence of a periodic orbit with frequency $2\pi p/q$, for some $p, q \in \mathbb{Z}_+$, is ensured if the drift c belongs to a whole connected interval $\mathcal{I}_{pq} \subseteq \mathbb{R}$. The existence and determination of such interval can be found through an implementation of the implicit function theorem or through a suitable parametric representation.

If we consider a sequence of rational numbers $\{p_n/q_n\}$ converging to an irrational number ω, we have numerical evidence, corroborated by the analytical expansion, that the intervals $\mathcal{I}_{p_n q_n}$ tend to the constant $c(\omega)$ related to the quasi–periodic orbit with frequency ω. In the same way, we have numerical evidence that periodic orbits of period p_n/q_n tend to the quasi–periodic orbit with frequency ω. Thus, the parametric representation allows us to relate the solutions of the periodic and quasi–periodic orbits. Through the parametric representation of periodic orbits, we are also able to determine the *Arnold's tongues*, which provide the region of existence of periodic orbits; they are found through the study of the behavior of the drift c as a function of the perturbing parameter ε. For a given periodic orbit the amplitude of the drift interval decreases as the perturbing parameter gets smaller; the variation of the drift as a function of the perturbing parameter defines the Arnold's tongues.

The analysis of the dissipative standard map provides interesting results concerning the spin–orbit resonances occurring in the Solar System. In particular, we are able to prove the existence of periodic orbits provided that the drift belongs to a given interval. From a physical point of view, this is very important because the drift is strictly related to the eccentricity of the Keplerian ellipse of the satellite around the planet; thus, it can be proved that spin–orbit resonances occur just for suitable values of the eccentricity.

0.3.4. Sitnikov's problem. In the last Chapter, we want to implement KAM and Nekhoroshev's theorems to an astronomical problem. If the system and the frequency of the motion satisfy suitable conditions, then, KAM theorem provides a strong stability property. Strong stability means that we can follow the motion and have information about it for all the times. In a similar way, the Nekhoroshev's theorem provides long stability properties of the system. In the last Chapter we show some applications of the two theorems to the Sitnikov's problem. Our aim is to provide new results about the stability properties of such problem by using constructive formulations of the two theorems. The Sitnikov's problem is one–dimensional and time dependent; we consider the equation of motion and we rewrite the problem in a Hamiltonian formulation by introducing action–angle variables. We construct a Birkhoff's normal form, which allows us to implement Nekhoroshev's and KAM theories. One aim is to provide Nekhoroshev's exponential stability estimates; this task has been achieved through the Pöschel formulation of Nekhoroshev's theorem ([**56**]). Then we show the existence of KAM tori around the elliptic fixed point through a suitable parametric representation of the torus.

The formulation of the problem that we have introduced depends on two small parameters, namely the eccentricity e of the two massive bodies and a rescaling parameter η measuring the distance of the elliptic fixed point placed in the origin of the phase–space. In our work, we provide the domains, in terms of the two small parameters e and η, in which the two theorems can be applied.

Let us remark that we have introduced a new formulation of integrability of the Sitnikov's problem. In fact, in classical literature, the problem is integrable by taking the eccentricity $e = 0$ and it is non–integrable for $e \neq 0$; in particular,the eccentricity measures the perturbation. On the contrary, we consider a Hamiltonian formulation such that the size of the perturbation is not measured only by the eccentricity, but also by another parameter, namely the distance from the elliptic fixed point η. Therefore, we remove the dependence of the angle variables to higher orders in such a way that the problem becomes integrable also for values of $e \neq 0$.

CHAPTER 1

Resonances in the Solar System

This Chapter is almost entirely the reproduction of the review paper "Resonances in the solar system" written in collaboration with Alessandra Celletti; it will appear in the proceedings of the meeting "Astronomia: storia e cultura" held in Campobasso (Italy) on May 21^{st}, 2009 (see [**16**]).

In this Chapter, we describe how the resonances work and we provide several examples of resonant bodies in the solar system. We describe the orbital resonances showing which effects they can have on the bodies involved and then we show many examples of them. Then, we describe the spin–orbit resonance and we provide a model which describes the problem. Successively, we provide some examples of the occurrence of the spin–orbit resonance.

1.1. Introduction

A resonance in Celestial Mechanics occurs when some of the quantities characterizing the motion of two or more celestial bodies are related in such a way that their ratio amounts to that of two small integers. Two main kinds of resonances are present in the solar system: *orbital resonances* and *spin–orbit resonances*. For the first kind we consider three bodies, for example Sun, Jupiter and an asteroid. We measure the orbital period of Jupiter and of the asteroid around the Sun; an orbital resonance occurs whenever the ratio of these periods is a rational number. In the case of the spin–orbit resonance, we consider a satellite moving around a central planet. We measure the period of revolution of the satellite around the planet, and the period of rotation of the satellite around itself; whenever the ratio of the two periods is a rational number, one speaks of a spin–orbit resonance. To have a physical meaning, the integers whose ratio provides the rational number must be typically small.

The solar system is plenty of resonances, both of orbital and rotational type. Once we will accumulate enough data concerning extra–solar planetary systems, it will be very interesting to see whether resonances within exoplanets are as frequent as in the solar system.

1.2. Orbital resonances

The most frequent resonance in the solar system is the *orbital resonance*, or *mean motion resonance*. It involves the orbital periods of two objects orbiting around a common primary. In particular, an orbital resonance occurs when the periods of revolution of two planets (satellites) orbiting around the Sun (the host planet) are such that their ratio is close to an integer fraction ([**53**]). Of course, in physical situations the ratio cannot be exactly equal to a rational number, but often a precision to the third or fourth decimal digit suffices. Let T_1 and T_2 be the orbital periods of the two celestial bodies. Let $p\ ,q \in \mathbb{Z}$ with $q \neq 0$. The two bodies are said to satisfy an orbital resonance of order $p : q$, whenever it is

$$\frac{T_1}{T_2} = \frac{p}{q}\ .$$

Therefore, an orbital resonance implies a periodic repetition of certain geometrical configurations between the two bodies, so that the reciprocal gravitational influence has a periodic character: their attraction increases when the two bodies approach each other, and it decreases when the two bodies are faraway. The periodic occurrence of the same dynamical configuration can contribute to stabilize or destabilize the orbit: one has stabilization whenever the two bodies move in a synchronized way so that they never approach too much, thus avoiding drastic changes of the orbits; viceversa, if the bodies approach closely, one orbit might slowly change, thus providing a modification of the trajectory which can become quite consistent over long time scales.

We will show different cases of orbital resonances in the solar system. Jupiter and Saturn are close to a 2:5 resonance: while Jupiter (the inner planet) completes five orbits around the Sun, Saturn (the outer planet) has made exactly two turns. Other examples are given by the Galilean satellites of Jupiter: Io–Europa and Europa–Ganymede are both in a 1:2 resonance (the *Laplace resonance*), Ganymede–Callisto are in a 1:4 resonance; concerning the satellites of Saturn, we find that Titan–Hyperion satisfy a 3:4 resonance, Mimas–Tethys and Enceladus–Dione are both in a 1:2 resonance, Titan–Iapetus are in a 1:5 resonance. Another very important resonance occurs between Neptune and Pluto, which satisfy a 2:3 resonance. Many other orbital resonances are present in the solar system; some of them are discussed below.

1.2.1. A zoo of resonant planets and satellites. Neptune–Pluto. As remarked before, orbital resonances can be extremely stable and self protecting: this is the case, for example, of the Neptune–Pluto pair. Pluto moves on a so highly eccentric orbit, that it crosses the orbit of the giant Neptune, which moves on an almost circular trajectory. Nevertheless the orbital resonance keeps Pluto away from Neptune, and it prevents the two planets from a collision as well as from a close encounter.

The orbital periods of Neptune and Pluto are, respectively, $T_N = 164.8$ years and $T_P = 247.9$ years: thus, their ratio is

$$\frac{T_P}{T_N} = 1.5042 \approx \frac{3}{2} \ ,$$

namely, while Pluto completes 2 orbits around the Sun, Neptune has made 3 revolutions. Let us assume that Neptune moves in a circular orbit and that the initial position of Pluto is at aphelion (namely, when the distance between the planet and the Sun is maximum). With reference to Figure 1.1, the alignments between Sun, Neptune and Pluto (namely the positions at which the gravitational interaction between the three bodies is stronger) take place at the initial position (marked by index 0), after 1 revolution of Pluto and 1.5 orbits of Neptune (marked by index 3), and again when the initial condition is restored (marked by index 6). In these configurations, Pluto is always at the aphelion and the distance from Neptune is maximum, so that Pluto is not strongly influenced by the gravitational attraction of Neptune.

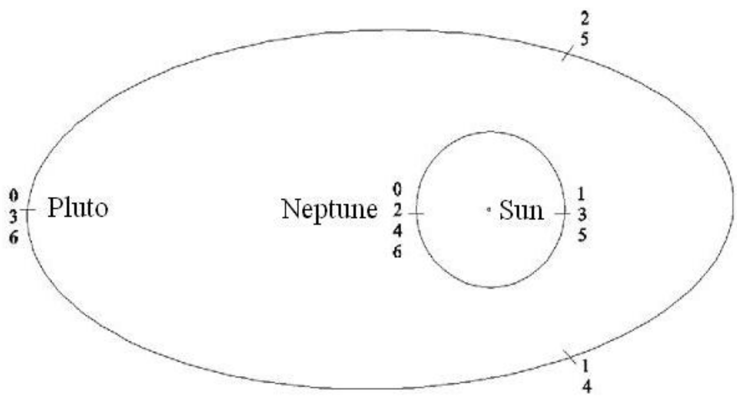

FIGURE 1.1. The resonance between Neptune and Pluto (after [**16**]).

Plutinos. There are many other objects, called Plutinos, sharing with Pluto the 2:3 resonance ([**53**]); their large number provides an indication of the importance of this resonance in shaping the dynamical structure of the *Transneptunian Belt*. Other orbital resonances can be found in the Kuiper Belt (which is a part of the Transneptunian Belt), like those of order 1:1 (*Neptune Trojans*), 1:2 (the *Twotinos*), as well as 3:5, 4:7 and 2:5.

After the discovery of the Plutinos, the official status of Pluto as a planet became controversial. Many scientists wondered whether Pluto should be considered as a separate body or just part of the Plutinos population. In 2006, a resolution of the IAU (International Astronomical Union) provided the official definition of a planet. According to this resolution, there are three main requirements needed to acquire the status of a planet:
1) the object must be in orbit around the Sun;
2) the object must be massive enough, so that it becomes a sphere in hydrostatic equilibrium under its own gravitational force;
3) the object must have cleared the neighborhood around its orbit.

Due to the presence of the Plutinos, Pluto does not satisfy the third requirement; for this reason, in 2006 the IAU assembly downgraded Pluto to the status of a "dwarf planet ", a celestial body satisfying the first two conditions, but not the third one.

Asteroid belt. We have mentioned that orbital resonances can also act to drastically change the trajectories. An important example can be found in the Asteroid Belt, the big region populated by small bodies in heliocentric orbits between Mars and Jupiter. If the number of asteroids is plotted as a function of their semimajor axis (recall that semimajor axis and orbital period are related by the third Kepler's law), one immediately notices a certain number of empty zones, the *Kirkwood gaps* ([**53**]). These gaps correspond to orbital resonances of order 1:2, 1:3, 2:5, 7:3 (compare with Figure 1.2). Asteroids once populating these regions have been ejected thanks to repeated perturbations due to Jupiter.

There are also populations of asteroids temporarily trapped in a resonance, like the Alinda family (close to the 1:3 resonance) and the Griqua family (corresponding to the 1:2 resonance). These groups are characterized by a very high eccentricity, which steadily increases due to the interaction with Jupiter, until some objects eventually have a close encounter with an inner planet that provokes their ejection from the resonance. In particular, chaotic mechanisms seem to be at the basis at the depletion of the 1:3 resonance ([**60**]).

On the contrary, there are regions in which the concentration of asteroids is very high; they correspond to specific resonances, like the Hilda asteroids in a 2:3 resonance with Jupiter, the Thule asteroids in a 3:4 resonance and the Trojan asteroids in a 1:1 resonance.

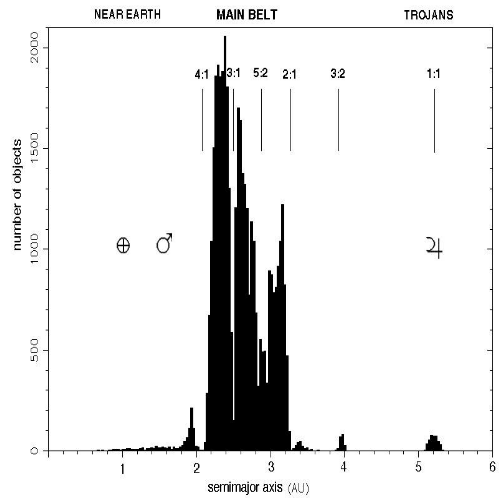

FIGURE 1.2. Asteroids histogram showing the number of asteroids versus their semimajor axis (after [**16**]).

Saturn's ring. The occurrence of orbital resonances is also found within planetary rings. For example, some depletions which are observed within Saturn's rings seem to be strictly related to orbital resonances with Saturn's moons ([**52**], [**53**]). In particular, the Cassini's division is a gap within Saturn's rings; a potential particle within the Cassini's division would be at a distance from the planet corresponding to a 1:2 resonance with Mimas (one of the satellites of Saturn). This means that the particles which would be located in the Cassini's division make two orbits, while Mimas completes one trajectory. This resonance causes Mimas' pulls on the ring particles to accumulate, destabilizing their orbits and leading to a sharp cutoff in the ring density. We also remark that some ringlets seem to be maintained by the gravitational effects of some small satellites, like Pandora, Prometheus and Janus.

Lagrangian points. A very peculiar resonance is that of order 1:1, namely the synchronous resonance. It occurs when the bodies share the same orbit. By definition a planet clears the neighborhood around its orbit by ejecting everything else around. Nevertheless, an exceptional case is represented by the 1:1 resonance and in particular by the *triangular Lagrangian points* ([**11**], [**52**], [**53**]). These positions correspond to the stationary solutions of the equations of motion describing the circular, restricted, three–body problem. This model is composed by three bodies of masses m_1, m_2, m_3, orbiting under their mutual gravitational influence. In the *restricted* framework, we assume that the third body has negligible mass with respect to the two primaries with masses m_1, m_2. Moreover, we suppose that the primaries move in circular orbits around their common center of mass.

The Lagrangian points correspond to five equilibrium positions of the equations of motion. In a rotating frame, at the Lagrangian points the gravitational attraction of the two primaries is counter–balanced by the centrifugal force, so that the third body is stationary with respect to the primaries (see Figure 1.3).

The first three solutions, found by L. Euler, are called L_1, L_2, L_3; they lie on the line defined by the two primaries (respectively, between them, beyond the smaller, beyond the larger). For this reason they are called *collinear equilibrium points* (see Figure 1.3). The other two solutions are L_4, L_5 and they were found by J. L. Lagrange. These points are located at the corners of two equilateral triangles, whose common base is defined by the line between the primaries (see Figure 1.3). Due to their particular configuration, these equilibrium positions are called *triangular Lagrangian points*.

When Lagrange studied these solutions, he did not know about any celestial body orbiting near the triangular positions; in fact, he assumed that such solutions were just a mathematical construction, without any physical relevance. It was only in 1906 that the first asteroid orbiting in a triangular Lagrangian point was observed; it was named Achilles. Since then, astronomers discovered a multitude of asteroids sharing the orbit of Jupiter, behind and ahead the planet, which are located very close to the triangular equilibrium solutions with Jupiter and the Sun (see Figure 1.4).

The asteroids located around the triangular Lagrangian positions on Jupiters orbit are denoted as the Greek asteroids (being the winners, they precede triumphantly the god Jupiter) and the Trojan asteroids (sadly lagging behind). However, Hector and Patroclus appear in the enemys camp, since they were discovered before the convention of naming Greeks those in L_4 and Trojans those in L_5 was invented. In many cases such distinction is not adopted and the two groups are generically referred to with the name *Trojans*.

Beside Jupiter, there exist other planets having small bodies located at their triangular Lagrangian points. For example, we observed asteroids in the triangular Lagrangian points of the Sun-Mars and Sun-Neptune systems. We can find small natural moons in the triangular Lagrangian positions of the system composed by Saturn and some of its satellites, like Tethys and Dione; finally, the triangular Lagrangian positions of the Earth-Sun system are populated by clouds of interplanetary dust ([**53**]).

We conclude by mentioning that the triangular Lagrangian points are stable equilibria provided that the primaries mass ratio satisfies a mathematical inequality, which is widely fulfilled by the Jupiter-Sun system ([**52**]).

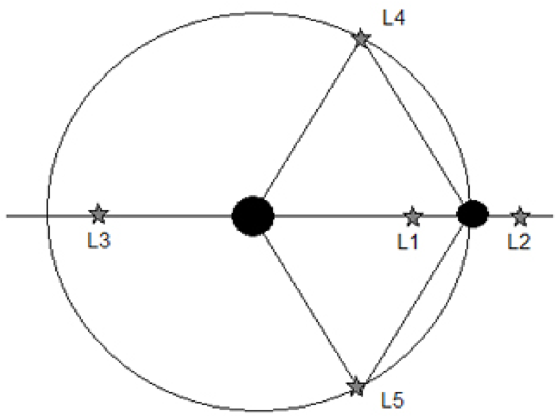

FIGURE 1.3. The Lagrangian triangular and collinear points (after [**16**]).

Laplace resonances. Another particular example of orbital resonance in the solar system is the Laplace resonance. It occurs when the

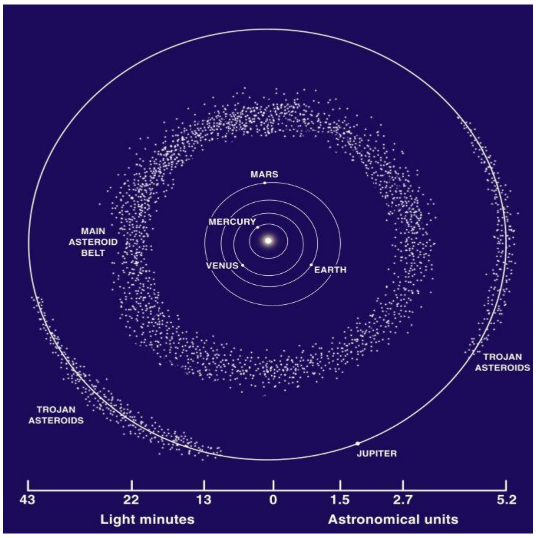

FIGURE 1.4. Greek and Trojan asteroids on Jupiter's orbit are spread around the triangular Lagrangian points (courtesy NASA).

frequencies (which are proportional to the inverse of the orbital periods) of three or more bodies satisfy a linear combination with integer coefficients. A concrete example can be found within Jupiters moons: the frequencies of Ganymede, Europa, Io are in a 1:2:4 orbital resonance. The pairs Io–Europa and Europa–Ganymede are both found in a 1:2 resonance: thus, the periods of revolution of Io and Ganymede are in the ratio 1:4. This peculiar resonance prevents the occurrence of triple conjunctions of the three satellites.

Titan–Hyperion. An interesting example of orbital resonance is provided by Titan and Hyperion (satellites of Saturn), which satisfy a resonance of order 3:4. Thanks to this dynamical configuration, Hyperion, a small and irregularly shaped satellite, is protected from a disruptive perturbing action of Saturn's largest moon, Titan. Being closer to the planet and moving faster, Titan periodically overtakes Hyperion; when this happens, the two bodies experience a minimum approach distance, while their mutual gravitational perturbation reaches a maximum. The existence of a resonance allows the conjunctions to take place only when Hyperion is at the apocenter of its orbit, which corresponds to the largest possible distance from Saturn, and therefore from Titan. As a consequence, the attraction due to Titan does not contribute to an ejection of Hyperion from Saturn's system.

1.3. Spin–orbit resonances

The table of "Physical and Photometric Data" published by the Astronomical Almanac provides an astonishing scenario (see Table 1): the biggest satellites of all planets always show the same face to their host planet. This situation is known for the Moon since antiquity; indeed, humankind have been able to observe the hidden face of the Moon only thanks to the Russian Lunik spacecraft, which circumnavigated the Moon in 1959. The physical reason behind the fact that the satellite always points the same hemisphere is the following: the period of revolution of the satellite around the planet is the same as the period of rotation of the satellite around its spin–axis. In this case one speaks of a *synchronous* or *1:1 spin–orbit resonance*. More generally, one has a spin–orbit resonance of order $p : q$ for some integers p, q with q non–zero, whenever the ratio of the revolutional (T_{rev}) to rotational (T_{rot}) periods amounts to p/q:

$$\frac{T_{rev}}{T_{rot}} = \frac{p}{q} \ , \qquad p, q \in \mathbb{Z} \ , \quad q \neq 0 \ .$$

In the solar system, the only exception to the synchronous resonance is provided by Mercury ([**27**]), which is observed to move in a 3:2 spin–orbit resonance, since twice the orbital period around the Sun equals three times its rotational period within an error of the order of 10^{-4}. In other words, within a very good approximation, during two orbital revolutions around the Sun, Mercury makes three rotations about its spin–axis.

TABLE 1. Physical data of the satellites: the satellite–to–planet mass ratio, the radius, the sidereal period of rotation P with S meaning synchronous with the orbital period and C meaning chaotic rotation (reproduced from The Astronomical Almanac Online and produced by the U.S. Naval Observatory and H.M. Nautical Almanac Office).

1.3.1. A model for the spin–orbit resonance. In order to write the equations of motion of the spin–orbit coupling between a satellite $\mathcal{S}$ and a planet $\mathcal{P}$, we can introduce a simplified model, based on the following assumptions:
(i) the satellite is a triaxial body, orbiting on a Keplerian ellipse around the planet;
(ii) the direction of the spin–axis coincides with that of the smallest physical axis of the ellipsoid;
iii) the spin–axis is perpendicular to the orbital plane;
iv) dissipative effects as well as perturbations due to other bodies are neglected.

Let us denote by a, e, r, f, respectively, the semimajor axis, eccentricity, orbital radius, true anomaly of the Keplerian orbit of the satellite. In particular, the quantities r and f are known functions of the time; for circular orbits the orbital radius is constant and the true anomaly is a linear function of the time. By a proper choice of the units of measure, let us normalize to one the gravitational constant and the period of revolution. Under the assumptions (i)–(iv), the equation of motion describing the spin–orbit problem takes the form (see, e.g., [**10**]):

$$\ddot{x} + \varepsilon \Big(\frac{a}{r}\Big)^3 \sin(2x - 2f) = 0 \ , \tag{1.1}$$

Planet	Satellite	Mass ratio	Radius (km)	P
Earth	Moon	0.0123	1737.4	S
Mars	Phobos	$1.672 \cdot 10^{-8}$	$13.4 \times 11.2 \times 9.2$	S
	Deimos	$2.43 \cdot 10^{-9}$	$7.5 \times 6.1 \times 5.2$	S
Jupiter	Io	$4.704 \cdot 10^{-5}$	$1829 \times 1819 \times 1816$	S
	Europa	$2.528 \cdot 10^{-5}$	1562	S
	Ganymede	$7.805 \cdot 10^{-5}$	2632	S
	Callisto	$5.667 \cdot 10^{-5}$	2409	S
	Amalthea	$1.10 \cdot 10^{-9}$	$125 \times 73 \times 64$	S
	Himalia	$2.2 \cdot 10^{-9}$	85	0.4
	Thebe		$58x49x42$	S
Saturn	Dione	$1.92 \cdot 10^{-6}$	562	S
	Rhea	$4.06 \cdot 10^{-6}$	764	S
	Titan	$2.366 \cdot 10^{-4}$	2575	S
	Hyperion	$1.00 \cdot 10^{-8}$	$164 \times 130 \times 107$	S
	Iapetus	$3.177 \cdot 10^{-6}$	736	S
	Phoebe	$1.454 \cdot 10^{-8}$	107	0.4
	Janus	$3.363 \cdot 10^{-9}$	$97 \times 95 \times 77$	S
	Epimetheus	$9.33 \cdot 10^{-10}$	$69 \times 55 \times 55$	S
	Prometheus	$2.75 \cdot 10^{-10}$	$74 \times 50 \times 34$	S
	Pandora	$2.39 \cdot 10^{-10}$	$55 \times 44 \times 31$	S
Uranus	Ariel	$1.56 \cdot 10^{-5}$	$581 \times 578 \times 578$	S
	Umbriel	$1.35 \cdot 10^{-5}$	585	S
	Titania	$4.06 \cdot 10^{-5}$	789	S
	Oberon	$3.47 \cdot 10^{-5}$	761	S
	Miranda	$0.08 \cdot 10^{-5}$	$240 \times 234 \times 233$	S
Neptune	Triton	$2.089 \cdot 10^{-4}$	1353	S
	Proteus		$218 \times 208 \times 201$	S
Pluto	Charon	0.1165	605	S

Table 1.

where the quantity x denotes the angle formed by the direction of the largest physical axis – belonging to the orbital plane – with a reference axis, say the perihelion line (see Figure 1.5) and the parameter ε is defined as $\varepsilon = \frac{3}{2}\frac{I_2-I_1}{I_3}$, where $I_1 < I_2 < I_3$ denote the principal moments of inertia.

We remark that the equation of motion is integrable in case of equatorial symmetry, say $I_1 = I_2$, such that $\varepsilon = 0$. For the Moon or Mercury the parameter ε is of the order of 10^{-4}. There exists a close relation between equation (1.1) and a standard pendulum equation, once (1.1) is averaged over a resonant angle.

The Fourier series expansion of equation (1.1) reads as

$$\ddot{x} \ + \ \varepsilon \sum_{m\neq 0, m=-\infty}^{+\infty} W\Big(\frac{m}{2}, e\Big) \ \sin(2x - mt) \ = \ 0 \ , \tag{1.2}$$

where the first few coefficients $W(\frac{m}{2}, e)$ are reported in Table 2; the coefficients have been expanded in power series of the orbital eccentricity as $W\Big(\frac{m}{2}, e\Big) \equiv W_0^m(e) + W_1^m(e) + W_2^m(e) + ...$, being $W_j^m(e) = O(e^j)$.

Let us now concentrate on a given resonance of order $p : 2$ for some $p \in \mathbf{Z}$. We introduce the *resonant angle* as $\gamma \equiv x - \frac{p}{2}t$; we can express equation (1.2) in terms of γ equation as

$$\ddot{\gamma}+\varepsilon W\Big(\frac{p}{2}, e\Big) \sin 2\gamma+\varepsilon \sum_{m\neq 0,p, \ m=-\infty}^{+\infty} W\Big(\frac{m}{2}, e\Big) \ \sin(2\gamma+(p-m)t) \ = \ 0 \ .$$

Averaging over the time, one obtains a *pendulum–like equation*

$$\ddot{\gamma} + \varepsilon W\Big(\frac{p}{2}, e\Big) \ \sin 2\gamma = 0 \ ,$$

which admits the energy integral

$$\frac{1}{2}\dot{\gamma}^2 - \frac{\varepsilon}{2} W\Big(\frac{p}{2}, e\Big) \cos 2\gamma = E \ ,$$

being E the total mechanical energy. The equilibrium points correspond to $\gamma = 0$ and $\gamma = \frac{\pi}{2}$ (modulus π). If $W(\frac{p}{2}, e) > 0$ then $\gamma = 0$

is stable, while $\gamma = \frac{\pi}{2}$ is unstable. The equilibrium correspond to the exact resonance and the librations correspond to small displacements around the resonance.

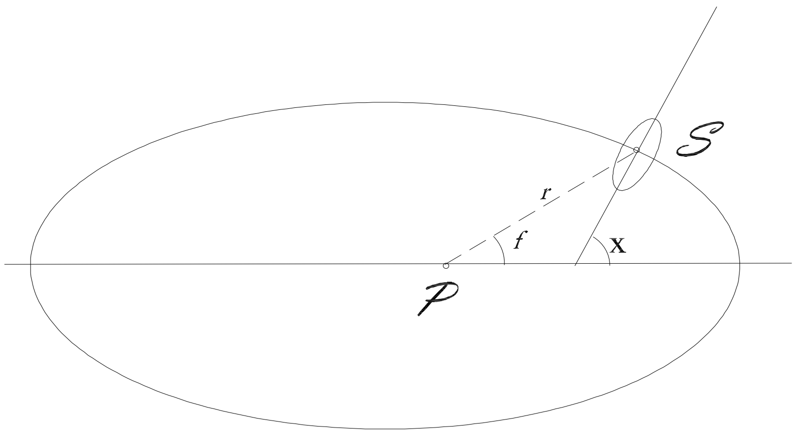

FIGURE 1.5. The geometry of the spin–orbit problem (after [**16**]).

1.3.2. Resonant planets and satellites. In this Section we review the main cases of bodies of the solar system trapped in a spin–orbit resonance. The survey starts from the inner body, Mercury, to the outermost Pluto.

Mercury. Around the middle of the XX century the general belief was that Mercury was rotating synchronously with the Sun. In that case Mercury should have shown a very hot hemisphere, permanently exposed to the Sun. Astronomical measurement did not agree with such assumption; around 1965 Giuseppe Colombo ([**26**], [**27**]) conjectured that Mercury was not rotating synchronously with the Sun. As a

$\frac{m}{2}$	$W_0^m(e)$	$W_1^m(e)$	$W_2^m(e)$	$W_3^m(e)$	$W_4^m(e)$	$W_5^m(e)$	$W_6^m(e)$
-1					$\frac{e^4}{24}$		$\frac{7e^6}{240}$
$-\frac{1}{2}$				$\frac{e^3}{48}$		$\frac{11e^5}{768}$	
$\frac{1}{2}$		$-\frac{e}{2}$		$\frac{e^3}{16}$		$-\frac{5e^5}{384}$	
1	1		$-\frac{5e^2}{2}$		$\frac{13e^4}{16}$		$-\frac{35e^6}{288}$
$\frac{3}{2}$		$\frac{7e}{2}$		$-\frac{123e^3}{16}$		$\frac{489e^5}{128}$	
2			$\frac{17e^2}{2}$		$-\frac{115e^4}{6}$		$\frac{601e^6}{48}$
$\frac{5}{2}$				$\frac{845e^3}{48}$		$-\frac{32525e^5}{768}$	
3					$\frac{533e^4}{16}$		$-\frac{13827e^6}{160}$

TABLE 2. Expansion in powers of e of the coefficients $W(\frac{m}{2}, e)$ appearing in (1.2).

consequence of the action of the solar torques on the permanent asymmetry of Mercury's equatorial plane, Colombo suggested that the ratio between the period of revolution and the period of rotation of Mercury was 3/2. The theoretical expectation was later confirmed by the observations performed by Mariner 10, a spacecraft launched in 1973 toward the inner planet.

Moon. The period of rotation of the Moon amounts to about 27.3 days and it coincides with the period of revolution around the Earth. As a consequence the Moon always points the same face to the Earth. Observers on the Earth can never see the far–side of the Moon. The hidden hemisphere was disclosed to humankind only in 1959, thanks to the images provided by the Russian spacecraft Lunik III. Indeed, due to lunar librations an Earth's observer can see about 59% of the Moon's surface.

Hyperion. The population of satellites around Saturn is very rich and one can find satellites of any size and shape. Among them, one of the most intriguing satellites is Hyperion, a small body orbiting between Titan and Iapetus on an almost circular and planar orbit. Its shape is rather irregular, as witnessed by its asymmetric dimensions (see Table 1). Hyperion's period of revolution amounts to about 21.28 days; J. Wisdom ([**61**]) conjectured that Hyperion was tumbling chaotically, due to its peculiar shape. Ground–based observations confirmed the prediction ([**45**]); as a consequence Hyperion became the first concrete example of chaos in the solar system.

Charon. The dwarf planet Pluto has three satellites; while two of them, Nix and Hydra, are very small, the closest satellite, Charon, has the peculiarity of being quite big in comparison to its planet (the radius amounts to about 604 km, while Pluto's mean radius is about 1151 km). Charon's orbital period amounts to about 6.387 days and it coincides with its rotational period; moreover, such period coincides also with the period of rotation of Pluto around its spin–axis. This situation is called *complete* spin–orbit resonance and it implies that both Pluto and Charon never turn their backs to each other.

CHAPTER 2

Aubry–Mather theory for twist maps

Let us consider an integrable system, namely a system for which a sufficient number of first integrals is available; if we add a small perturbation to the system we get a new system very close to the first one to which we refer as a *nearly–integrable system*.

The solution of a nearly–integrable system can not be written in an explicit way; but, if we know the dynamics of the integrable one, from the KAM theory and from the Aubry–Mather theory we can have many information about the dynamics of the perturbed system.

For this reason we want to describe some results about these theories. In the first Section we provide a short description of the KAM theory in the conservative setting for a time–dependent Hamiltonian in an n–dimensional space. The theory can be extended also to dissipative systems. In the second Section we provide a more detailed review about the Aubry–Mather theory, focusing on twist maps and in particular on dissipative twist maps.

2.1. The KAM theory

The KAM theory (acronym of the three mathematicians A. N. Kolmogorov, V. I. Arnold and J. Moser who developed the theory) provides many information about the dynamics of systems close to an integrable one. If we consider an integrable system described by the Hamiltonian $H(I, \phi, t) = H(I)$ with $I \in \mathbb{R}^n$ and $\phi,\ t \in \mathbb{T}^n$, we know that the dynamics is ruled by regular bounded and quasi–periodic motions;

the phase–space is $2n$–dimensional and if we fix a level of energy for the system we can find some invariant sets of dimension n given by $I = const.$ These sets are tori and on them quasi–periodic motions take place. The frequency $\omega \in \mathbb{R}^n$ of such motion is given by

$$\dot{\phi} = \frac{\partial H}{\partial I} = \omega \ .$$

Let us add in the Hamiltonian a small perturbation depending also on the angle variables, say

$$H(I, \phi, t) = H_0(I) + \varepsilon H_1(I, \phi, t) \ , \tag{2.1}$$

where $\varepsilon \geq 0$ is the perturbing parameter and H_0, H_1 are smooth functions; we wonder how the dynamics changes under the perturbation. From KAM theory we know that "most" of the invariant tori which foliate the phase–space of the integrable system obtained by taking $\varepsilon = 0$ survive under a "small" perturbation (meaning a "small" value of ε). "Most" of them means that a set of tori with full Lebesgue measure can be found: in particular the KAM theorem states that given an Hamiltonian of the form (2.1) satisfying a non-degeneracy assumption, then, all the tori with frequency satisfying the Diophantine condition survive under a small perturbation provided the size of the perturbation is sufficiently small. We recall that an irrational number ω satisfies the Diophantine condition if there exist suitable constants γ, $\tau > 0$ such that

$$|\omega \cdot m + n| \geq \frac{1}{\gamma |m|^\tau}$$

for any m, $n \in \mathbb{Z}^n \setminus \{0\}$. This condition is necessary in order to guarantee the convergence of the series describing the equation of the torus. In fact, from perturbation theory, some terms of the form $|\omega \cdot m + n|$ come out; they are at the denominator, they can be very small and for this reason they are called *small divisors.* If the Diophantine condition holds, the convergence of the series in which the small divisors appear, is guaranteed. It can be shown that in the sense of Lebesgue measure, almost all $\omega \in \mathbb{R}^n$ satisfy the Diophantine condition. From the KAM theory we also know that invariant tori surviving under the perturbation are just a little deformed and displaced with respect to the integrable ones and they are called KAM tori. Moreover, we know that the motions taking place on the KAM tori are quasi–periodic with the same frequency of the corresponding motion of the unperturbed system.

We know that the perturbed system is not integrable, therefore we can not find an explicit solution of the equations of motion but the persistence of KAM tori provides important properties about the stability of the dynamics: in fact, in low dimension ($n \leq 2$), the KAM tori constitute obstructions for the dynamics and confine the motions in bounded regions. If the number of degrees of freedom is $n = 2$, the phase–space is 4–dimensional and an energy level is a 3–dimensional space, while the KAM tori are 2–dimensional surfaces; this means that such tori separate the energy levels in bounded regions and a generic orbit either lie on an invariant torus or it is trapped between two of them for all times. In both cases the motion is confined and it will be very close to its initial conditions.

2.2. The Aubry–Mather theory

KAM theory ensures that the most of the invariant circles survive in systems that are small perturbation of integrable systems. Now we wonder what happens to those circles which do not persist under the perturbation and therefore break-down. The Aubry–Mather theory gives some answers: it claims that when an invariant circle breaks–down, it is replaced by an invariant set on which the orbits preserve many features of those they have before the break–down. From the point of view of the Aubry–Mather theory, all the invariant sets in which the dynamics takes place, are called *Aubry–Mather sets* (in the following we will provide a rigorous definition), apart from the nature of the rotation number and from the size of the perturbation. According to whether the rotation number associated to the set is a rational or an irrational number, the nature of the set can vary. If the rotation number is rational it can be formed by periodic orbits; if it is irrational the Aubry–Mather set can be an invariant circle on which a quasi–periodic orbit takes place or it can be a particular set occurring when the invariant circle with that given irrational rotation number does not persist. This particular set is a *Cantor set* and it is called *Cantorus.*

Let us define a Cantor set (see [**1**]):

DEFINITION 2.1. *A Cantor set is a set which is perfect and nowhere dense.*

A set is *perfect* if it is equal to its set of accumulation points and it is *nowhere dense* if its closure has an empty interior. Let S^1 be the unit circle and let us suppose that $f : S^1 \to S^1$ is a homeomorphism with irrational rotation number, and let $E(x)$, with $x \in S^1$, be the set of accumulation points of the sequence $\{f^n(x)\}_{n=1}^{\infty}$ where f^n is the n^{th} iteration of f. Then we can state the following:

PROPOSITION 2.2. *The set $E(x)$ is independent of x. Moreover, $E = E(x)$ is the unique, minimal closed invariant set of f.*

Moreover the following Proposition can be proved (see [**1**]);

PROPOSITION 2.3. *The set E is either the whole of S^1 or it is a Cantor set.*

The existence of Cantori is based on this proposition and of course on the Aubry–Mather theorem.

2.2.1. Area–preserving twist maps. Let us provide some definitions and notations. Let $\tilde{A}$ be the unit cylinder $S^1 \times \mathbb{R}$. The lift to $\mathbb{R}^2$ of a set $\tilde{B} \subset \tilde{A}$ is denoted by B, and the lift to $\mathbb{R}^2$ of a function $\tilde{f}$ on the cylinder is denoted by f.

DEFINITION 2.4. *A diffeomorphism $f : \mathbb{R}^2 \to \mathbb{R}^2$, $f = f(\theta, r)$ is called twist map if:*
1) f commutes with T where $T : \mathbb{R}^2 \to \mathbb{R}^2$ is the unit translation $T(\theta, r) = (\theta + 1, r)$,
2) f is orientation preserving,
3) there exists $\delta > 0$ such that for all $(\theta, r) \in \mathbb{R}^2$ one has

$$\frac{\partial(\pi_1 f(\theta, r))}{\partial r} > \delta \tag{2.2}$$

where $\pi_1 : \mathbb{R}^2 \to \mathbb{R}^2$ is the projection $\pi_1(\theta, r) = \theta$.

From condition 1), it follows that f is the lift of a unique map $\tilde{f} : \tilde{A} \to \tilde{A}$ of the cylinder; from 2) it follows that $\tilde{f}$ is end preserving (namely it preserves the orientation of the boundary of an annular region contained into the cylinder); finally, from 3) it follows that the image under f of a vertical line is the graph of a continuous function (i.e. the vertical line is necessarily deviated, see Figure 2.1).

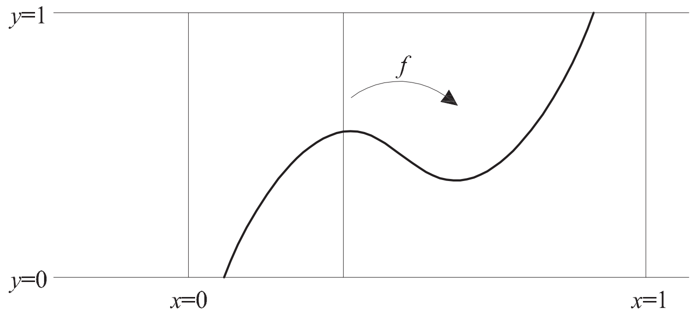

FIGURE 2.1. Geometrically, the twist condition states that the image of a segment $x = const$ forms a graph over the x axis (after [**50**]).

Let us define the rotation number of a set as follows:

DEFINITION 2.5. *Let $f : A \to A$ be a twist map and $z \in A$; then the rotation number of f in z is*

$$\rho(f, z) = \lim_{n\to\infty} \frac{\pi_1(f^n(z))}{n}, \tag{2.3}$$

if it exists.

Let $\tilde{C}$ be a curve belonging to the cylinder and homeomorphic in S^1; then, if we consider $\tilde{f}$ restricted to $\tilde{C}$, it can be proved that the limit exists and it does not depend on the point $z \in \tilde{C}$ (see [**?**]); therefore we can associate the rotation number to the curve $\tilde{C}$.

DEFINITION 2.6. *A point $(\theta, r) \in \mathbb{R}^2$ is called p/q–periodic if there exist $p \in \mathbb{Z}$ and $q \in \mathbb{Z}^+$ with $(p, q) = 1$, such that $f^q(\theta, r) = (\theta + p, r)$, where f^q is the q^{th} iteration of the map f.*

Using the same notation of Definition 2.4, we can provide the following:

DEFINITION 2.7. *An Aubry–Mather set for the twist map f, is a minimal closed set M, invariant under f and under T, on which the projection π_1 is injective and f is order preserving, i.e. for all x_1, $x_2 \in M$*

$$\pi_1(x_1) < \pi_1(x_2) \;\Rightarrow\; \pi_1(f(x_1)) < \pi_1(f(x_2)) \;. \tag{2.4}$$

The sets satisfying equation (2.4) are called *f–ordered.* In Figure 2.2 we show two examples of sets, the former is an f–ordered set and the latter is a non–f–ordered set. All points of an f–ordered set have the same rotation number (see [**1**], [**5**], [**38**]): this means that a unique rotation number is associated with any Aubry–Mather set M.

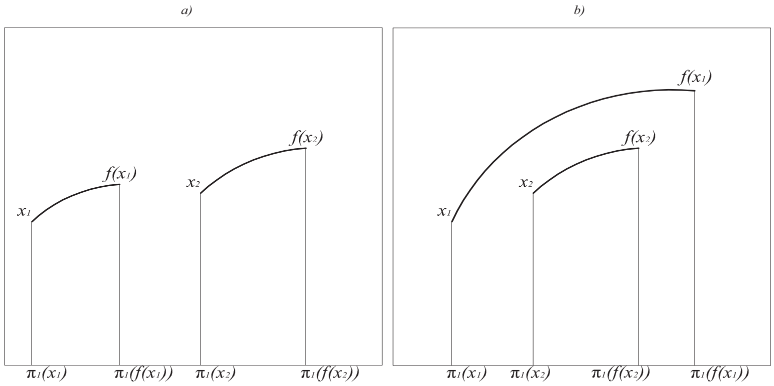

FIGURE 2.2. a) Example of a f–ordered set: the set $\{x_1, x_2\}$ satisfies (2.4); b) example of a non–f–ordered set: the set $\{x_1, x_2\}$ does not satisfy (2.4).

As already said before, this number can be rational and in this case the set M can be formed by an ordered collection of periodic orbits, otherwise the number can be irrational and M could be a Cantor set. It could be that M is an invariant circle both if the rotation number is rational or irrational (see [**38**]).

DEFINITION 2.8. *Let us define the orbit under f of a point $z = (\theta, r) \in A$ as the set given by $O(f, z) = \{f^k(z) + (l, 0) : k, l \in \mathbb{Z}\}$; we will say that z is a Birkhoff p/q–periodic point if it is p/q–periodic and if its orbit $O(f, z)$ is f–ordered.*

This means that the orbit of a Birkhoff p/q–periodic point belongs to an Aubry–Mather set; in fact, it is minimal if p, q are relatively prime and it is closed; being formed by a finite number of points.

Let us see some steps leading to the statement of the Aubry–Mather theorem, whose results are obtained independently by the two mathematicians.

The first step is the well–known so called *"last geometric Poincaré theorem"*. Let us see a simple version (see []):

Theorem 2.9. *Let f be an area–preserving map on the compact annulus moving two points on the boundary circles on opposite directions (twist condition). Then f has at least two fixed points.*

In 1912, Poincaré just enounces the theorem, but he does not prove it. One year later, Birkhoff proves an analogous result with a weaker thesis in the statement, namely "at least one fixed point". In 1925, Birkhoff provides a new version of the theorem that is named as the Poincaré–Birkhoff theorem. Let us consider a map $f : A \to A$ not twist, but such that it satisfies the twist condition on the boundary, namely, said ρ_0 and ρ_1 the two rotation numbers of f restricted respectively to $\mathbb{R} \times \{0\}$ and $\mathbb{R} \times \{1\}$, it must be $\rho_0 < \rho_1$. The Poincaré–Birkhoff theorem states the following (compare with [**38**]):

Theorem 2.10. *Let f be the lift of an area–preserving map on the cylinder such that it satisfies the boundary twist condition. If $p/q \in [\rho_0, \rho_1]$ and $(p, q) = 1$, then f has at least two p/q–periodic orbits. Moreover if $\rho_0 < 0 < \rho_1$, then f has at least two fixed points.*

Birkhoff does not say what happens to the orbits with different rotation numbers and he does not provide any information about the nature of periodic orbits he speaks about. Aubry and Mather prove that the orbits of theorem 2.10 are ordered orbits (they are Birkhoff orbits) and moreover they prove the existence of quasi–periodic orbits.

In an integrable system, the orbits of a twist map f have the following properties:

1) they lie on invariant circles;
2) they are cycle ordered;
3) they exist for any rotation number in $(-\infty, +\infty)$;
4) they minimize the action.

If we perturb the system, KAM theorem ensures that "most part" (i.e. a set of full measure) of invariant circles survive under a small perturbation provided the small perturbation is sufficiently small and the rotation numbers of such invariant circles satisfy the Diophantine condition.

The Aubry–Mather theory states that the circles that do not survive and that break–down are replaced by invariant sets on which the orbits keep some of the properties they have in the unperturbed case. These sets are the Aubry–Mather sets. Let us state the Aubry–Mather theorem (see []) after the following definition:

DEFINITION 2.11. *Consider a twist map $f : A \to A$; consider f restricted to $C_0 = \mathbb{R} \times \{0\}$ and $C_1 = \mathbb{R} \times \{1\}$; let ρ_0 and ρ_1 be the two rotation numbers associated to C_0 and C_1, respectively; then $\rho_1 > \rho_0$ and $[\rho_0, \rho_1]$ is called twist or rotation interval.*

THEOREM 2.12. *Let f be the lift of an area–preserving twist map on the cylinder. Then f has Aubry–Mather sets with rotation number ω for all $\omega \in [\rho_0, \rho_1]$.*

Moreover, the theorem provides some properties of such sets:

THEOREM 2.13. *Let M be an Aubry–Mather set for the lift f of an area–preserving twist map on the cylinder. Then*
1) *M forms a graph on its projection $\pi_1(M)$; this projection is Lipschitz with Lipschitz constant L depending just on the twist constant given by*

$$L = \inf_{(\theta,r)\in M} \frac{\partial(\pi_1 f(\theta, r))}{\partial r} \; ;$$

2) *all the orbits in M are f–ordered and all of them have the same rotation number. It is called rotation number of M and it is noted by $\rho(M)$;*

3) *the projection* $\pi_1(M)$ *is a closed invariant set for the lift of a homeomorphism on the circle and* f *restricted to* M *is conjugated to the lift of a homeomorphism through* π_1.

From Proposition 2.3 and from Theorem 2.12, we can deduce that, if ω is a rational number, then the Aubry–Mather set is a collection of periodic orbits, while, if ω is irrational, then the Aubry–Mather set could be either an invariant circle or a Cantorus.

2.2.2. Katok's results. In [**44**], A. Katok gives more information about the properties of Aubry–Mather sets; in particular, quasi–periodic sets and Cantori can be obtained as limit of Birkhoff periodic orbits. Its proof holds for area–preserving twist maps, and more general, he replaces the hypothesis of area–preserving twist maps with twist maps which preserve a positive measure.

He proves a new version of Aubry–Mather theorem and he provides a proof based on two different steps: the first one is valid for any twist homeomorphism $f : A \to A$, independently of the fact that it is area–preserving. It is stated in the following theorem (compare with [**44**]):

THEOREM 2.14. *(Katok) Let* f *be a twist homeomorphism. If* f *has a Birkhoff* p/q*–periodic orbit for any rational number* p/q *in the twist interval* $[\rho_0, \rho_1]$*, then* f *also possesses a minimal Aubry–Mather set with any irrational rotation number in the twist interval.*

The Theorem 2.14 tells us that if f has a Birkhoff p/q–periodic orbit for any $p/q \in [\rho_0, \rho_1]$, then f has Aubry–Mather sets with rotation numbers ω for any $\omega \in [\rho_0, \rho_1]$.

This means that invariant Cantor sets are possible in non–area–preserving systems provided appropriate Birkhoff periodic points are present.

In order to prove the Aubry–Mather theorem from theorem 2.14, we need a result ensuring the existence of Birkhoff p/q–periodic orbits. Such existence is provided by a generalized version of Poincaré-Birkhoff theorem (see [**44**]):

Theorem 2.15. *Let f be a twist homeomorphism preserving a positive measure on open sets and let p/q belong to the twist interval. Then, f has a Birkhoff p/q–periodic orbit.*

If in addition f is a C^1 diffeomorphism then, under the same assumptions, f has two different Birkhoff p/q–periodic orbits which form together an Aubry–Mather set.

To summarize, the previous two theorems provide the result obtained by Aubry and Mather for a twist map which preserves a positive measure:

Theorem 2.16. *Let f be a twist homeomorphism on the cylinder, preserving a positive measure on open sets, with twist interval $[\rho_0, \rho_1]$. Then for any $\rho \in [\rho_0, \rho_1]$, f has an Aubry–Mather set with rotation number ρ.*

Katok proves another important property about Aubry–Mather sets, namely, he proves that they can be obtained as limit of Birkhoff periodic orbits. It follows from the following proposition:

Proposition 2.17. *Let f be a twist homeomorphism. Then*
a) the set of all Aubry–Mather sets for a twist homeomorphism is closed in Hausdorff topology;
b) the rotation number $\rho(M)$ for an Aubry-Mather set M is continuous in Hausdorff topology.

The Theorem 2.14 ensures the existence of Aubry–Mather sets for any rotation number in the twist interval and the Proposition 2.17

guarantees that, given a sequence of rational numbers $\{\frac{p_n}{q_n}\}$ converging to an irrational number ω, the p_n/q_n–periodic orbits converge to the quasi–periodic orbit with rotation number ω.

2.2.3. Dissipative twist maps. We wonder if in dissipative systems some sets similar to the Aubry–Mather sets can appear and if we can extend the Aubry–Mather theorem for dissipative twist maps.

Let us start by defining a dissipative twist map.

Definition 2.18. *Let $f : \mathbb{R}^2 \to \mathbb{R}^2$ be a diffeomorphism satisfying conditions* 1), 2) *and* 3) *of definition 2.4. We will say that f is dissipative if it satisfies the following conditions:*
4) *there exists $\lambda \in (0,1)$ such that for any $x \in \mathbb{R}^2$ we have $0 < \det Df(x) \leq \lambda$, where $Df(x)$ is the Jacobian of the map f;*
5) *there exists an $M \in \mathbb{R}^+$ such that for any $N \geq M$, $S^1 \times [-N, N]$ is a trapping region for f (B is a trapping region for f if it is an annular region such that its image under f belongs to the interior of B).*

Condition 5) is not really necessary to have a dissipative map, but it is a requirement for some theorems we will see in the following.

Let us start with some remarks.

Remark 2.1. $i)$ *In a dissipative system only one invariant circle can exist (if there are two invariant circles, the area between them would be preserved under the action of the map and this cannot happen, due to the fact that the system is dissipative).*
$ii)$ *Birkhoff periodic orbits can persist under a small dissipative perturbation (see* [**1**]*).*
$iii)$ *Given the existence of Birkhoff periodic orbits, Katok theorem 2.14 allows us to conclude that Aubry–Mather sets exist for any irrational number in the twist interval.*

Let us suppose the existence of Birkhoff periodic orbits; then, Katok theorem allows us to claim that Aubry–Mather sets with irrational rotation numbers must occur. Remark *i*) tells us that at most one invariant circle can exist; on the other hands, Katok theorem states that Aubry–Mather sets must occur for any irrational number within the twist interval; this means that some of these Aubry–Mather sets should be Cantor sets.

Let us recall the requirements of Theorem 2.14:

- Existence of a twist homeomorphism with not trivial rotation interval (if the rotation interval is just a number, the theorem has no relevance).
- Existence of Birkhoff p/q–periodic orbits for any rational number belonging to this interval.

We also note that stable points of area–preserving maps should become asymptotically stable if we add a dissipation. This means that, if Birkhoff periodic points exist, they should appear on attractive sets of the dissipative twist map. We want to recall the definition of an attractive set:

Definition 2.19. *We will say that an f–invariant set Γ is weakly attractive if, for any neighborhood N of Γ, there exists a neighborhood M of Γ in N such that $f(M) \subset M$. If, moreover, M can be chosen such that $\Gamma = \bigcap_{n=0}^{\infty} f^n(M)$, then we will say that Γ is attractive. If an attractive set contains a dense orbit of f, we will say that it is an attractor.*

Casdagli [**9**] and Le Calvez [**46**] extend the Aubry–Mather theory to dissipative twist maps. They generalize the Aubry–Mather theorem when the attractive set of the whole cylinder lies in a compact subcylinder for which the map has a non–trivial rotation interval.

Let us see how the rotation interval for an attractive set of a dissipative twist map can be defined, namely how its endpoints ρ_i and ρ_e can be defined. Let H be the set of compact connected sets separating the cylinder, and let $\Gamma \in H$ be an invariant set for f. Let us associate with Γ (compare with [**5**], [**9**]), two real numbers that are respectively, the internal rotation number ρ_i and the external rotation number ρ_e, as follows. Let us start with the definition of ρ_e: let $L = \{(x, y) \in \mathbb{R}^2 | x \in \mathbb{R}, y = y_0\}$ be a horizontal line lying above Γ (see Figure 2.3). Let us denote by Γ' those points belonging to Γ such that their vertical projection on L is bijective (the marked line in Figure 2.3). Let $\pi : L \to \Gamma'$ be the vertical projection from L to Γ'. Then ρ_e is defined by $-\rho(g)$ where $\rho(g)$ is the rotation number of the map $g : L \to L$ defined as $g(\theta) = \pi^{-1} \circ f^{-1} \circ \pi(\theta)$. It can be shown that $f^{-1}(\Gamma') \subset \Gamma'$ so that g is well defined. Moreover, $\rho(g)$ is well defined since g is the lift of a circle map and it is monotonic (see [**?**]). Similarly, we can define ρ_i considering the horizontal line lying below Γ. Figure 2.3 shows an invariant set $\Gamma \in H$ and how the map g can be defined.

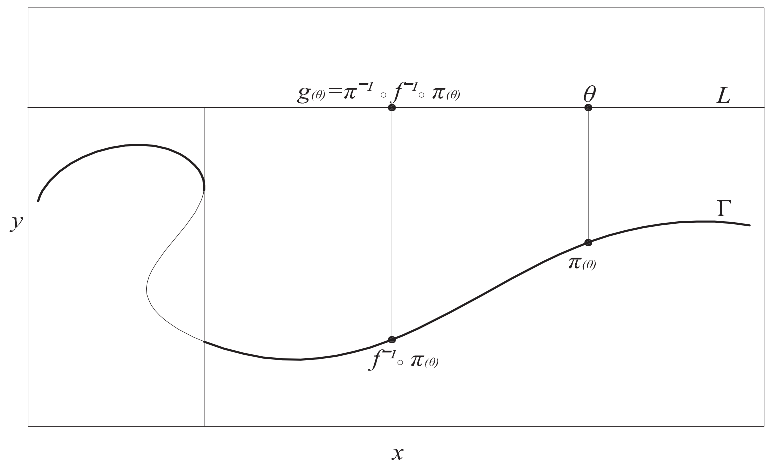

FIGURE 2.3. The Figure shows the projections defining the external rotation number for an invariant set $\Gamma \in H$.

Casdagli proves that a dissipative twist map with a trapping region (i.e. which satisfies condition 5) of Definition 2.18), has a unique Birkhoff attractive set. The Birkhoff set is defined as follows:

DEFINITION 2.20. *Let B be a compact connected f–invariant set which separates the cylinder $S^1 \times \mathbb{R}$ and such that it is a trapping region for f. Let $\Lambda(B) = \bigcap_{n=0}^{\infty} f^n(B)$. Then, we will call Birkhoff set, the set $B(f) = \partial(\Lambda(B))_{inf} \cap \partial(\Lambda(B))_{sup}$*

We recall that if Λ is a compact connected set which separates the cylinder C, we denote with Λ_{inf} and with Λ_{sup} the two unlimited components, respectively, inferior and superior of $C \setminus \Lambda$.

The set $B(f)$ is sometimes wrongly called "attractor": actually, it is not necessary an attractor because it could not contain dense orbits. More precisely, we can state that $B(f)$ is an attractive set and it separates the cylinder in two connected components. Figures 2.4 and 2.5 show two examples of invariant attractive sets.

In some cases $B(f)$ is simply an invariant circle which runs around the cylinder (invariant rotational circle) and in this case its rotation interval is trivial because it is reduced to only one point. In this case we can find periodic points which lie outside the Birkhoff set, and it happens because $B(f)$ does not describe the whole dynamics of f.

However, when $B(f)$ is an invariant rotational circle, it can contain Birkhoff periodic points, whenever the rotation number is a rational number. On the contrary, if we do not know anything about the nature of $B(f)$, we can not guarantee the existence of Birkhoff periodic points

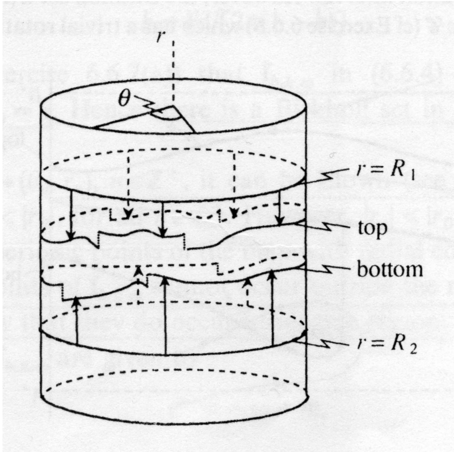

FIGURE 2.4. Schematic illustration of the top and bottom of a Birkhoff attracting set. The circles $r = R_1$ and $r = R_2$ allows us to define the rotation interval. Observe that the top and the bottom of an attracting set are not necessarily continuous curves (after [**1**]).

on $B(f)$. For this reason the following result by Casdagli (absolutely not trivial) is the key to apply Katok Theorem 2.14.

THEOREM 2.21. *Let the Birkhoff set $B(f)$ have internal and external rotation numbers ρ_i and ρ_e, with $\rho_i \leq \rho_e$. Then $B(f)$ contains Birkhoff p/q–periodic orbits for all $p/q \in [\rho_i, \rho_e]$.*

We recall that, when the twist map considered is area–preserving, rotational circles must necessary intersect their images under the map. This topological property of area–preserving twist maps plays a very important role in the occurrence of their Birkhoff periodic points. In non–area–preserving twist maps, it can be proved that the Birkhoff set $B(f)$ has an analogous property, more precisely the *intersection property* which we define as follows:

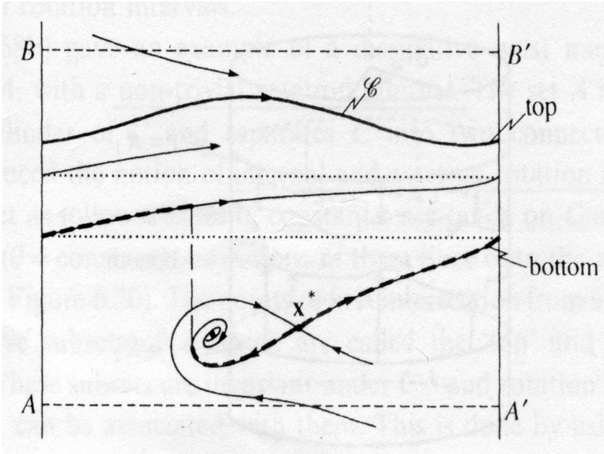

FIGURE 2.5. In the Figure the line AB and $A'B'$ are identified. It is shown an invariant circle $\mathcal{C}$ such that $\rho(f_{|\mathcal{C}}) = \alpha$; a focus and a saddle point x^*. The union of $\mathcal{C}$ and the unstable manifolds of the saddle is an attractive set A for f. The top of A is $\mathcal{C}$, while its bottom set is a segment of the unstable manifolds of x^*. Thus $\rho_i = 0$ and $\rho_e = \alpha$, so that A has a non–trivial rotation interval. However the Birkhoff set $B(f)$ is simply the circle $\mathcal{C}$ which as a trivial rotation interval (after [**1**]).

DEFINITION 2.22. *We say that an f–invariant set $\Gamma \in H$ has the intersection property if given any set $C \in H$ with $C \cap \Gamma \neq \emptyset$, then $C \cap f(C) \neq \emptyset$.*

In [**9**] the author easily proves that the set $B(f)$ satisfies this property and he explicitly uses the property to prove Theorem 2.21. Then, an analogue of Aubry–Mather theorem follows from Katok's result 2.14.

THEOREM 2.23. *Let $B(f)$ be a Birkhoff set with non–trivial rotation interval $[\rho_i, \rho_e]$, with $\rho_i < \rho_e$. Then, for every rational number*

$p/q \in [\rho_i, \rho_e]$, $B(f)$ contains a Birkhoff p/q–periodic orbit and, for every irrational number $\omega \in [\rho_i, \rho_e]$, $B(f)$ contains an Aubry–Mather set with rotation number ω.

Let us remark that the trapping hypothesis does not guarantee that the Birkhoff set has a non–trivial rotation interval (see [**1**]). In particular, the existence of a non–trivial rotation interval for the Birkhoff set is not obvious and in [**9**], the author does not prove such existence. Such proof can be provided through the *Shadowing Lemma* and from some properties of the stable and unstable manifolds of the periodic points belonging to the attractive set of the map f.

Let f be a C^ℓ–diffemorphism on $\mathbb{R}^2$ with a hyperbolic invariant set Λ and recall that the orbit of a point $x_0 \in \mathbb{R}^2$ under f is the sequence of points $\{x_i\}$, where $x_i = f^i(x_0)$, so that $x_{i+1} = f(x_i)$. Let $W^s(x, f)$ and $W^u(x, f)$ be, respectively, the stable and unstable manifolds of a given point $x \in \Lambda$ under f. Let $f : \mathbb{R}^2 \to \mathbb{R}^2$ have also an annular trapping region T, and let A be the attractive set $A = \bigcap_{n\in\mathbb{Z}^+} f^n(T)$.

Our aim is to prove that there exists orbits in Λ with a range of rotation numbers and we will do it by making use of the Shadowing Lemma. We omit the intermediate steps and we states the following theorem which guarantees that there exists a non trivial rotation interval for a Birkhoff set, namely for the attractive set A defined above.

THEOREM 2.24. *Let $y \in A$ be a periodic point of f of period q and rotation number p/q where p, q are relatively prime. Suppose that $W^u(y, f^q)$ intersect $W^s(f^k(y), f^q)$ transversely for some $0 < k < q$. Then there exists a non–trivial interval I containing p/q such that, for every $\alpha \in I$, there is a point with polar coordinates $(\theta, r) \in A$ with rotation number $\rho(\theta, r) = \alpha$. Furthermore, there are points in A for which the rotation number does not exist.*

This theorem gives sufficient conditions for the existence of a non–trivial rotation interval associated with a given attractive set A, and it completes the results about the possibility of the existence of cantori in dissipative twist maps.

CHAPTER 3

On the dynamics of the dissipative standard map

The evolution of a physical problem can be described through some continuous functions of the time or through functions defined at discrete intervals of the time. In the first case we refer to a *continuous dynamical system*, while in the second case we refer to a *discrete dynamical system*.

The evolution of an ℓ–dimensional discrete system is described by a mapping represented by a set of equations of the form

$$\underline{x}_{n+1} = \underline{f}(\underline{x}_n) \ , \quad n \in \mathbb{N} \ , \tag{3.1}$$

where $\underline{x} = (x_1, \ldots, x_\ell) \in \mathbb{R}^\ell$ and $\underline{f} = (f_1, \ldots, f_\ell) \in \mathbb{R}^\ell$. Such equations describe the dynamics at the discrete time $n+1$ as a function of the solution at the time n; this means that the solution x_n of (3.1) at the time n with initial datum x_0 is obtained by iterating the mapping starting from x_0. In this Chapter we will describe the dynamics of a particular discrete mapping, namely the *dissipative standard map* which is related to the spin–orbit problem through a suitable integration.

First we characterize the conservative mapping showing which kinds of motion take place and then we compare the conservative mapping with the dissipative one. Successively, we present some new results about the existence of periodic orbits in the dissipative standard map. We prove, through a suitable parameterization and through the implementation of the implicit function theorem, the existence of periodic orbits within an interval of a drift parameter involved in the equation of the dissipative standard map; moreover, through the study of the behavior of the drift as function of the perturbing parameter, we define explicitly the Arnold's tongues in which periodic orbits with a given period can be found. Arnold's tongues are well–known structures (compare with [**6**], [**59**]); from a physical point of view, our results allow as to connect the occurrence of the spin–orbit resonances (associated with periodic solutions) to the eccentricity of the Keplerian orbit of the satellite (corresponding to the drift parameter).

Furthermore, the parametric representation of the solution allows us to write the solution of rotational tori and, therefore, to relate periodic orbits to quasi–periodic orbits.

The content of this Chapter is included in a paper written in collaboration with A. Celletti (see [**15**]).

3.1. The conservative standard map

Let us introduce the well–known discrete dynamical system called *standard map* introduced by B.V. Chirikov in [**25**] and defined by the equations

$$\begin{cases} y_{n+1} = y_n + \varepsilon f(x_n) \\ x_{n+1} = x_n + y_{n+1} \ , \end{cases} \tag{3.2}$$

where $x_n \in \mathbb{T} = \mathbb{R}/(2\pi\mathbb{Z})$, $y_n \in \mathbb{R}$, ε is a positive real parameter, called *perturbing parameter* and $f = f(x)$ is an analytic, periodic function. In particular the *classical standard map* is obtained by setting $f(x) = \sin(x)$:

$$\begin{cases} y_{n+1} = y_n + \varepsilon \sin x_n \\ x_{n+1} = x_n + y_{n+1} \ , \end{cases} \tag{3.3}$$

In the following, we will refer to the standard map, with the formulation given in equation (3.3). We will show some properties of the standard map and of its dynamics.

The mapping (3.3) is conservative because the phase space area is preserved under the action of the map. Indeed, we can show that the determinant of the corresponding Jacobian associated to the map is equal to one: setting $f_x(x_n) \equiv \frac{\partial f(x_n)}{\partial x} = \cos(x_n)$, we have

$$\det \begin{pmatrix} \frac{\partial y_n}{\partial y} & \frac{\partial y_n}{\partial x} \\ \frac{\partial x_n}{\partial y} & \frac{\partial x_n}{\partial x} \end{pmatrix} = \det \begin{pmatrix} 1 & \varepsilon f_x(x_n) \\ 1 & 1 + \varepsilon f_x(x_n) \end{pmatrix} = 1 \ .$$

Another important property of the standard map is its integrability for $\varepsilon = 0$. If we neglect the perturbation taking $\varepsilon = 0$, the mapping (3.3) reduces to

$$\begin{cases} y_{n+1} = y_n \\ x_{n+1} = x_n + y_{n+1} \ , \end{cases} \tag{3.4}$$

so that, the map is integrable and the solution can be written in a very simple way because, as we can see, y_n is constantly equal to the initial value y_0, and $x_n = x_0 + ny_0$ for any $n \geq 0$.

In this case the coordinate y_n is fixed while x_n varies as $x_n = x_0 + ny_0$; in the case in which the initial condition y_0 is equal to a rational multiple of 2π, the trajectory is a periodic orbit: if the initial datum is of the form $(y_0, x_0) = (2\pi \frac{p}{q}, x_0)$ with p, q positive coprime integers and $x_0 \in \mathbb{T}$, the successive iterations of the x coordinate are given by the following sequence: $x_0 + 2\pi \cdot \frac{p}{q}$, $x_0 + 2\pi \cdot 2 \cdot \frac{p}{q}, \cdots, x_0 + 2\pi \cdot q \cdot \frac{p}{q} = x_0 + 2\pi$; since x_0 varies on the torus, after q iterations it comes back to its initial position: therefore, we get a periodic orbit of period q. The quantity p measures how many times the interval $[0, 2\pi)$ is run before coming back to the starting position.

The situation is completely different if we consider an irrational initial condition y_0: fixed the initial value y_0, the y coordinate remains always constant under any number of iterations, while, since $x_n = x_0 + ny_0$, the x coordinate fills densely the line $y = y_0$ as the number of iterations increases. The orbit, given by a straight line, is a *quasi–periodic invariant curve* (see Figure 3.1a): on this curve a quasi–periodic motion takes place, and any point of the x coordinate never comes back on itself.

In order to distinguish between periodic and quasi–periodic orbits we introduce the *rotation number* ω defined by the quantity

$$\omega = \lim_{n\to\infty} \frac{x_n - x_0}{n} \ .$$

The rotation number, when it exists, is the frequency of the motion: as we have already seen, in the unperturbed case ($\varepsilon = 0$) the equations of the standard map reduce to the system (3.4) that can be written as

$$\begin{cases} y_n = y_0 \\ x_n = x_0 + n y_0 \ , \end{cases}$$

where (x_0, y_0) is the initial condition. If the rotation number can be written as $\omega = 2\pi\frac{p}{q}$ with p, q positive coprime integers, then $y_q = y_0$, $x_q = x_0 + 2\pi q = x_0$ and the motion is periodic with frequency ω; if ω and 2π are incommensurable, i.e. $\frac{\omega}{2\pi}$ is an irrational number, then the dynamics associated to (3.4) is quasi–periodic.

As we have shown, in the unperturbed case, the dynamics of the standard map is completely known and it is fully described by periodic and quasi–periodic motions. Let us show how the dynamics changes when we introduce the perturbation: for $\varepsilon \neq 0$ the mapping becomes non–integrable, in fact it is not possible to find an explicit solution and chaotic motions might appear. For ε not zero but sufficiently small, the quasi–periodic invariant curves, called *rotational invariant curves*, are slightly displaced and deformed with respect to the integrable case. The periodic orbits are surrounded by closed trajectories, called *librational curves.* As ε increases the librational curves increase their amplitude, the rotational invariant curves are more and more deformed and distorted, and for a given value of ε they break–down, leaving place to the *cantori*, which are still invariant sets, but they are graphs of a Cantor set (for a more detailed description of cantori, we refer to Chapter 2); moreover, chaotic motions start to appear and they fill an increasing region. These phenomenons are shown in Figure 3.1, which shows the evolution of the classical standard map as the perturbing parameter ε varies: we can see how the invariant curves are deformed, how they break–down as ε increases, or how they are destroyed and they do not exist for a critical value of ε.

The existence of the rotational invariant curves provides an important property of stability: a solution with a given initial value can not cross a rotational invariant curve, so if we take an initial condition between two different rotational invariant curves, the solution starting from that initial condition will be trapped between the two curves for all times. On the contrary, their break–down, starting with the appearance of cantori, allows the solution to diffuse in an extended region of the phase space.

3.2. The dissipative standard map

The equations (3.3), can be modified in order to introduce a dissipation. In particular, we can define the *dissipative standard map* as

$$\begin{cases} y_{n+1} = by_n + c + \varepsilon \sin x_n \\ x_{n+1} = x_n + y_{n+1} \ , \end{cases} \tag{3.5}$$

where $x_n \in \mathbb{T} = \mathbb{R}/(2\pi\mathbb{Z})$, $y_n \in \mathbb{R}$, $\varepsilon > 0$ is the *perturbing parameter*, $b \in \mathbb{R}_+$ is the *dissipative parameter* and $c > 0$ is a *drift parameter*. It is easy to show that the parameter b is the determinant of the Jacobian associated to (3.5); in fact, with the same notation used in the

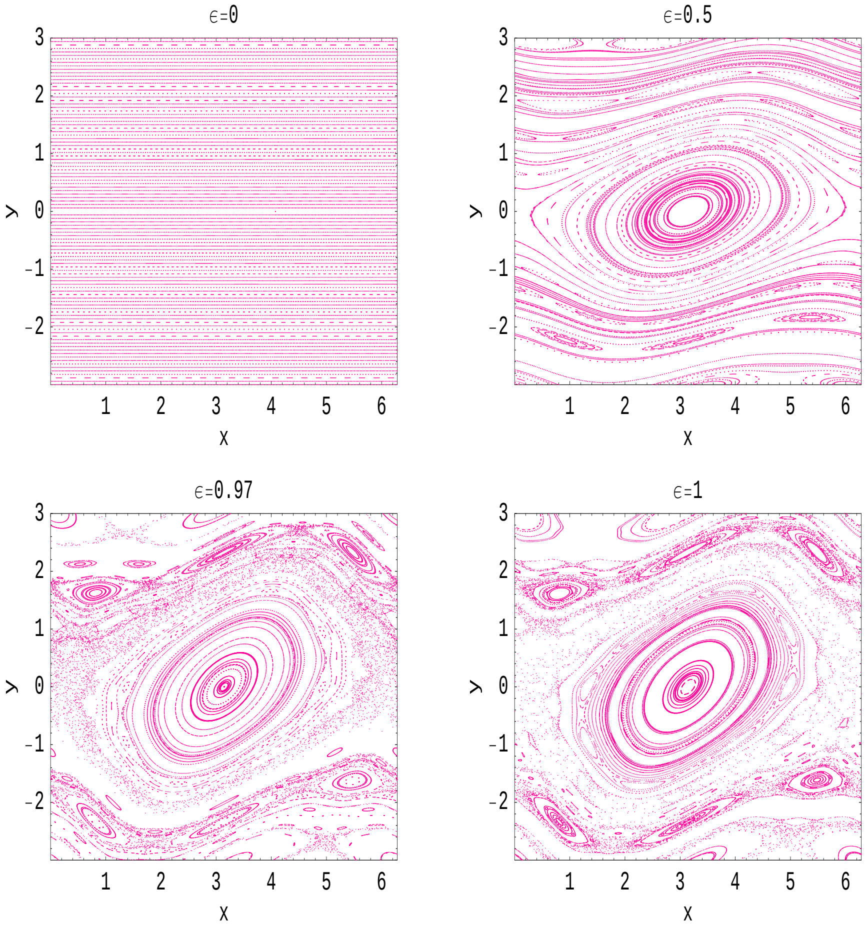

FIGURE 3.1. Dynamics of the classical standard map, starting with $x_0 = \pi$ and varying 100 initial conditions y_0 within the interval $[-3, 3]$ as ε increases: a) $\varepsilon = 0$, b) $\varepsilon = 0.5$, c) $\varepsilon = 0.97$, d) $\varepsilon = 1$.

conservative case, one has:

$$\det \begin{pmatrix} \frac{\partial y_n}{\partial y} & \frac{\partial y_n}{\partial x} \\ \frac{\partial x_n}{\partial y} & \frac{\partial x_n}{\partial x} \end{pmatrix} = \det \begin{pmatrix} b & \varepsilon f_x(x_n) \\ b & 1 + \varepsilon f_x(x_n) \end{pmatrix} = b \ .$$

We can distinguish four different cases as b varies.

- If $b = 1$ and $c = 0$, the map is the conservative standard mapping (3.3).

- If $b = 0$, one obtains the one-dimensional mapping $x_{n+1} = x_n + c + \varepsilon \sin x_n$; moreover, if $\varepsilon = 0$ one obtains the circle map $x_{n+1} = x_n + c$.
- If $0 < b < 1$ the mapping is dissipative and in particular it is contractive.
- If $b > 1$ the mapping is expansive.

In the following, when we speak about dissipative standard map, we will always refer to the third case of contractive mapping.

Let us show some properties about the dynamics of the dissipative standard map. We can find attracting periodic orbits, invariant curves and strange attractors: we can see that stable periodic orbits become attractive, and that periodic orbits and an invariant curve can coexist. In particular, a big difference with the conservative standard map is that in the dissipative case, only one invariant curve can exist: in fact, if we have two invariant curves, the area between them is preserved, contrary to the assumption that the system is dissipative. Finally, strange attractors are very complicate geometrical structures and they are shown to have a non–integer dimension, namely a *fractal* dimension.

If we define

$$\alpha \equiv \frac{c}{1-b}$$

we can see that for $\varepsilon = 0$ the trajectory $\{y_n = \alpha\} \times \mathbb{T}$ is invariant; in fact, the invariance relation

$$y_{n+1} = y_n = by_n + c \ ,$$

admits the solution $y_n = \alpha$ with α being given by

$$\alpha = b\alpha + c \quad \Rightarrow \quad \alpha \equiv \frac{c}{1-b} \ .$$

From the last relation we can see that the drift c can be written as $c = \alpha(1-b)$ and therefore it becomes zero as $b = 1$ as in the conservative case.

3.3. A parametric representation of periodic orbits in the conservative case

The existence of periodic orbits is very important to understand the dynamics of the perturbed standard map as the perturbing parameter ε varies. We have seen for the conservative case that an invariant curve is deformed as ε increases and it is destroyed at a certain value of ε. Moreover, periodic orbits with very large period can approximate very well the dynamics of an invariant curve. So, we can study the properties of an invariant curve (for example the break–down threshold (compare with [**39**]) of an invariant curve with irrational rotation number ω), using the stability properties of periodic orbits with frequencies given by the rational approximants to ω.

We would like to show some results about the existence of periodic orbits for the conservative standard map; in this Section we will present the results given in [**17**]. Let us consider the mapping defined by the equation (3.3); considering that $x_{n+1} - x_n = y_{n+1}$ and $x_n - x_{n-1} = y_n$, one obtains

$$x_{n+1} - 2x_n + x_{n-1} = \varepsilon \sin x_n \ . \tag{3.6}$$

We look for a periodic solution with rational frequency $\omega = 2\pi p/q$ for some p, $q \in \mathbb{Z}_+$, with p, q coprime, such that it satisfies the periodicity condition

$$\begin{cases} x_{n+q} = x_n + 2\pi p \\ y_{n+q} = y_n \ . \end{cases} \tag{3.7}$$

Then we parameterize the solution as

$$x_n = \theta_n + u(\theta_n) \ , \quad \theta_n \in \mathbb{T} \ , \tag{3.8}$$

where $u(\theta_n)$ is a continuous, $2\pi p$–periodic function and the linear flow θ_n is such that $\theta_{n+1} = \theta_n + \omega$. Then we expand the function u in

Fourier–Taylor series as

$$u(\theta_n) \equiv \sum_{j=1}^{\infty} \varepsilon^j u_j(\theta_n) = \sum_{j=1}^{\infty} \varepsilon^j \sum_{\ell=1}^{\min(j,q)} a_{\ell j} \sin(\ell\theta_n) \ , \tag{3.9}$$

where the real coefficients $a_{\ell j}$ will be determined as follows. Inserting the parameterization (3.8) in (3.6), it follows that the function u must satisfy the equation

$$u(\theta_n + 2\pi\frac{p}{q}) - 2u(\theta_n) + u(\theta_n - 2\pi\frac{p}{q}) = \varepsilon \sin(\theta_n + u(\theta_n)) \ . \tag{3.10}$$

Inserting (3.9) in the previous equation and equating the same orders of ε, after a suitable expansion of the right hand side $\varepsilon \sin(\theta_n + u(\theta_n))$ around ε, one obtains the expression of the coefficients $a_{\ell j}$. We omit the computations (for more details see [**17**]), but we just want to remark that when we equate terms of order ε^q (where q is the period of the periodic orbit we are considering), one has to choose θ_n such that $\sin(q\theta_n) = 0$. Such choice compensates the zero term $\cos(2\pi q\frac{p}{q} - 1)$ occurring at the q^{th} order and it fixes the value of θ_0, since $\theta_n = \theta_0 + 2\pi n\frac{p}{q}$ for the linearity of the flow θ_n. Therefore, one has two solutions (modulus 2π):

$$\theta_0 = \frac{\pi}{q} \quad \text{and} \quad \theta_0 = \frac{2\pi}{q} \ .$$

It is possible to show that the orbit starting at $\theta_0 = \frac{\pi}{q}$ is stable for q odd and unstable for q even, while the one starting at $\theta_0 = \frac{2\pi}{q}$ is stable for q even and unstable for q odd (see [**17**]).

As written before, the coefficients $a_{\ell j}$ can be computed recursively from the previous equations: by the computations, we can see that the coefficient a_{qq} appearing in the function $u_q(\theta_n) = \sum_{\ell=1}^{q} a_{\ell q} \sin(\ell\theta_n)$ is not determined because it disappears from the equations. But it has no consequences because this term does not contribute to the general solution: in fact we can see that

$$u_q(\theta_0) = \sum_{\ell=1}^{q} a_{\ell q} \sin(\ell\theta_0) = \sum_{\ell=1}^{q-1} a_{\ell q} \sin(\ell\theta_0)$$

since the choice of θ_0 is such that $\sin(q\theta_0) = 0$.

Remark 3.1. *In the next Section, we will see that in the dissipative case, the problem about the disappearance of the coefficients of the q^{th} order can not be avoided, and it leads to a completely different solution.*

3.4. Periodic orbits in the dissipative standard map

In this Section we extend the results about the existence of periodic orbits to the dissipative standard map; we could see that there are many differences with respect to the conservative case: for example in the dissipative case, there exist many periodic orbits of a given period, while in the conservative case we have just two periodic orbits, one stable and the other one unstable; stable periodic orbits in the dissipative case are attractive. Another difference is that in the conservative case we are able to write the full expression of the equation defining the periodic orbit through the parameterization, while in the dissipative case we can not find the full expression, but just an approximation to the order of the period.

We will see that in the dissipative case, the drift c plays a very important role for the existence of periodic orbits: we will show that periodic orbits of frequency $2\pi p/q$, for some $p, q \in \mathbb{Z}_+$, can be found within a whole interval of the drift, say $\mathcal{I}_{pq}$.

Let us summarize the main results obtained about the parameterization of periodic orbits. We define again the dissipative standard mapping as

$$\begin{cases} y_{n+1} = by_n + c + \varepsilon \sin x_n \\ x_{n+1} = x_n + y_{n+1} \ , \end{cases} \tag{3.11}$$

where $x_n \in \mathbb{T} = \mathbb{R}/(2\pi\mathbb{Z})$, $y_n \in \mathbb{R}$, $0 < b < 1$, $\varepsilon > 0$, $c > 0$. A parametric representation of the solution is obtained by setting

$$x_n = \theta_n + u(\theta_n) \ , \quad \theta_n \in \mathbb{T} \ , \tag{3.12}$$

where $u(\theta_n)$ is a continuous, periodic function and the parametric coordinate θ_n evolves linearly. The function u can be written as a series expansion in ε, say $u(\theta_n) = \sum_{j=1}^{\infty} u_j(\theta_n)\varepsilon^j$, where the terms $u_j(\theta_n)$ can be determined by solving suitable recursive equations. The drift c can be also expanded in Taylor series as $c = \sum_{j=0}^{\infty} c_j \varepsilon^j$ for some real quantities c_j. We will show that in the periodic case the series expansion for u can be determined up to the order $j = q-1$. Moreover, the terms c_1, ..., c_{q-1} defining the Taylor series of the drift up to the order $q-1$ are real numbers, while the quantity c_q (coming out from the q^{th} order) is a continuous periodic function of θ_n, namely $c_q = c_q(\theta_n)$. As a consequence, for $\theta_n \in [0, 2\pi)$ the drift is constrained to belong to an interval, say $c \in \mathcal{I}_{pq}$. In the following, we will see that the determination of such interval can be also found through an implementation of the implicit function theorem.

3.4.1. A parametric representation of periodic orbits in the dissipative case. Let us show in detail the results about the parameterization. We parameterize a solution with frequency $\omega \in \mathbb{R}$ associated to the dissipative standard map (3.11) as in equation (3.12), where the parametric coordinate θ_n evolves linearly as $\theta_{n+1} = \theta_n + \omega$. Then the unknown function $u = u(\theta_n)$ is the solution of equation (3.14) given in the following Lemma.

LEMMA 3.1. *Defining the quantity*

$$\gamma \equiv (1-b)\omega - c \ , \tag{3.13}$$

then the function $u = u(\theta_n)$ *associated to the solution* (3.12) *of the dissipative standard map* (3.11) *must satisfy the equation*

$$u(\theta_n + \omega) - (1+b)u(\theta_n) + bu(\theta_n - \omega) + \gamma = \varepsilon \sin(\theta_n + u(\theta_n)) \ . \quad (3.14)$$

Proof.

From (3.11) we get

$$\begin{aligned} x_{n+1} - x_n = y_{n+1} &= by_n + c + \varepsilon \sin x_n \\ &= b(x_n - x_{n-1}) + c + \varepsilon \sin x_n \ , \end{aligned}$$

which provides the following equation:

$$x_{n+1} - (1+b)x_n + bx_{n-1} - c - \varepsilon \sin x_n = 0 \ . \quad (3.15)$$

Inserting the parameterization (3.12) in (3.15) and using (3.13), we can easily see that the function $u(\theta_n)$ must satisfy (3.14). $\square$

Equation (3.14) is valid both for invariant attractors and for periodic orbits. In this Section we are interested in the parameterization of periodic orbits; to this end we set $\omega = 2\pi p/q$ for some p, $q \in \mathbb{Z}_+$ coprime. A periodic solution (x_n, y_n) of frequency ω for the mapping (3.11), must satisfy the following periodicity condition

$$\begin{cases} x_{n+q} = x_n + 2\pi p \\ y_{n+q} = y_n \ . \end{cases}$$

We want to prove the following important result about the existence of periodic orbits for the dissipative standard map:

Proposition 3.2. *Let* $M : \mathbb{R} \times \mathbb{T} \to \mathbb{R} \times \mathbb{T}$ *be the map defined in* (3.11) *and let* $p, q \in \mathbb{Z}_+$ *coprime. Then, for fixed values of* b, ε, *say* $b = \bar{b}$, $\varepsilon = \bar{\varepsilon}$, *one can find an interval* $\mathcal{I}_{pq} \subset \mathbb{R}$, *such that for any* $c \in \mathcal{I}_{pq}$, *the map* M *admits at least a periodic orbit of period* p/q.

To prove the above statement we start by finding a parameterization of the form (3.12) for the periodic orbit with frequency ω; to this end, we look for a solution of equation (3.14). We define the function u for any $\theta \in [0, 2\pi)$, although the periodic orbit consist of q points. The first point $x_0 = \theta_0 + u(\theta_0)$ is obtained from an initial datum $\theta = \theta_0$ and the other $q-1$ points are computed iterating the initial datum by the law of evolution of the flow θ_n, namely $\theta_n = \theta_0 + 2\pi np/q$. Then, to find the solution u of (3.14), we expand the function $u(\theta_n)$ in Taylor series as

$$u(\theta_n) = \sum_{j=1}^{+\infty} u_j(\theta_n)\varepsilon^j \ , \tag{3.16}$$

for some real functions u_j which can be expanded in Fourier series as

$$u_j(\theta_n) = \sum_{\ell=1}^{+\infty} \Big(a_{\ell j} \sin(\ell\theta_n) + b_{\ell j} \cos(\ell\theta_n) \Big) \ , \tag{3.17}$$

where the unknown real coefficients $a_{\ell j}$, $b_{\ell j}$ will be explicitly computed. We also expand the drift c in Taylor series as

$$c = \sum_{j=0}^{\infty} c_j \varepsilon^j \ ,$$

with $c_j \in \mathbb{R}$ where we fix $c_0 = (1-b)\omega$, which corresponds to the solution with $y_0 = \omega$ for the unperturbed system with $\varepsilon = 0$. Similarly we expand γ defined in (3.13) as

$$\gamma = \sum_{j=1}^{\infty} \gamma_j \varepsilon^j \ , \tag{3.18}$$

where γ_j are suitable real coefficients.

Proposition 3.3. *Consider a periodic orbit of frequency* $2\pi p/q$ *with* p, $q \in \mathbb{Z}_+$*; given the parameterization* (3.12) *and the expansions*

(3.16), (3.17), (3.18), *the following equation holds for any* $j > 0$*:*

$$
\begin{aligned}
\sum_{j=1}^{\infty} \ \varepsilon^j \ \sum_{\ell=1}^{\infty} \Big\{ & \sin(\ell\theta_n)\Big[(1+b)a_{\ell j}\alpha_\ell^{(p,q)} - (1-b)b_{\ell j}\beta_\ell^{(p,q)}\Big] \\
& + \cos(\ell\theta_n)\Big[(1-b)a_{\ell j}\beta_\ell^{(p,q)} + (1+b)b_{\ell j}\alpha_\ell^{(p,q)}\Big] + \gamma_j\Big\} \\
= \ & \sum_{j=1}^{\infty} \varepsilon^j \Big\{ \sum_{\ell=1}^{j} \Big[S_{\ell j}^{(p,q)} \sin(\ell\theta_n) + C_{\ell j}^{(p,q)} \cos(\ell\theta_n)\Big] \\
& + D_j^{(p,q)}\Big\} \ , \qquad (3.19)
\end{aligned}
$$

for some unknown real coefficients $a_{\ell j}$*,* $b_{\ell j}$*,* γ_j*. The real constants* $\alpha_\ell^{(p,q)}$*,* $\beta_\ell^{(p,q)}$ *are given by*

$$
\begin{aligned}
\alpha_\ell^{(p,q)} &= \cos(2\pi\ell \cdot \tfrac{p}{q}) - 1 \\
\beta_\ell^{(p,q)} &= \sin(2\pi\ell \cdot \tfrac{p}{q}) \ ,
\end{aligned}
\qquad (3.20)
$$

while the quantities $S_{\ell j}^{(p,q)}$*,* $C_{\ell j}^{(p,q)}$ *and* $D_j^{(p,q)}$ *depend on the terms* $a_{\ell i}$*,* $b_{\ell,i}$ *for* $i = 1, \cdots, j-1$*.*

Proof.

The equation (3.19) is obtained by inserting the Taylor–Fourier expansions (3.16), (3.17), (3.18) in the parametric equation (3.14). In fact, the left hand side of (3.14) can be written as

$$\begin{aligned}
\sum_{j=1}^{+\infty} \quad \varepsilon^j \quad & \Big\{ \sum_{\ell=1}^{+\infty} \Big[a_{\ell j} \sin(\ell\theta_n + 2\pi\frac{p}{q}) + b_{\ell j} \cos(\ell\theta_n + 2\pi\frac{p}{q}) \Big] \\
& -(1+b) \Big[a_{\ell j} \sin(\ell\theta_n) + b_{\ell j} \cos(\ell\theta_n) \Big] \Big\} \\
& +b \sum_{j=1}^{+\infty} \varepsilon^j \sum_{\ell=1}^{+\infty} \Big\{ a_{\ell j} \sin(\ell\theta_n - 2\pi\frac{p}{q}) + b_{\ell j} \cos(\ell\theta_n - 2\pi\frac{p}{q}) \Big\} + \gamma \\
= \quad & \sum_{j=1}^{+\infty} \varepsilon^j \sum_{\ell=1}^{\infty} \Big\{ (1+b) a_{\ell j} \sin(\ell\theta_n) \cos(2\pi\ell\frac{p}{q}) \\
& +(1-b) a_{\ell j} \cos(\ell\theta_n) \sin(2\pi\ell\frac{p}{q}) + (1+b) b_{\ell j} \cos(\ell\theta_n) \cos(2\pi\ell\frac{p}{q}) \\
& -(1-b) b_{\ell j} \sin(\ell\theta_n) \sin(2\pi\ell\frac{p}{q}) \\
& -(1+b)(a_{\ell j} \sin(\ell\theta_n) + b_{\ell j} \cos(\ell\theta_n)) \Big\} + \sum_{j=1}^{+\infty} \gamma_j \varepsilon^j \ ,
\end{aligned}$$

which coincides with the left hand side of (3.19), recalling that $\alpha_\ell^{(p,q)}$, $\beta_\ell^{(p,q)}$ are defined in (3.20).

The right hand side of equation (3.19) is obtained as follows. Let us consider a generic function $g(\theta_n)$, then the function $g(\theta_n + u)$ with u as in (3.16) can be expanded as

$$g(\theta_n + u) = \sum_{j=1}^{\infty} \varepsilon^j \sum_{\underline{k} \in \mathcal{K}_j} \left(\partial_x^{k_1 + \dots + k_j} g \right) \prod_{\ell=1}^{j} \frac{(u_\ell)^{k_j}}{k_j!} + g(\theta_n) \ ,$$

where $\underline{k} = (k_1, \cdots, k_j) \in \mathbb{N}^j$ and $\mathcal{K}_j \equiv \{\underline{k} : \sum_{\ell=1}^{j} \ell k_\ell = j\}$; the order j of the ε-expansion of the function $g(\theta_n + u)$ is written as the sum of products of the u_ℓ with $\ell = 1, \cdots, j$, which corresponds to a sum of products of the derivatives of g and of the functions $u_\ell(\theta_n)$ for $\ell = 1, ..., j$. In the specific case $g(\theta_n) \equiv \sin\theta_n$, by some computations, such products can be written as a linear combination of the functions $\sin(\ell\theta_n)$ and $\cos(\ell\theta_n)$ for $\ell = 0, ..., j$; the coefficients of these linear combinations are functions depending on the coefficients $a_{\ell i}$, $b_{\ell i}$ with $\ell = 1, \cdots, i$ and $i = 1, \cdots, j-1$, and they will define $S_{\ell j}^{(p,q)}$, $C_{\ell j}^{(p,q)}$, $D_j^{(p,q)}$.

In the case $g(\theta_n) \equiv \sin\theta_n$, the quantities $S_{\ell j}^{(p,q)}$, $C_{\ell j}^{(p,q)}$, $D_j^{(p,q)}$ can be computed explicitly in a recursive way. By (3.16) and (3.17), we have

$$\begin{aligned} \varepsilon\sin(\theta+u) &= \varepsilon\sin(\theta+\sum_{j=1}^{\infty}\varepsilon^j u_j(\theta)) \\ &= \varepsilon\sin\left(\theta+\sum_{j=1}^{\infty}\varepsilon^j\sum_{\ell=1}^{j}(a_{\ell j}\sin(\ell\theta_n)+b_{\ell j}\cos(\ell\theta_n))\right) \\ &\equiv \sum_{j=1}^{\infty}\varepsilon^j\Big[\sum_{\ell=1}^{j}(S_{\ell j}\sin(\ell\theta_n)+C_{\ell j}\cos(\ell\theta_n))+D_j\Big] \ , \end{aligned} \tag{3.21}$$

where we impose the last equality. Let us define the complex functions $d_k = d_k(\theta_n)$ such that

$$e^{i(\theta_n+u(\theta_n))} = \sum_{k=0}^{\infty} d_k(\theta_n)\varepsilon^k \ . \tag{3.22}$$

Differentiating (3.22) with respect to ε, we obtain

$$i\ \sum_{j=1}^{\infty} d_j(\theta_n)\varepsilon^j\ \sum_{\ell=1}^{\infty}\ell u_\ell\varepsilon^{\ell-1} = \sum_{k=1}^{\infty} k d_k(\theta_n)\varepsilon^{k-1} \ .$$

Equating same powers of ε, we obtain the recursive relations defining d_k in terms of u_1, ..., u_k, d_0,..., d_{k-1}:

$$\begin{aligned} d_0(\theta_n) &= e^{i\theta_n} \\ d_k(\theta_n) &= \frac{i}{k}\sum_{j=1}^{k} j u_j(\theta_n) d_{k-j}(\theta_n) \ . \end{aligned}$$

Denoting by $\bar{d}$ the complex conjugate of d, we can easily show by induction that the function $(d_k(\theta_n) - \bar{d}_k(\theta_n))/(2i)$ can be expressed in the form

$$\frac{d_k(\theta_n) - \bar{d}_k(\theta_n)}{2i} = \sum_{\ell=1}^{k+1} (A_{\ell k} \sin(\ell\theta_n) + B_{\ell k} \cos(\ell\theta_n)) + E_k \ , \qquad k \geq 0 \tag{3.23}$$

for suitable $A_{\ell k}$, $B_{\ell k}$ $(\ell = 1, ..., k+1)$ and E_k. For $k = 0$ we obtain that

$$\frac{d_0(\theta_n) - \bar{d}_0(\theta_n)}{2i} = \sin\theta_n \ .$$

Assuming that (3.23) holds for $k-1$, we have

$$\begin{aligned} \frac{d_k(\theta_n) - \bar{d}_k(\theta_n)}{2i} &= \frac{i}{k} \sum_{j=1}^{k} j u_j(\theta_n) \Big[\frac{d_{k-j}(\theta_n) - \bar{d}_{k-j}(\theta_n)}{2i} \Big] \\ &= \frac{i}{k} \sum_{j=1}^{k} j \sum_{\ell=1}^{j} (a_{\ell j} \sin(\ell\theta_n) + b_{\ell j} \cos(\ell\theta_n)) \\ &\quad \Big\{ \sum_{\ell=1}^{k-j+1} \Big[A_{\ell,k-j} \sin(\ell\theta_n) + B_{\ell,k-j} \cos(\ell\theta_n) \Big] \\ &\quad + E_{k-j} \Big\} \ , \end{aligned} \tag{3.24}$$

which is of the form (3.23) for suitable coefficients $A_{\ell k}$, $B_{\ell k}$, E_k, depending on $a_{\ell j}$, $b_{\ell j}$ for $j = 1, ..., k$, $\ell = 1, ..., j$. Notice that (3.24) provides a recursive formula for computing $A_{\ell k}$, $B_{\ell k}$, E_k. Recalling the first and the last term in (3.21) and equating same powers of ε, we get

$$\frac{1}{2i} \big(d_{j-1}(\theta_n) - \bar{d}_{j-1}(\theta_n) \big) = \sum_{\ell=1}^{j} (S_{\ell j} \sin(\ell\theta_n) + C_{\ell j} \cos(\ell\theta_n)) + D_j \ ,$$

for $j \geq 1$, where $S_{\ell j} \equiv A_{\ell,j-1}$, $C_{\ell j} \equiv B_{\ell,j-1}$, $D_j \equiv E_{j-1}$ (namely $S_{\ell j}^{(p,q)}$, $C_{\ell j}^{(p,q)}$ are functions depending on $a_{\ell i}$, $b_{\ell i}$ for $i = 1, \cdots, j-1$) $\Box$

Finding the solution $u(\theta_n)$ of the parametric equation (3.14) is equivalent to solve the main equation (3.19). In concrete computations, where $S_{\ell j}^{(p,q)}$, $C_{\ell j}^{(p,q)}$, $D_j^{(p,q)}$ are determined explicitly, we equate same orders of ε, so to obtain some equations which allow us to determine the unknowns $a_{\ell j}$, $b_{\ell j}$ and γ_j.

Remark 3.2. *For the specific case of the standard map* (3.11)*, containing just one harmonic, the following properties hold:*

i) in (3.21) *the index* ℓ *runs from* 0 *to* j*; therefore, the unknowns* $a_{\ell j}$ *and* $b_{\ell j}$ *are zero for all* $\ell > j$*;*

ii) for j *even, only* ℓ *even appears in* (3.21)*; therefore, if* j *is even, all* $a_{\ell j}$*'s and* $b_{\ell j}$*'s are zero for* ℓ *odd;*

iii) similarly, if j *is odd, all* $a_{\ell j}$*'s and* $b_{\ell j}$*'s are zero for* ℓ *even.*

In order to solve (3.19) we proceed as follows. Equating same orders of ε in (3.19), we obtain three different cases according to whether j is less, equal or greater than q. We start by considering $j < q$; then, for all $\ell = 1, ..., j$, we get the following linear system in the unknowns $a_{\ell j}$, $b_{\ell j}$ and γ_j:

$$\begin{cases} (1+b)\alpha_\ell^{(p,q)} a_{\ell j} - (1-b)\beta_\ell^{(p,q)} b_{\ell j} = S_{\ell j}^{(p,q)} \ , \\ (1-b)\beta_\ell^{(p,q)} a_{\ell j} + (1+b)\alpha_\ell^{(p,q)} b_{\ell j} = C_{\ell j}^{(p,q)} \ , \\ \gamma_j = D_j^{(p,q)} \qquad\qquad \text{for} \quad j \quad \text{even} \ , \\ \gamma_j = 0 \qquad\qquad\qquad \text{for} \quad j \quad \text{odd} \ . \end{cases} \tag{3.25}$$

We remark that $S_{\ell j}^{(p,q)}$, $C_{\ell j}^{(p,q)}$ and $D_j^{(p,q)}$ depend on the $a_{\ell i}$, $b_{\ell i}$ for $i = 1, \cdots, j-1$, so that they are known whenever the functions u_i at the previous orders are known. The solution of (3.25) provides the unknowns $a_{\ell j}$, $b_{\ell j}$ and γ_j for $\ell = 1, \cdots, j$ and $j = 1, \cdots, q-1$.

We are now able to determine the function $u(\theta_n)$ and the quantity γ up to the order $q-1$ of their Taylor expansions. Let us denote by $u^{(q-1)}(\theta_n)$ and $\gamma^{(q-1)}$ the truncations to the order $q-1$ of the ε-expansions of $u(\theta_n)$ and γ, namely

$$u^{(q-1)}(\theta_n) = \sum_{j=1}^{q-1} u_j(\theta_n)\varepsilon^j \ , \qquad \gamma^{(q-1)} \equiv \sum_{j=1}^{q-1} \gamma_j \varepsilon^j \ ,$$

where the functions $u_j(\theta_n)$ are given as in (3.17). From the expansion of γ, we compute the expansion of the drift as

$$c^{(q-1)} \equiv \sum_{j=0}^{q-1} c_j \varepsilon^j \ ,$$

where we recall that the relation between c and γ is given by the equation (3.13) and therefore $c_0 = (1-b)\omega$ and $c_j = -\gamma_j$.

When we equate terms of the same order $j = q$, we see that the coefficients $\alpha_q^{(p,q)}$ and $\beta_q^{(p,q)}$ are equal to zero, being

$$\begin{aligned} \alpha_q^{(p,q)} &= \cos(2\pi q \cdot \tfrac{p}{q}) - 1 = 0 \\ \beta_q^{(p,q)} &= \sin(2\pi q \cdot \tfrac{p}{q}) = 0 \ . \end{aligned} \tag{3.26}$$

As a consequence, the unknowns a_{qq} and b_{qq} disappear from the left hand side of equation (3.19) and they cannot be determined. Therefore, the Taylor coefficient $u_q(\theta_n)$ remains undetermined. On the other hand, using (3.26), the order q of the right hand side of (3.19) is not zero, so that such equation holds provided

$$\gamma_q = S_{qq}^{(p,q)} \sin(q\theta_n) + C_{qq}^{(p,q)} \cos(q\theta_n) + D_q^{(p,q)} \ . \tag{3.27}$$

The consequence of the previous equation is very important since it shows that γ_q depends on θ_0, namely $\gamma_q = \gamma_q(\theta_0)$ (we recall that the relation between θ_n and θ_0 is given by $\theta_n = \theta_0 + 2\pi np/q$); in particular, being $\gamma_q(\theta_0)$ a bounded periodic function, for θ_0 varying in $[0, 2\pi)$, the quantity γ_q varies within an interval of the form $[\gamma_-, \gamma_+]$ for some endpoints $\gamma_-, \gamma_+ \in \mathbb{R}$.

For $j > q$ all the u_j's and γ_j's remain undetermined, since they depend on $u_q(\theta_n)$ which is undetermined.

Up to now we have obtained the following result: the solution $u(\theta_n)$ associated to a periodic orbit of frequency $2\pi p/q$ is given up to the order $q-1$, and the orders equal or greater than q remain undetermined; as we have stressed in Remark 3.1 in Section 3.3, the problem can not be avoided because, in the dissipative case, the Fourier coefficients a_{qq} and b_{qq} contribute both to the general solution u. Regarding the drift, the existence of the periodic orbit is ensured whenever γ_q belongs to the interval $[\gamma_-, \gamma_+]$. In particular, we can write the expansion of the drift c up to the order q as

$$c^{(q)} \equiv c^{(q)}(\theta_n) = c_0 + \varepsilon c_1 + \varepsilon^2 c_2 + \cdots + \varepsilon^{q-1} c_{q-1} + \varepsilon^q c_q(\theta_n) \ , \qquad (3.28)$$

where $c_0, \ldots, c_{q-1}$ are constants (depending on $\bar{b}$, p, q), while $c_q = c_q(\theta_n)$ belongs to an interval $\tilde{\mathcal{I}}_{pq} \equiv [c_-^{(p,q)}, c_+^{(p,q)}]$ whose endpoints are given by the minimum and the maximum of the function (3.27) (depending on $\bar{b}$, p, q too). In order to make this computation explicit, we provide in the next Section, the determination of the parametric representation for the specific case $p = 1$, $q = 3$.

Remark 3.3. *In Section 3.5 we will deal with quasi–periodic attractors with an irrational frequency ω and we will see that in the parametric representation, the difference with the periodic case relies on the fact that the series expansions* (3.16)*,* (3.17)*,* (3.18) *can be computed recursively at any order; concerning the drift, the quantities γ_j (equivalently c_j) are always constants and they are identically zero at odd orders.*

3.4.2. The parametric representation of the $2\pi/3$–periodic orbit. In this Section we show a concrete example for the parametric representation of the periodic orbit with frequency $2\pi/3$. We start by writing the Taylor expansion of the term $\varepsilon \sin(\theta_n + u(\theta_n))$ up to the order $q = 3$ with $u(\theta_n)$ as in (3.16):

$$\begin{aligned} \varepsilon \quad & \sin(\theta_n + \sum_{j=1}^{2} \varepsilon^j u_j(\theta_n)) \\ = \quad & \varepsilon \sin\theta_n + \varepsilon^2 u_1 \cos\theta_n + \varepsilon^3 \big(u_2 \cos\theta_n - \frac{1}{2}(u_1)^2 \sin\theta_n\big) \ . \end{aligned} \qquad (3.29)$$

Let

$$\begin{aligned} \alpha_\ell^{(1,3)} &\equiv \alpha_\ell = \cos(2\pi\ell \cdot \tfrac{1}{3}) - 1 \\ \beta_\ell^{(1,3)} &\equiv \beta_\ell = \sin(2\pi\ell \cdot \tfrac{1}{3}) \ . \end{aligned} \tag{3.30}$$

Then, we equate same orders of ε in equation (3.19), taking into account the expansion (3.29). For $j = 1$ we have:

$$\begin{aligned} \sin\theta_n & \quad \Big[\alpha_1(1+b)a_{11} - \beta_1(1-b)b_{11}\Big] \\ + & \quad \cos\theta_n \Big[\beta_1(1-b)a_{11} + \alpha_1(1+b)b_{11}\Big] + \gamma_j = \sin\theta_n \ , \end{aligned}$$

which is equivalent to the following linear system in the unknowns a_{11}, b_{11} and γ_1:

$$\begin{cases} \alpha_1(1+b)a_{11} - \beta_1(1-b)b_{11} = 1 \\ \beta_1(1-b)a_{11} + \alpha_1(1+b)b_{11} = 0 \\ \gamma_1 = 0 \ . \end{cases}$$

As we have seen in Remark 3.2, we stress that the coefficients $a_{\ell 1}$ and $b_{\ell 1}$ are zero for $\ell > 1$. The first two equations of the previous system allow us to determine the two unknowns a_{11} and b_{11}. Recalling (3.30), we get:

$$\begin{cases} a_{11} = -\frac{1+b}{2(1+b+b^2)} \\ b_{11} = -\frac{1-b}{2\sqrt{3}(1+b+b^2)} \ . \end{cases} \tag{3.31}$$

The function u_1 is therefore determined as $u_1(\theta_n) = a_{11}\sin\theta_n + b_{11}\cos\theta_n$ with $\gamma_1 = 0$.

Let us continue with the computation of the solution of (3.19) to the second order. Using the above expression for $u_1(\theta_n)$ and taking the second order in ε of equation (3.19), we get the expression:

$$\begin{aligned} \sin 2\theta_n & \quad \Big[\alpha_2(1+b)a_{22} - \beta_2(1-b)b_{22}\Big] \\ + & \quad \cos 2\theta_n \Big[\beta_2(1-b)a_{22} + \alpha_2(1+b)b_{22}\Big] + \gamma_2 \\ = & \quad \frac{1}{2}a_{11}\sin 2\theta_n + \frac{1}{2}b_{11}\cos 2\theta_n + \frac{1}{2}b_{11} \ , \end{aligned}$$

from which we obtain the following linear system in the unknowns a_{22}, b_{22} and γ_2:

$$\begin{cases} \alpha_2(1+b)a_{22} - \beta_2(1-b)b_{22} = \frac{1}{2}a_{11} \\ \beta_2(1-b)a_{22} + \alpha_2(1+b)b_{22} = \frac{1}{2}b_{11} \\ \gamma_2 = \frac{1}{2}b_{11} \ . \end{cases}$$

From (3.30) we have $\alpha_2 = -\frac{3}{2}$, $\beta_2 = -\frac{\sqrt{3}}{2}$, so that we determine a_{22}, b_{22}, γ_2 as

$$\begin{cases} a_{22} = -\frac{1}{6(1+b+b^2)} \\ b_{22} = 0 \\ \gamma_2 = -\frac{1-b}{4\sqrt{3}(1+b+b^2)} \ . \end{cases} \tag{3.32}$$

Since the coefficients $a_{\ell 2}$ and $b_{\ell 2}$ are zero for $\ell = 1$ and $\ell > 2$ (see Remark 3.2), the function u_2 is given by $u_2 = a_{22}\sin 2\theta_n$.

Let us conclude with the computation of the third order, which corresponds to the case $j = q$. Considering the third order of (3.29) and inserting the known functions u_1 and u_2, we get a linear combination of sines and cosines with known coefficients. Taking the third order in ε of equation (3.19), we get the following expression:

$$\begin{aligned} \sin\theta_n \quad & \Big[\alpha_1(1+b)a_{13} - \beta_1(1-b)b_{13}\Big] \\ + \quad & \cos\theta_n\Big[\beta_1(1-b)a_{13} + \alpha_1(1+b)b_{13}\Big] \\ + \quad & \sin 3\theta_n\Big[\alpha_3(1+b)a_{33} - \beta_3(1-b)b_{33}\Big] \\ + \quad & \cos 3\theta_n\Big[\beta_3(1-b)a_{33} + \alpha_3(1+b)b_{33}\Big] + \gamma_3 \\ = \quad & \sin\theta_n\Big[\frac{1}{2}a_{22} - \frac{3}{8}a_{11}^2 - \frac{1}{8}b_{11}^2\Big] + \cos\theta_n\Big[-\frac{1}{4}a_{11}b_{11}\Big] \\ + \quad & \sin 3\theta_n\Big[\frac{1}{2}a_{22} + \frac{1}{8}a_{11}^2 - \frac{1}{8}b_{11}^2\Big] + \cos 3\theta_n\Big[\frac{1}{4}a_{11}b_{11}\Big] \ . \end{aligned} \tag{3.33}$$

First we note that the coefficients α_3 and β_3 are zero; therefore in the left hand side of (3.33) the coefficients of $\sin 3\theta_n$ and $\cos 3\theta_n$ are zero. As a consequence, the unknowns a_{33} and b_{33} disappear from the previous equation and they cannot be determined. Equating the coefficients of

$\sin\theta_n$, $\cos\theta_n$, we determine a_{13}, b_{13}. Moreover, equation (3.33) holds provided

$$\gamma_3 = S_{33}^{(1,3)} \sin(3\theta_n) + C_{33}^{(1,3)} \cos(3\theta_n) \ ,$$

with

$$S_{33}^{(1,3)} = \frac{1}{2}a_{22} + \frac{1}{8}a_{11}^2 - \frac{1}{8}b_{11}^2 \ , \quad C_{33}^{(1,3)} = \frac{1}{4}a_{11}b_{11} \ .$$

so that we have an expression of γ_3 as a function of θ_n (namely θ_0).

In conclusion, the truncation of the function $u(\theta_n)$ up to the second order is given by

$$u^{(2)}(\theta_n) = \varepsilon(a_{11}\sin\theta_n + b_{11}\cos\theta_n) + \varepsilon^2 a_{22}\sin 2\theta_n$$

with a_{11}, b_{11}, a_{22} as in (3.31), (3.32). The approximation to the third order in ε of the drift is given by

$$c^{(3)} = c_0 + \varepsilon^2 c_2 + \varepsilon^3 c_3 \ ,$$

where c_0, c_2, c_3 take the expressions

$$\begin{aligned} c_0 \quad &= 2\pi\frac{1}{3}(1-b) \ , \qquad c_2 = \frac{1-b}{4\sqrt{3}(1+b+b^2)} \ , \\ c_3(\theta_n) \quad &= -(S_{33}^{(1,3)}\sin 3\theta_n + C_{33}^{(1,3)}\cos 3\theta_n) \ . \end{aligned}$$

The term c_3 varies within the interval $[c_-, c_+]$ with endpoints given by the minimum and the maximum of c_3 as θ_n varies in $[0, 2\pi)$; therefore, the whole drift $c^{(3)}$ belongs to an interval, say $\mathcal{I}_{13}$, in which the existence of the periodic orbit of period 3 is ensured.

We provide a concrete example of the interval $\mathcal{I}_{13}$ that varies as the parameters b and ε vary. For example, we fix $b = 0.5$, $\varepsilon = 0.5$; then, the drift parameter c can vary within the interval $\mathcal{I}_{13} = (1.04872, 1.06629)$. In Figure 3.2 we consider four different values of c within and outside $\mathcal{I}_{13}$. Figures 3.2a, 3.2d show that outside the interval, the parameterization does not correspond to a periodic orbit, while a periodic orbit of period 3 is found in the interval $\mathcal{I}_{13}$ as shown in Figures 3.2b, 3.2c.

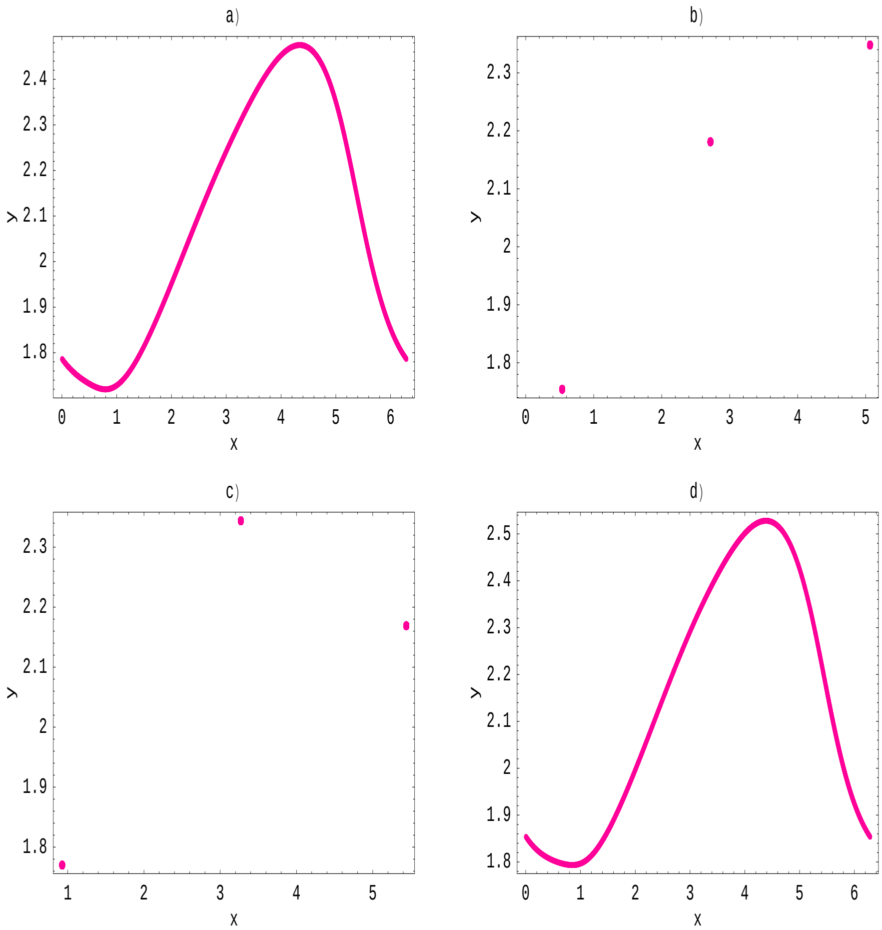

FIGURE 3.2. The evolution of the parametric representation of the $2\pi/3$–periodic orbit has been computed for $b = 0.5$ and $\varepsilon = 0.5$; the figures show four different orbits for different values of the drift c: a) $c = 1.04$, b) $c = 1.05$, c) $c = 1.06$, d) $c = 1.07$.

3.4.3. An implementation of the Implicit Function Theorem. As written before, the existence of periodic orbits for the mapping (3.11) can be obtained analytically by implementing the Implicit

Function Theorem in the following way. Let us define the vector function $\underline{F} = (F_1, F_2)$ as:

$$\underline{F}(x_0, y_0; b, \varepsilon, c) = M^q(x_0, y_0; b, \varepsilon, c) - (x_0, y_0) - (2\pi p, 0) \ , \qquad (3.34)$$

where (x_0, y_0) are the initial conditions and M^q is the q^{th} iteration of the mapping (3.11). Then, the following theorem holds:

THEOREM 3.4. *(Implicit Function Theorem) Let* $\underline{z} = (x, y)$ *and for some* $\overline{b}$, $\overline{\varepsilon}$, $\overline{c} > 0$ *introduce the parameters* $\rho_{\overline{b}}$, $\rho_{\overline{\varepsilon}}$, $\rho_{\overline{c}}$, $\rho_{\underline{z}_0} \in \mathbb{R}_+$*; define the domains* $\mathcal{D} = \Big\{(b, \varepsilon, c) \in \mathbb{R}^3 : \ |b - \overline{b}| < \rho_{\overline{b}}, \ |\varepsilon - \overline{\varepsilon}| < \rho_{\overline{\varepsilon}}, \ |c - \overline{c}| < \rho_{\overline{c}}\Big\}$, $\mathcal{B} \equiv \{\underline{z} \in \mathbb{R}^2 : \ |\underline{z} - \underline{z}_0| < \rho_{\underline{z}_0}\}$. *Let us consider the function* $\underline{F} : (\underline{z}, b, \varepsilon, c) \in \mathcal{B} \times \mathcal{D} \to \underline{F}(\underline{z}; b, \varepsilon, c) \in \mathbb{R}^2$ *defined as in* (3.34)*. Having fixed the initial condition* $\underline{z}_0 = (x_0, y_0)$*, assume that*

$$\underline{F}(\underline{z}_0; \overline{b}, \overline{\varepsilon}, \overline{c}) = \underline{0}$$

and that

$$\det \left(\frac{\partial \underline{F}}{\partial \underline{z}}\right)_{|_{(\underline{z}_0, \overline{b}, \overline{\varepsilon}, \overline{c})}} \neq 0 \ .$$

If $\rho_{\underline{z}_0}$, $\rho_{\overline{b}}$, $\rho_{\overline{\varepsilon}}$, $\rho_{\overline{c}} \in \mathbb{R}_+$ *satisfy a smallness condition, defined by some function* C *of the form*

$$C = C(\rho_{\underline{z}_0}, \rho_{\overline{b}}, \rho_{\overline{\varepsilon}}, \rho_{\overline{c}}) < 1 \ , \qquad (3.35)$$

then there exists a unique, continuous vector function $\underline{f} = \underline{f}(b, \varepsilon, c)$*, such that* $\underline{f}(\overline{b}, \overline{\varepsilon}, \overline{c}) = \underline{z}_0$ *and* $\underline{F}(\underline{f}(b, \varepsilon, c); b, \varepsilon, c) = \underline{0}$ *for any* $(b, \varepsilon, c) \in \mathcal{D}$*.*

We want to provide an explicit expression for condition (3.35) and we do it by writing the function $\underline{F} \equiv (F_1, F_2)$ in (3.34) in an explicit form as

$$\begin{cases} F_1(x_0, y_0) = y_0(b^q - 1) + \sum_{j=0}^{q-1} b^j c + \varepsilon \sum_{j=0}^{q-1} b^{q-1-j} \sin x_j \\ F_2(x_0, y_0) = \sum_{j=1}^{q} y_j - 2\pi p \ , \end{cases} \tag{3.36}$$

where x_j and y_j can be recursively written as a function of the initial conditions (x_0, y_0):

$$\begin{cases} y_j(x_0, y_0) = b^j y_0 + \sum_{k=0}^{j-1} b^k c + \varepsilon \sum_{k=0}^{j-1} b^{j-1-k} \sin x_k \\ x_j(x_0, y_0) = x_0 + \sum_{k=1}^{j} y_k \ . \end{cases} \tag{3.37}$$

If the function $\underline{F}(x_0, y_0; b, \varepsilon, c) = \underline{0}$, then the point (x_0, y_0) belongs to a periodic orbit of frequency $2\pi p/q$ for some b, ε, c. Let us fix the parameters as $b = \bar{b}$, $\varepsilon = \bar{\varepsilon}$, $c = \bar{c}$ for some $\bar{b}$, $\bar{\varepsilon}$, $\bar{c} > 0$; through an implementation of the implicit function theorem we can to determine a neighborhood of the parameters $\bar{b}$, $\bar{\varepsilon}$, $\bar{c}$ in which there exists a periodic orbit of frequency $2\pi p/q$ with initial conditions in a neighborhood of (x_0, y_0).

Let $\underline{z} \equiv (x_0, y_0)$; we immediately remark that for $\varepsilon = 0$ the Jacobian associated to (3.36) is zero, being

$$\Big(\frac{\partial \underline{F}}{\partial \underline{z}}(\underline{z}_0)\Big) = \begin{pmatrix} b^q - 1 & 0 \\ \sum_{j=1}^{q} b^j & 0 \end{pmatrix} \ .$$

For this reason we need to consider a value of ε different from zero and then we compute the Jacobian matrix as follows. Let

$$\Big(\frac{\partial \underline{F}}{\partial \underline{z}}(\underline{z}_0; b, \varepsilon, c)\Big) = \begin{pmatrix} \alpha & \beta \\ \gamma & \delta \end{pmatrix} \ ,$$

where α, β, γ, δ depend on b, ε, c, and they can be written as follows:

$$\begin{cases} \alpha = \dfrac{\partial F_1}{\partial y_0}(x_0, y_0; b, \varepsilon, c) = b^q - 1 + \varepsilon \displaystyle\sum_{j=1}^{q-1} b^{q-1-j} \cos x_j \frac{\partial x_j}{\partial y_0} \\ \beta = \dfrac{\partial F_1}{\partial x_0}(x_0, y_0; b, \varepsilon, c) = \varepsilon \displaystyle\sum_{j=0}^{q-1} b^{q-1-j} \cos x_j \frac{\partial x_j}{\partial x_0} \\ \gamma = \dfrac{\partial F_2}{\partial y_0}(x_0, y_0; b, \varepsilon, c) = \displaystyle\sum_{j=1}^{q} \frac{\partial y_j}{\partial y_0} = \frac{\partial x_q}{\partial y_0} \\ \delta = \dfrac{\partial F_2}{\partial x_0}(x_0, y_0; b, \varepsilon, c) = \displaystyle\sum_{j=1}^{q} \frac{\partial y_j}{\partial x_0} \ , \end{cases}$$

with x_j, y_j defined in (3.37). Let us introduce the positive parameters $\rho_{\underline{z}_0}$, $\rho_{\overline{b}}$, $\rho_{\overline{\varepsilon}}$, $\rho_{\overline{c}}$; consider the domains $\mathcal{D}$ and $\mathcal{B}$ defined in Theorem 3.4. According to [**13**], the values $\rho_{\underline{z}_0}$, $\rho_{\overline{b}}$, $\rho_{\overline{\varepsilon}}$, $\rho_{\overline{c}}$ must satisfy the following condition:

$$C = 4m^2 \cdot \|\underline{F}(\underline{z}_0; b, \varepsilon, c)\| \cdot \left\| \frac{\partial^2 \underline{F}}{\partial \underline{z}^2} \right\| < 1 \ , \tag{3.38}$$

where m is the norm of the inverse of the Jacobian matrix, which can be written as

$$m = \left| \left(\frac{\partial \underline{F}}{\partial \underline{z}}(\underline{z}_0; b, \varepsilon, c) \right)^{-1} \right| = \sup_{(b,\varepsilon,c)\in\mathcal{D}} \left| \frac{1}{\alpha\delta - \beta\gamma} \right| \cdot \sup_{(b,\varepsilon,c)\in\mathcal{D}} (|\beta| + |\delta|, |\alpha| + |\gamma|) \ . \tag{3.39}$$

We remark that the norm of the function $\underline{F}$ can be evaluated as

$$\|\underline{F}\| = \sup_{(b,\varepsilon,c)\in\mathcal{D}} (|F_1|, |F_2|) \ , \tag{3.40}$$

and finally the norm of the second derivatives of $\underline{F}$ can be defined as

$$\begin{aligned} \left\| \frac{\partial^2 \underline{F}}{\partial \underline{z}^2} \right\| \ &= \sup_{\{\underline{z}\in\mathcal{B},\ (b,\varepsilon,c)\in\mathcal{D}\}} \left(\left\| \frac{\partial^2 F_1}{\partial y^2} \right\| + \left\| \frac{\partial^2 F_1}{\partial x^2} \right\| + 2 \left\| \frac{\partial^2 F_1}{\partial y \partial x} \right\|, \right. \\ &\left. \left\| \frac{\partial^2 F_2}{\partial y^2} \right\| + \left\| \frac{\partial^2 F_2}{\partial x^2} \right\| + 2 \left\| \frac{\partial^2 F_2}{\partial y \partial x} \right\| \right) \ . \end{aligned} \tag{3.41}$$

If we put together (3.39), (3.40), (3.41) we can explicitly evaluate (3.38), which is indeed of the form (3.35).

If we fix $\rho_{\underline{z}_0}$, $\rho_{\overline{b}}$, $\rho_{\overline{\varepsilon}}$, then the condition (3.35) depends only on $\rho_{\overline{c}}$, say

$$C = C(\rho_{\overline{c}}) < 1 \ . \tag{3.42}$$

If we solve the inequality (3.42), considering the explicit form given above, we find that the parameter c is again constrained to an interval in agreement with what was found using the parametric representation. The size of this interval depends on the values of $\rho_{\underline{z}_0}$, $\rho_{\overline{b}}$, $\rho_{\overline{\varepsilon}}$: if such values increase, then $\rho_{\overline{c}}$ decreases and if they overcome a critical value, then the inequality (3.42) has no solution. In Table 1, we report a comparison of the size of the intervals of c found numerically, denoted by Δc^{Num}, with those found through an implementation of the Implicit Function Theorem, denoted by Δc^{IFT}. We focus on orbits of frequency $2\pi/3$, having fixed the values of the parameters b, ε, ρ, where $\rho = \max(\rho_{\underline{z}_0}, \rho_{\overline{b}}, \rho_{\overline{\varepsilon}})$. Moreover, we take the initial conditions using the first–order parameterization: we can set $x_0 = \theta_0 + \varepsilon u_1(\theta_0)$, $y_0 = \omega + \varepsilon u_1(\theta_0) - \varepsilon u_1(\theta_0 - \omega)$, where, in principle, θ_0 can be arbitrarily chosen. An optimal choice for θ_0 can be taken as one of the solutions corresponding to the average value of c within the interval for which the periodic orbit exists. To be sure that the initial datum belongs to the periodic orbit, we perform a sufficient number of iterations to reach the attractor; we also check that such initial condition is well inside the basin of attraction of the periodic orbit.

From Table 1, we can note that the size of the interval Δc^{IFT} is always consistently less than the size of the interval Δc^{Num}. Moreover, if we compare the three values for $b = 0.5$ and $\varepsilon = 0.8$ we can see how the size Δc^{IFT} decreases whenever ρ increases. Table 1 shows that in general the agreement between the analytical and numerical values is quite good; closer values could be obtained through a more refined version of the Implicit Function Theorem.

b	ε	ρ	Δc^{IFT}	Δc^{Num}
0.5	0.5	10^{-3}	$2.89 \cdot 10^{-3}$	$1.71 \cdot 10^{-2}$
0.5	0.8	10^{-4}	$6.18 \cdot 10^{-2}$	$6.74 \cdot 10^{-2}$
0.5	0.8	10^{-3}	$6.15 \cdot 10^{-2}$	$6.74 \cdot 10^{-2}$
0.5	0.8	10^{-2}	$3.54 \cdot 10^{-2}$	$6.74 \cdot 10^{-2}$
0.8	0.5	10^{-3}	$1.10 \cdot 10^{-3}$	$1.25 \cdot 10^{-2}$
0.8	0.8	10^{-3}	$3.06 \cdot 10^{-2}$	$4.83 \cdot 10^{-2}$

TABLE 1. Comparison between the amplitudes of the intervals of c found numerically (Δc^{Num}) and by an implementation of the implicit function theorem (Δc^{IFT}) for orbits of frequency $2\pi/3$.

3.5. Invariant attractors by a Newton's method.

The aim of the parameterization of periodic orbits is to find the link between periodic orbits and invariant attractors. In fact, the parametric representation allow us to relate the solutions of periodic and quasi–periodic attractors.

To this end, in this Section, we want to find a solution of the parametric equation (3.14) for an invariant attractor with irrational diophantine frequency $\omega \in \mathbb{R}$. We recall that an irrational number ω is called *diophantine* if it satisfies the diophantine condition, i.e. it is such that $|\frac{\omega}{2\pi}n + m|^{-1} \leq C|n|^\tau$, for any $n \in \mathbb{Z}_+$, $m \in \mathbb{Z}$ and for some positive constants C, τ with $\tau \geq 1$. Let us define the operators D_1 and D_b as

$$D_1 u(\theta_n) \equiv u(\theta_n + \frac{\omega}{2}) - u(\theta_n - \frac{\omega}{2}) \, , \qquad D_b u(\theta_n) \equiv u(\theta_n + \frac{\omega}{2}) - b u(\theta_n - \frac{\omega}{2})$$

and let $\Delta_b \equiv D_b D_1 = D_1 D_b$. Then, equation (3.14) can be written as

$$\Delta_b u(\theta_n) - \varepsilon \sin(\theta_n + u(\theta_n)) + \gamma = 0 \, . \tag{3.43}$$

The solution of (3.43) can be found provided the constant γ satisfies

$$\gamma = -\langle u_\theta \Delta_b u \rangle \ , \tag{3.44}$$

where $u_\theta \equiv \frac{\partial u(\theta)}{\partial \theta}$ and $\langle \cdot \rangle$ denotes the average over $\theta_n \in \mathbb{T}$. In fact, if we multiply (3.43) by $1 + u_\theta$, we compute the average over $\theta_n \in \mathbb{T}$ and if we take into account that $\langle u_\theta \rangle = 0$, $\langle \Delta_b u \rangle = 0$ and that $\langle (1 + u_\theta) \sin(\theta_n + u) \rangle = 0$, we obtain (3.44)

As in Section 3.4.1, we expand the function u and the quantity γ in Taylor series around $\varepsilon = 0$ as in (3.16) and (3.18); then we insert these expansions in (3.43)–(3.44) and equating same orders of ε we obtain an explicit expression for the terms u_j, γ_j. Then, by (3.14), it is easy to show that the first order term u_1 must satisfy the equation

$$u_1(\theta_n + \omega) - (1 + b)u_1(\theta_n) + bu_1(\theta_n - \omega) = \sin \theta_n \ ; \tag{3.45}$$

inserting in (3.45) the Fourier expansion of u_1 given by

$$u_1(\theta_n) = \sum_{k \in \mathbb{Z}} \hat{u}_k^{(1)} e^{ik\theta_n} \ ,$$

we obtain the Fourier coefficients

$$\hat{u}_{\pm 1}^{(1)} = \pm \frac{1}{2i(e^{\pm i\omega} - (1 + b) + be^{\mp i\omega})} \ ,$$

which provide the (real) solution

$$u_1(\theta_n) = \frac{(b - 1)\cos\theta_n \cot\frac{\omega}{2} - (b + 1)\sin\theta_n}{2(1 + b^2 - 2b\cos\omega)} \ .$$

This solution can be compared with that found in the periodic case to see that they are analogous. Through similar computations we can determine higher order terms. Notice that for $0 < b < 1$ the above function does not contain zero divisors (as it may happen in the conservative case $b = 1$), though the divisors can be arbitrarily small. By (3.44) one obtains $\gamma_1 = 0$ and it can be shown that $\gamma_{2k+1} = 0$, while $\gamma_{2k} \neq 0$ for any $k \in \mathbb{Z}_+$.

We remark that in the irrational case the Taylor–expansions of the function u and the term γ can be computed explicitly to any finite order N. Moreover, we can associate a specific value of the drift c with a rotational torus. More precisely, a quasi–periodic orbit with an irrational frequency ω there exists for a specific value of the drift, namely $c = c(\omega)$.

In order to find a better approximate solution of (3.43), one can implement a Newton's procedure starting from an approximate solution given by a finite truncation up to a given integer order N, of the power series expansions (3.16), (3.18). More precisely, we can start with an initial approximate solution of the form

$$u^{(N)}(\theta_n) = \sum_{j=1}^{N} u_j(\theta_n)\varepsilon^j \ , \qquad \gamma^{(N)} = \sum_{j=1}^{N} \gamma_j \varepsilon^j \ . \tag{3.46}$$

The functions $u^{(N)}(\theta_n)$ and $\gamma^{(N)}$ satisfy (3.43) up to an error term $e^{(N)}(\theta_n)$, namely

$$\Delta_b u^{(N)}(\theta_n) - \varepsilon \sin(\theta_n + u^{(N)}(\theta_n)) + \gamma^{(N)} = e^{(N)}(\theta_n) \ ,$$

where $e^{(N)}(\theta_n)$ is of order $O(\varepsilon^{N+1})$. Then we can implement a Newton's method as described in [**14**] adapted to the case of the standard map: we start from an initial approximate solution $(u^{(N)}(\theta_n), \gamma^{(N)})$ with associated error term $e^{(N)}$, and then we define a new solution which satisfies (3.43) with an error term quadratically smaller than $e^{(N)}(\theta_n)$. More precisely, we define the quadratic approximation as

$$u^{(2N)}(\theta_n) \equiv u^{(N)}(\theta_n) + u^{(c)}(\theta_n) \ , \qquad \gamma^{(2N)} \equiv \gamma^{(N)} + \gamma^{(c)} \ , \tag{3.47}$$

where the corrections $u^{(c)}(\theta_n)$ and $\gamma^{(c)}$ are given by the following formulae (see [**14**] for complete details) after having introduced the following auxiliary quantities

$$\begin{aligned}
V &\equiv 1+\frac{\partial u^{(N)}}{\partial\theta}\ , \qquad\qquad W\equiv V(\theta_n+\frac{\omega}{2})V(\theta_n-\frac{\omega}{2})\ ,\\
E &\equiv Ve^{(N)}\ , \qquad\qquad \bar{E}\equiv\langle E\rangle\ , \qquad\qquad \tilde{E}\equiv E-\bar{E}\ ,\\
a &\equiv \frac{\langle W^{-1}D_b^{-1}\tilde{E}\rangle-\bar{E}\langle W^{-1}D_b^{-1}u_\theta^{(N)}\rangle}{\langle W^{-1}\rangle-(b-1)\langle W^{-1}D_b^{-1}u_\theta^{(N)}\rangle}\ ,\\
E_1 &\equiv D_b^{-1}\tilde{E}+a(-1+(b-1)D_b^{-1}u_\theta^{(N)})-\bar{E}D_b^{-1}u_\theta^{(N)}\ ,\\
\hat{w} &\equiv -VD_1^{-1}(W^{-1}E_1)\ ;
\end{aligned}\tag{3.48}$$

then, the corrections introduced in (3.47) are given by:

$$u^{(c)}\equiv\hat{w}-V\langle\hat{w}\rangle\ , \qquad\qquad \gamma^{(c)}\equiv\gamma^{(N)}-\bar{E}+(b-1)a\ .$$

In this way, a solution provided by the implementation of the formulae (3.48) is such that the associated error term is of order ε^{2N}; therefore, larger is N, closer is the approximation to the real solution. As an example, we compute the explicit solution (3.46) up to $N=7$ and then we implement the formulae (3.48) to determine $u^{(14)}$. Let $\tilde{u}^{(k)}$ denote the truncation of the ε–expansion of $u^{(14)}$ to the order k. An approximate solution $(\tilde{x},\tilde{y})$ of the invariant attractor with frequency ω is given by the following expression:

$$\left\{\begin{array}{l}\tilde{x}=\theta_n+\tilde{u}^{(k)}(\theta_n)\\ \tilde{y}=\omega+\tilde{u}^{(k)}(\theta_n)-\tilde{u}^{(k)}(\theta_n-\omega)\ .\end{array}\right.\tag{3.49}$$

In order to evaluate how such approximation is good we present a concrete example provided by the invariant attractor with frequency $2\pi\omega_g$, where $\omega_g\equiv\frac{\sqrt{5}-1}{2}$ is the golden ratio.

We compute the analytical solution using equation (3.49), setting $k=14$, fixing $b=0.9$ and taking different values of the perturbing parameter, i.e. $\varepsilon=0.8,\ 0.9,\ 0.98$; each solution is obtained using a grid of 3 000 values of $\theta_n\in[0,2\pi)$. We also computed the numerical solution, iterating the mapping (3.11) starting from the initial point of the analytical approximation. Let $(x_j^{(a)}, y_j^{(a)})$ and $(x_j^{(n)}, y_j^{(n)})$, $j = 1, ..., 3000$, be, respectively, the analytical and the numerical trajectories. Figure 3.3 reports the graphs obtained computing the distance between the analytical and numerical solutions, namely the graph over 3 000 iterations of the error quantity

$$\sqrt{\frac{(x_j^{(a)} - x_j^{(n)})^2 + (y_j^{(a)} - y_j^{(n)})^2}{\frac{1}{2}[(x_j^{(n)})^2 + (y_j^{(n)})^2 + (x_j^{(a)})^2 + (y_j^{(a)})^2]}}\ , \qquad j = 1, ..., 3000\ . \quad (3.50)$$

The agreement between the two approximations is good as far as ε is small; when the perturbing parameter increases, the graphs show a larger discrepancy between the analytical and numerical approximations, until the breakdown threshold is reached (in this case the breakdown threshold amounts to about 0.972, see [**?**]). It is obvious that, for higher values of the perturbing parameter, a refined description requires an approximation to larger orders (and consequently a much higher computational effort).

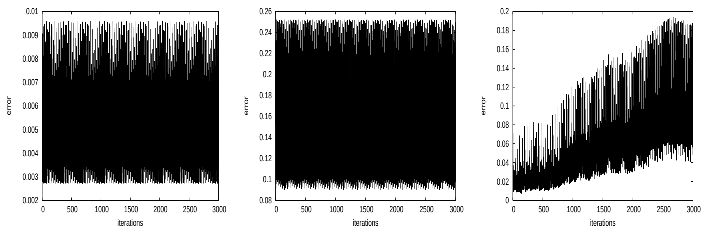

FIGURE 3.3. Graphs of the error quantity (3.50), measuring the distance between the analytical and the numerical approximation (see (3.49)) of the invariant attractor with frequency $2\pi\omega_g$ for $b = 0.9$, $k = 14$ and $a)$ $\varepsilon = 0.8$, $b)$ $\varepsilon = 0.9$, $c)$ $\varepsilon = 0.98$ (after [**15**]).

3.6. Drift convergence and Arnold's tongues

3.6.1. Arnold's tongues. The parametric representation of periodic orbits shown in Section 3.4.1 tells us that for each rational number p/q, the existence of a periodic orbit of period p/q is ensured if the drift parameter varies within an interval. By equation (3.28) it is obvious that the interval depends on the perturbing and dissipative parameters. More precisely for a given period p/q and for a fixed value of the dissipation b, the amplitude of the drift interval decreases as the perturbing parameter gets smaller. Indeed, Figure 3.4 shows the variation of the drift as a function of the perturbing parameter for three periodic orbits with frequency $2\pi \cdot 1/3$, $2\pi \cdot 1/2$, $2\pi \cdot 2/3$ and for two values of the dissipative parameter, i.e. $b = 0.5$ and $b = 0.8$ (respectively, Figure 3.4a and Figure 3.4b). If we plot the drift parameter versus the perturbing parameter we can recognize the typical structures of *Arnold's tongues* (compare with [**6**], [**59**]). Within each Arnold's tongue the periodic orbit is stable, where the stability is evaluated by computing the eigenvalues of the monodromy matrix along a full cycle of the periodic orbit. The stable periodic orbits become unstable through a saddle–node bifurcation, when approaching the boundary of the Arnold tongue.

3.6.2. Drift convergence. The parametric representation (Section 3.4.1) of the periodic orbits and the construction of quasi–periodic attractors (Section 3.5) provide many information about the relation between periodic and invariant attractors. In particular, we recall that a whole interval $\mathcal{I}_{pq}$ of the drift is associated with a periodic orbit of period p/q, while a unique constant $c = c(\omega)$ is associated with a quasi–periodic orbit of frequency ω.

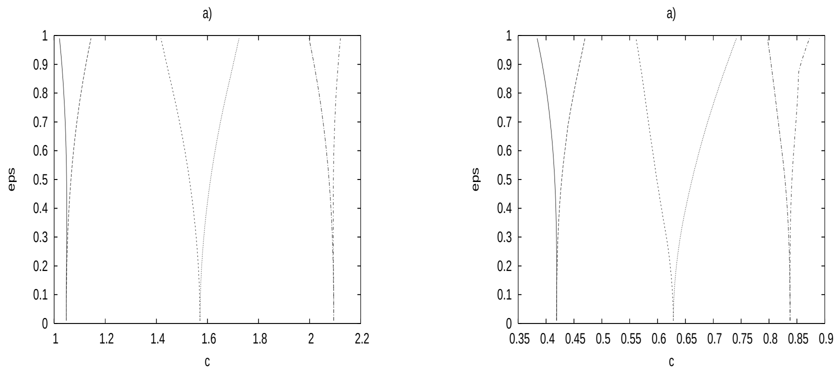

FIGURE 3.4. Arnold's tongues providing the drift c as a function of ε. Each plot shows the tongues associated to three different periodic orbits, precisely with frequencies $2\pi\cdot 1/3$ (left), $2\pi\cdot 1/2$ (center), $2\pi\cdot 2/3$ (right). a) $b = 0.5$, b) $b = 0.8$ (after [**15**]).

If we consider a sequence of rational numbers p_j/q_j converging to an irrational number ω, we have numerical evidence, corroborated by the analytical expansion, that the sequence of the intervals $\mathcal{I}_{p_j/q_j}$ tends to the constant c related to the orbit with frequency ω. Moreover, by equation (3.28), we can see that the size of the interval $\mathcal{I}_{p_j/q_j}$ decreases as q increases. In the same way we have numerical evidence that periodic orbits of period p_j/q_j tend to the quasi–periodic orbit with frequency ω. Let us show a concrete example: we explicitly determine the functions $u_j = u_j(\theta_n)$ up to the order 6. Then, we evaluate an approximation to the 6^{th} order of the expansion of the drift (see (3.18)) for the periodic orbits with frequencies $2\pi p_j/q_j$, where p_j/q_j is equal to a rational approximant to the golden number $\omega_g \equiv \frac{\sqrt{5}-1}{2}$. Let us denote by $\gamma^{(6)}_{p_j/q_j}$ and $\gamma^{(6)}_{\omega_g}$ the approximate drifts, respectively, of periodic orbits and the orbit associated to the golden frequency. Figure 3.5 provides the logarithm of the difference $|\gamma^{(6)}_{p_j/q_j} - \gamma^{(6)}_{\omega_g}|$ as j increases; the plot shows a fast convergence of the periodic drifts associated to the Fibonacci numbers p_j/q_j to that of the invariant attractor. However, this approximation to the 6^{th} order is valid only for small values of ε. For higher values of ε, we need a higher order expansion or a numerical evaluation to obtain more refined results. In Table 2 we report an average value of the drift within each interval $\mathcal{I}_{p_j/q_j}$ found through a numerical evaluation to show how the average value of the drift tends to the drift of the invariant attractor with frequency $2\pi\omega_g$.

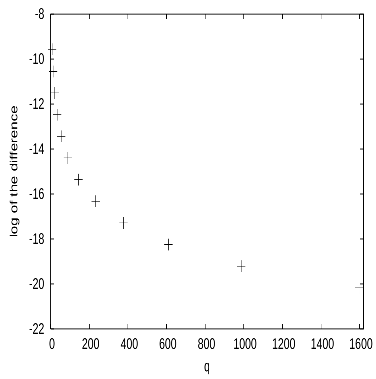

FIGURE 3.5. Plot of the logarithm of the absolute value of the difference of γ_{p_j/q_j} minus γ_{ω_g} versus q_j for $b = 0.9$, $\varepsilon = 0.5$ (after [**15**]).

p/q	c	p/q	c
1/2	0.322143	21/34	0.385862
2/3	0.421515	34/55	0.386159
3/5	0.375734	55/89	0.386046
5/8	0.390044	89/144	0.386089
8/13	0.384586	144/233	0.386072
13/21	0.386640	233/377	0.386079

TABLE 2. The drift parameter for several periodic orbits approximating the golden ratio for $b = 0.9$, $\varepsilon = 0.9$. The value of the drift for the golden ratio amounts to $c = 0.386077$.

CHAPTER 4

Some new results on the Sitnikov's problem

The problem we are going to introduce is one of the most simple applications of the three–body–problem, but not trivial; it is an example of a non–integrable dynamical system in which chaos could appear. In particular, in such problem we can find oscillatory motions, quasi–periodic and chaotic motions.

In this Chapter we derive the model in terms of the Hamiltonian formulation of the system. Then, we introduce the action–angle variables and we approximate the system by a perturbed harmonic oscillator. Through suitable transformations, we remove the perturbation to higher orders and we construct the Birkhoff normal form. Normal forms are crucial to understand the dynamical behavior on long time scales. It is possible to implement theories, like Nekhoroshev's theorem using the Pöschel formulation ([**56**]). We apply this theorem in order to find the Nekhoroshev's domain of the parameters involved in which Nekhoroshev exponential stability estimates can be found. To this end, we show the existence of KAM tori using a suitable parameterization in order to write an approximate representation of KAM tori around the elliptic fixed point of the system.

Some results of this Chapter are taken from an original research in collaboration with C. Lhotka [**29**].

4.1. A brief history of the Sitnikov's problem

The *Sitnikov's problem* was introduced by K. A. Sitnikov in 1960; he treated this problem in order to show the existence of oscillatory motions for the three–body–problem ([**57**]). The model describes the motion of a massless body moving on a straight line perpendicular to the plane of two primaries which move on Keplerian orbits with eccentricity e (compare with Figure 4.1 and with Section 4.2). The problem has 1 and 1/2 degrees of freedom, due to the explicit dependence of the time and moreover it depends on the parameter e. A simplified problem was treated by W. D. MacMillan in 1913 (see [**48**]) who studied the case of zero eccentricity of the primaries' orbits and he solved analytically the problems in terms of elliptic functions. J. Moser in 1973 (compare with [**51**]) showed that the problem is not globally integrable and chaotic orbits exist for a certain set of initial conditions. In 2002, S. B. Faruque (see [**37**]) provided analytical approximations to the MacMillan problem in terms of series expansions in the parameters of the system.

Concerning the elliptic case (eccentricity different from zero), the first derivation of some analytic expressions in terms of initial conditions and primaries' eccentricity have been introduced by J. Liu and Y.S. Sun in 1990 (see [**47**]). They replaced the periodic differential equations by an autonomous mapping representing a surface of section over one primary revolution. Later, in 1992 (see [**41**]), J. Hagel, using perturbation theory, obtained a solution of the linearized equation of motion and then he extended the problem by including nonlinear forces: the solution gives a good approximation for small oscillations of the third body. In 1993, R. Dvorak (see [**30**]) using numerical integrations showed that invariant curves exist for small oscillations centering on the barycenter. In 2005, J. Hagel and C. Lhotka (see [**42**]) derived an analytical approximated solution using Floquet and Courant–Snyder theories.

In recent years the problem has been extended to the case in which the third body has a non–negligible mass, and therefore it influences the motion of the primaries (*extended Sitnikov's problem*). It was treated by R. Dvorak and Y. S. Sun in 1997 (see [**32**]) and by P. Soulis, T. Bountis and R. Dvorak in 2007 (see [**58**]); in the latter paper the authors also treated the case in which the third body is not constrained to be on a straight line and it can move off the z–axis (*generalized extended Sitnikov's problem*). Finally the extended problem was treated by J. Hagel in 2009 (see [**40**]) to show perihelion motion of the primaries' orbits in the circular limit.

4.2. Mathematical formulation

Two bodies of equal mass $m_1 = m_2$ (called *primeries*) move under Newton's law of attraction on Keplerian orbits; they orbit on a plane around the common barycenter, moving in an antisymmetrical way ($r_1 = -r_2$). A third massless point is constrained to move on a straight line L perpendicular to the plane of the primaries and passing through the barycenter of the primaries (see Figure 4.1). Since the mass of the third body can be neglected, the motion of the first two bodies is not affected by the third body. Moreover, due to the symmetric configuration of the model, the third body will remain on the line L. The problem consists in the study of the dynamical evolution of the third body, which is periodically subjected to the action of the primaries.

We normalize the time so that the period of the primaries is 2π, and the mass unit so that the total mass is one, i.e. we consider $m_1 = m_2 = 1/2$

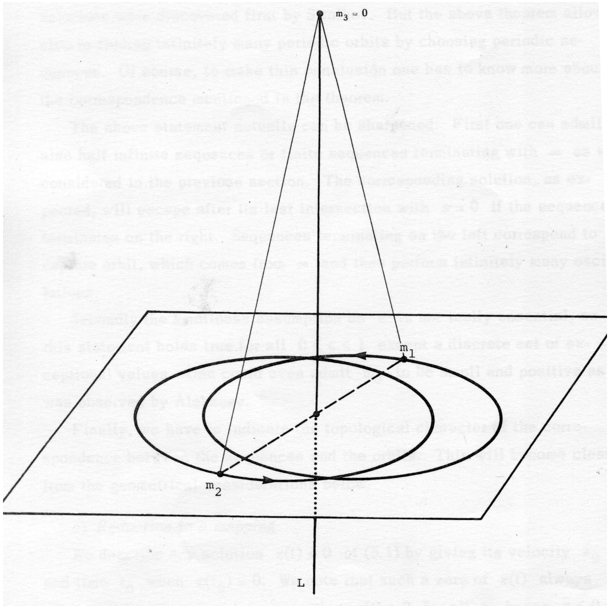

FIGURE 4.1. The Sitnikov's model (after [**51**]).

and the length unit so that the gravitational constant G is equal to one. Let z be the coordinate describing the motion of the third body. The Hamiltonian describing the system is given by

$$H(y,z,t) = \frac{1}{2}y^2 - \frac{1}{\sqrt{r(t)^2 + z^2}} , \tag{4.1}$$

where $y = \dot{z}$ and $r(t)$ is the distance between one of the primaries and the barycenter. If the eccentricity is zero, the motion of the primaries is circular; then $r(t)$ is a constant ($r = 1/2$) and we get an integrable system (MacMillan problem). If the eccentricity is different from zero, then $r(t)$ is a known function of the time and it can be expanded in Taylor series around $e = 0$. It can be written as (compare with [**7**]):

$$r(t) = \frac{1}{2}\Big(1 + \sum_{n=1}^{\infty} r_n(t)e^n\Big) , \tag{4.2}$$

where the terms r_n are trigonometric polynomials in the time t. Up to the fourth order we have:

$$\begin{aligned} r_1(t) &= -\cos t \ , \\ r_2(t) &= \frac{1}{2}(1-\cos 2t) \ , \\ r_3(t) &= \frac{3}{8}(\cos t - \cos 3t) \ , \\ r_4(t) &= \frac{1}{3}(\cos 2t - \cos 4t) \ . \end{aligned}$$

We can also rewrite the fractional term of the Hamiltonian as

$$\frac{1}{\sqrt{r(t)^2+z^2}} = \frac{1}{r}\frac{1}{\sqrt{1+(\frac{z}{r})^2}} = \frac{1}{r}\sum_{k=0}^{\infty}\begin{pmatrix} -\frac{1}{2} \\ k \end{pmatrix}\left(\frac{z}{r}\right)^{2k} \ , \qquad (4.3)$$

where the brackets are the binomial coefficient and the convergence of the series is guaranteed provided $|z(t)/r(t)| < 1$.

By setting

$$\begin{aligned} \dot{z} &= y \\ \dot{y} &= -\frac{\partial H}{\partial z} \ , \end{aligned}$$

the equation of motion derived from (4.1) is given by

$$\ddot{z} = -\frac{z}{\sqrt{(r(t)^2+z^2)^3}} \ . \qquad (4.4)$$

Inserting (4.3), the equation of motion takes the form:

$$\ddot{z} = \sum_{k=0}^{\infty}\begin{pmatrix} -\frac{3}{2} \\ k \end{pmatrix}\left(\frac{z^{2k+1}}{r(t)^{2k+3}}\right) \ . \qquad (4.5)$$

Expanding it up to a finite order N, we get the equation of motion in the following polynomial way:

$$\ddot{z} = -8z - \sum_{\beta=0}^{N}\ \sum_{\alpha=0}^{\beta}\left(c_{\alpha,\beta-\alpha}\ e^{\alpha}z^{\beta-\alpha}\cos(kt) + d_{\alpha,\beta}\ e^{\alpha}z^{\beta-\alpha}\right) \ , \qquad (4.6)$$

where $c_{m,n} \in \mathbb{R}$, $d_{m,n} \in \mathbb{R}$, $k \in Z$ are suitable constants.

For the integrable approximation $e = 0$ and small oscillations, i.e. $z << 1$ the approximate equation of motion (4.6) turns out to be the equation of the harmonic oscillator with natural frequency $\omega = \sqrt{8}$. In this assumption, the massless body performs small oscillations with frequency ω around an elliptic fixed point centered at the origin (see Figure 4.2). We provide the expansion of (4.6) up to the order $N = 4$:

$$\begin{aligned}\ddot{z} &+ [8 + 24e\cos t + e^2(12 + 36\cos 2t) + e^3(27\cos t + 53\cos 3t)]z \\ &+ (-48 - 240e\cos t)z^3 = 0 \ . \end{aligned} \tag{4.7}$$

The double sum in (4.6) is therefore, the perturbation of an harmonic oscillator. We can see that it also contains of non zero average terms (the part given by the $d_{m,n}$ coefficients). In the next Section, we will perform canonical transformations in order to remove this perturbation to higher orders and to obtain a Birkhoff normal form.

In Figure 4.2 we show a phase portrait (with the Poincaré section condition $r(t) = r_{min}$) for the value of the eccentricity $e = 0.1$. We can observe the elliptic fixed point at the origin; close to the linear problem, for very small oscillations around the barycenter, we can observe closed invariant curves; these closed curves exist up to a certain value of the initial conditions; moving away for the barycenter the curves break–down and unbounded and chaotic motions are possible. In the domain of closed invariant curves we can observe islands which exist around stable periodic orbits of the problem. It is known (compare with [**28**]) that in between such islands we can have hyperbolic points, separatrices and sometimes only thin layers of chaotic motions. Nevertheless, these motions are bounded and never lead to escape. Outside the "main island" we see two islands of invariant curves around a stable point which correspond to the 2:1 resonance, where the primaries make two compete revolutions whereas the third body completes exactly one oscillation (for a more detailed description of the phase–space of the Sitnikov's problem as the eccentricity e varies, see [**30**], [**31**]).

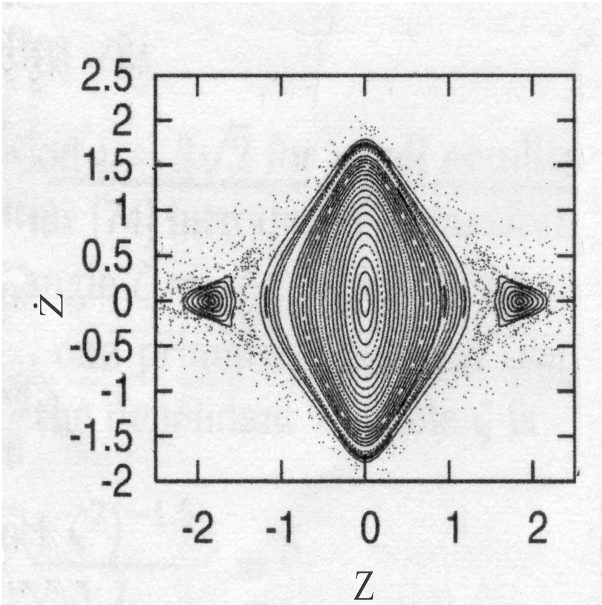

FIGURE 4.2. Phase portrait of the Sitnikov's model for the eccentricity $e = 0.1$ (after [**31**]).

To understand the nonlinear and time dependent effects close to the center $z = 0$, we perform a canonical transformation to action–angle variables of the harmonic oscillator and, doing this, we also rescale the action variable by some $\eta > 0$, obtaining the following transformation:

$$\begin{cases} y = \sqrt{2\omega\eta J_1}\cos\varphi \\ z = \sqrt{\frac{2}{\omega}\eta J_1}\sin\varphi \end{cases} , \qquad \omega = \sqrt{8}\ . \tag{4.8}$$

In this way the new action J_1 becomes of order unity and the parameter η measures the distance from the origin. We note that, in order to obtain a symplectic transformation, we have to multiply the resulting Hamiltonian by η^{-1}. Taking into account the equation (4.6), the transformation (4.8) allows us to rewrite the Hamiltonian into a more suitable form to apply canonical perturbation theory. Furthermore, before rewriting the new Hamiltonian, we want to introduce a new set of variables $(J_2, \phi_2 = t)$ to extend the phase–space; then, the new Hamiltonian takes the form:

$$\begin{aligned} H &= \omega J_1 + J_2 + \sum_{k=1}^{N} p_k(J_1; e, \eta) \\ &\quad + \sum_{(k,l)\in\mathbb{Z}^2} q_{k,l}(J_1; e, \eta) \cdot \cos(k\phi_1 + l\phi_2), \end{aligned} \tag{4.9}$$

where p_k and $q_{k,l}$ are polynomials in J_1, e, η (for easier notation we denote the new Hamiltonian with the same symbol H). Note that, the sums represent the perturbation of the system; it is again split into non–zero and zero average contributions, like in the formulations of the equations of motion (4.6).

For the ongoing analysis it is important to estimate the region of convergence of the series in e and η. For this reason it is preferable to reorder the terms in the Hamiltonian (4.9) such that the Hamiltonian can be written into the form:

$$H = h_0(J_1, J_2) + \sum_{k=1}^{N} h_k \ , \tag{4.10}$$

such that the following holds for any k:

$$\left| \frac{h_{k+1}}{h_k} \right| < 1 \ , \tag{4.11}$$

so that the D'Alambert criterion can be applied. Since the terms h_k in general will depend on both the eccentricity e and the parameter η, being J_1 and J_2 of order $O(1)$, the criterion (4.11) has to be fulfilled in the whole domain of interest of e and η. Thus, up to order $N = 16$ (which is the machine precision limit), we found the critical values $e_{crit} \simeq 0.612$ and $\eta_{crit} \simeq 0.4$. Therefore, we have to limit the domain for the ongoing analysis to $(e, \eta) \in (0, e_{crit}) \times (0, \eta_{crit})$.

Up to 5^{th} order the Hamiltonian written in terms of h_k is given by:

$$
\begin{aligned}
h_0 &= \sqrt{8}J_1 + J_2 \ , \\
h_1 &= 0 \ , \\
h_2 &= 0 \ , \\
h_3 &= \frac{3\sqrt{2}}{2}eJ_1\cos(2\phi_1-\phi_2) + 3\sqrt{2}eJ_1\cos\phi_2 + \frac{3\sqrt{2}}{2}eJ_1\cos(2\phi_1+\phi_2) \ , \\
h_4 &= \frac{3\sqrt{2}}{2}e^2J_1 - \frac{9}{4}\eta J_1^2 + \frac{3}{2}e^2J_1\cos 2\phi_1 + \frac{9\sqrt{2}}{2}e^2J_1\cos 2\phi_2 \\
&\quad + \frac{9\sqrt{2}}{4}e^2J_1\cos(2\phi_1+2\phi_2) + \frac{9\sqrt{2}}{4}e^2J_1\cos(2\phi_1-2\phi_2) \\
&\quad - 3\eta J_1^2\cos 2\phi_1 - \frac{3}{4}\eta J_1^2\cos 4\phi_1 \ , \\
h_5 &= \frac{27\sqrt{2}}{16}e^3J_1\cos(2\phi_1-\phi_2) + \frac{27\sqrt{2}}{8}e^3J_1\cos\phi_2 + \frac{53\sqrt{2}}{8}e^3J_1\cos 3\phi_2 \\
&\quad + \frac{27\sqrt{2}}{16}e^3J_1\cos(2\phi_1+\phi_2) + \frac{53\sqrt{2}}{16}e^3J_1\cos(2\phi_1+3\phi_2) \\
&\quad + \frac{53\sqrt{2}}{16}e^3J_1\cos(2\phi_1-3\phi_2) - \frac{15}{2}eJ_1^2\eta\cos(2\phi_1-\phi_2) \\
&\quad - \frac{15}{8}\cos(4\phi_1-\phi_2) - \frac{45}{4}eJ_1^2\eta\cos(\phi_2) \\
&\quad - \frac{15}{2}eJ_1^2\eta\cos(2\phi_1+\phi_2) - \frac{15}{8}eJ_1^2\eta\cos(4\phi_1+\phi_2) \ . \qquad (4.12)
\end{aligned}
$$

4.3. New formulation of the problem

In this Sections we perform a suitable sequence of canonical transformations in order to obtain a new Hamiltonian close to an integrable one starting from (4.12), namely we will remove the perturbation to higher orders. The implementation of the algorithm is performed by standard Lie–transformation theory by using a sequence of near–to–identity transformations. This allows us to find a new set of variables

$(J_k^{(r)}, \phi_k^{(r)})$, $k = 1, 2$ in which the Hamiltonian (4.12) takes the form:

$$\begin{aligned} H^{(r)}(J_1^{(r)}, J_2^{(r)}, \phi_1^{(r)}, \phi_2^{(r)}; e, \eta) &= Z^{(r)}(J_1^{(r)}, J_2^{(r)}; e, \eta) \\ &\quad + R^{(r+1)}(J_1^{(r)}, J_2^{(r)}, \phi_1^{(r)}, \phi_2^{(r)}; e, \eta) \end{aligned} \tag{4.13}$$

which define the Birkhoff normal form of a nearly–integrable Hamiltonian system. The upper index (r) labels the variables at the r^{th} normalization step, $Z^{(r)}$ is called the *normal form* term, $R^{(r)}$ the *remainder* of the Birkhoff normal form, which is at the basis to introduce the concept of the optimal order of truncation and exponential stability (this is strongly connected to Nekhoroshev's theory [**54**]). In fact, we will see that the size of the remainder provides the size of the perturbation. Next, we will use the normal form of the approximate Hamiltonian formulation (4.12) at order r closest to the optimal order of truncation; we will find a parameterization of a torus persisting under the perturbation of the remainder, and we will perform the Nekhoroshev's estimates around it.

4.3.1. The Birkhoff normal form. In this Section we present an algorithm which allows us to rewrite the Hamiltonian (4.12) in a more suitable way in which the perturbation is removed to higher orders; the explicit computations are based on a program developed by C. Efthymiopoulos (compare with [**33**]). Let us consider equation (4.10); the equations of motion are given by

$$\begin{aligned} \dot{\phi}_k &= \frac{\partial H}{\partial J_k} = \omega_k(J) + \sum_{k=1}^{N} \frac{\partial h_k}{\partial J_k}(J, \phi) \\ \dot{J}_k &= -\frac{\partial H}{\partial \phi_k} = -\sum_{k=1}^{N} \frac{\partial h_k}{\partial \phi_k}(J, \phi) \ , \end{aligned} \tag{4.14}$$

for $k = 1, 2$, where $\omega_k = \partial h_0 / \partial J_k$ is the frequency of the unperturbed system, $J = (J_1, J_2)$, $\phi = (\phi_1, \phi_2)$.

The idea is to find a canonical transformation $(J,\phi) \to (J',\phi')$ from old to new variables, such that the nonlinear effects become negligible:

$$\begin{aligned} \dot{\phi}'_k &= \frac{\partial H'}{\partial J'_k} = \omega'_k(J') + O_r(J',\phi') \\ \dot{J}'_k &= -\frac{\partial H'}{\partial \phi'_k} = O_r(J',\phi') \ , \end{aligned} \tag{4.15}$$

where H' is the Hamiltonian in the new variables, ω' denotes the new frequency in terms of the new variables and $O_r(J',\phi')$ is the non–normal form contribution. The equations (4.15) define the normal form of the dynamical system; the new Hamiltonian H' is called the *Birkhoff normal form.*

The transformation is obtained using the method of Lie–series. We summarize the computational algorithm, which is needed in the calculations. Given an Hamiltonian of the form $H = H_0 + \varepsilon H_1$, let us define the Lie–derivative as

$$l_W = \{\cdot, W\} \ ,$$

where the curly brackets stand for the Poisson brackets; then, the Lie–operator can be defined as its exponential as:

$$L_W = \exp l_W \ .$$

This operator has many properties; in particular we need two of them: $i)$ we use the fundamental result that the time–evolution of the action–angle variables of a Hamiltonian system $H(J,\phi)$ can be written in terms of

$$\begin{aligned} J(t) &= \exp\{t l_H J(0)\} \\ \phi(t) &= \exp\{t l_H \phi(0)\} \ , \end{aligned}$$

which generates a symplectic transformation in phase space. The idea is to use this property to construct a symplectic transformation in order to remove the perturbation to higher orders of ε. Therefore, an

ε–close canonical transformation (where ε is a small parameter) from old $(J^{(0)}, \phi^{(0)})$ to new $(J^{(1)}, \phi^{(1)})$ variables can be implemented using the Lie–operator:

$$\begin{aligned} J^{(1)} &= \exp\{\varepsilon l_{W_1} J^{(0)}\} \\ \phi^{(1)} &= \exp\{\varepsilon l_{W_1} \phi^{(0)}\} \ , \end{aligned}$$

where we have replaced the Hamiltonian through a generating function W_1 and the time flow in t through the parameter flow in ε.

ii) The Lie–operator is flat, i.e. given a function f, then

$$f(L_W J, L_W \phi) = L_W(J, \phi) \ ;$$

this means that under a change of variables, the Hamiltonian transforms as follows

$$H^{(1)}(J^{(1)}, \phi^{(1)}) = \exp\{\varepsilon l_{W_1} H^{(0)}(J^{(0)}, \phi^{(0)})\} \ .$$

Expanding the exponential and the perturbing part into Taylor series in ε as

$$H^{(1)} = (1 + \varepsilon l_{W_1} + \ldots)(h_0(J) + h_1(J, \phi) + \ldots) \ ,$$

we get order by order the following terms: at ε^0 we get h_0, at ε^1 we get $l_{W_1} h_0 + h_1$, and similar for higher orders. Our aim is to remove the dependence of the angles to higher orders. To this end, we write the generating function W (that removes the perturbation) as $W = \sum_k W_k$; then we implement the Poisson brackets to obtain:

$$\{h_0, W_1\} + h_1 = 0 \ , \tag{4.16}$$

which is called *homological equation*. Let us consider the Fourier expansion of h_1 as

$$h_1 = \sum_{k \in \mathbb{Z}} \hat{h}_{1,k}(J) \exp\{i \cdot k \cdot \phi\} \ ,$$

then, the homological equation can be solved, provided that the generating function W_1 itself has the form

$$\tilde{W}_1 = \sum_{k \in \mathbb{Z}} w_{1,k}(J) \exp\{i \cdot k \cdot \phi\} \ .$$

The coefficients $w_{1,k}$ can be found by implementing the Poisson brackets, calculating the derivatives and comparing coefficients of the same Fourier orders. We obtain an explicit expression for the coefficients given by

$$w_{1,k} = \frac{\hat{h}_{1,k}}{i \cdot k \cdot \omega} \ . \tag{4.17}$$

In (4.17), the terms of the form $k \cdot \omega$ appear at the denominator. It is therefore necessary to exclude Fourier terms containing zero divisors. We can do it in the assumption to be far away from the resonances. This completes one iteration of the Lie–transformation method. In a similar way, we can eliminate terms of second and higher orders up to r so to obtain the Hamiltonian in normal form as in (4.13), namely

$$H^{(r)}(J^{(r)}, \phi^{(r)}; e, \eta) = Z^{(r)}(J^{(r)}; e, \eta) + R^{(r+1)}(J^{(r)}, \phi^{(r)}; e, \eta) \ , \tag{4.18}$$

where $Z^{(r)}$ and $R^{(r+1)}$ are, respectively, the normal form and remainder at order r. If we fix an order of truncation $r = r_0$, the frequency is fixed as $\omega'_k(J) = \partial Z^{(r_0)}/\partial J'^{(r_0)}_k$ while the higher order terms can be bounded by the norm of the remainder, namely $\partial R^{(r_0+1)}/\partial \phi'^{(r_0)}_k$.

4.3.2. Application to the Sitnikov's problem. In the case of the Sitnikov's problem, we aim to transform the Hamiltonian (4.10), given up to r^{th} order through (4.12), into the form (4.18) by the method of Lie–transformations described above. The Hamiltonian is already in a proper form, therefore we implement the homological equations (4.16) and we solve it for suitable generating functions. We will show the explicit calculation up to the order 4.

At the 0^{th} order, the solution, as already indicated, is the identity given by $k_0 = \sqrt{8}J_1 + J_2$. We omit the 1^{st} and 2^{nd} order; in fact, since $h_1 = h_2 = 0$ we get from straightforward arguments that $k_1 = k_2 = 0$ with the generating functions $W_1 = W_2 = 0$. At the 3^{rd} order, the homological equation takes the form:

$$\begin{aligned}\frac{\partial W_3}{\partial \phi_2} + \sqrt{8}\frac{\partial W_3}{\partial \phi_1} &- 3\sqrt{2}eJ_1\cos\phi_2 - \frac{3\sqrt{2}}{2}eJ_1\cos(2\phi_1 - \phi_2) \\ &- \frac{3\sqrt{2}}{2}eJ_1\cos(2\phi_1 + \phi_2) = 0 \ , \end{aligned} \tag{4.19}$$

from which we determine W_3 as:

$$\begin{aligned} W_3 &= \frac{3\sqrt{2}eJ_1\sin(2\phi_1 - \phi_2)}{4\sqrt{8} - 2} + 3\sqrt{2}eJ_1\sin(\phi_2) \\ &+ \frac{3\sqrt{2}eJ_1\sin(2\phi_1 + \phi_2)}{4\sqrt{8} + 2} \ ; \end{aligned} \tag{4.20}$$

from this equation we get $k_3 = 0$. Repeating the procedure we get at 4^{th} order the homological equation

$$\begin{aligned}\frac{\partial W_4}{\partial \phi_2} + \sqrt{8}\frac{\partial W_4}{\partial \phi_1} &- \frac{3\sqrt{2}}{2}e^2J_1\cos 2\phi_1 - \frac{9\sqrt{2}}{2}e^2J_1\cos 2\phi_2 \\ &- \frac{9\sqrt{2}}{4}e^2J_1\cos(2\phi_1 + 2\phi_2) - \frac{9\sqrt{2}}{4}e^2J_1\cos(2\phi_1 - 2\phi_2) \\ &- \frac{3\sqrt{2}}{2}e^2J_1 + 3J_1^2\eta\cos 2\phi_1 + \frac{3}{4}J_1^2\eta\cos 4\phi_1 \\ &+ \frac{9}{4}J_1^2\eta = 0 \ ; \end{aligned} \tag{4.21}$$

the function W_4 is therefore given explicitly by solving (4.21). We obtain the term k_4 as follows:

$$k_4 = \frac{1}{4}\left(6\sqrt{2}e^2J_1 - 9\eta J_1^2\right) \ . \tag{4.22}$$

With the help of the algebraic manipulator Mathematica we have obtained the non resonant normal form up to order 16. We omit the calculations and we write the normalized Hamiltonian as:

$$H^{(16)} = Z^{(16)} + R^{(17)}$$

where

$$\begin{aligned} Z^{(16)} &= \frac{315}{64\sqrt{2}}e^8 J_1 - \frac{945}{16}e^6 J_1^2 \eta - \frac{364575}{11408\sqrt{2}}e^6 J_1 \\ &+ \frac{4725}{16\sqrt{2}}e^4 J_1^3 \eta^2 + \frac{443745}{3472}e^4 J_1^2 \eta + \frac{48087\sqrt{2}}{6727}e^4 J_1 \\ &- \frac{14559}{1736\sqrt{2}}e^4 J_1 - \frac{11025}{64}e^2 J_1^4 \eta^3 - \frac{2511345}{15748\sqrt{2}}e^2 J_1^3 \eta^2 \\ &- \frac{8919}{7688}e^2 J_1^2 \eta + \frac{1}{4}\left(6\sqrt{2}e^2 J_1 - 9J_1^2 \eta\right) - \frac{36}{31}\sqrt{2}e^2 J_1 \\ &+ \frac{3969}{128\sqrt{2}}J_1^5 \eta^4 + \frac{625}{64}J_1^4 \eta^3 + \frac{47}{32\sqrt{2}}J_1^3 \eta^2 \\ &+ \sqrt{8}J_1 + J_2 \ . \end{aligned} \tag{4.23}$$

As we can see the normal form depends explicitly on the action variables J and on the parameters e and η.

For the Nekhoroshev's estimates the remainder plays a very important role because the estimates are derived from it, and it represents the perturbation. To get optimal results, it is necessary to reach the optimal order of truncation, such to render the perturbation exponentially small, i.e. we are looking for a normal form of order $r = r_{opt}$, such that the norm of the remainder $\|R^{(r+1)}(J_1, J_2, \phi_1, \phi_2; e, \eta)\|$ becomes minimal. In our case, the norm of the remainder depends on the parameters e and η (note that we require J_1, J_2 being of order unity). We calculated the normal form for fixed $e = e_0$ and $\eta = \eta_0$ up to order $r = 40$ (by using a program developed by C. Efthymiopoulos [**33**]) and we see as the norms of the remainder depend on r. We found three different behavior according to different values of (e, η). We give specific examples of the behavior of the norms in Figure 4.3, which demonstrates the dependence on the optimal order of truncation by the parameters e and η.

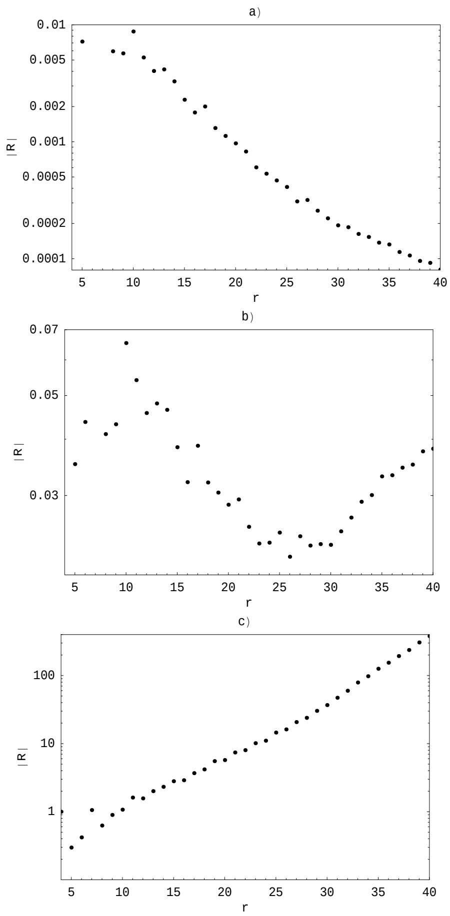

FIGURE 4.3. The remainder R as function of the order of truncation r is plotted as e and η vary. a) In the case $e = 0.02$, $\eta = 0.01$ the norm is a decreasing function of the order r; b) In the case $e = 0.04$, $\eta = 0.03$ the norm has a minimum between the order 5 and the order 40; c) In the case $e = 0.04$, $\eta = 0.09$ the norm is an increasing function of the order r (after [**29**]).

4.4. Nekhoroshev's estimates

In this Section we first show a short description of the Nekhoroshev's theorem, which provides information about the long term stability properties of nearly–integrable systems. The original statement of the theorem (see [**54**]) concerns Hamiltonians having a property called *steepness*, but this concept can be replaced by other more familiar hypotheses. The theorem was reformulated by many authors (compare with [**4**], [**34**], [**35**], [**36**], [**56**]), who replaced the steepness condition with other conditions as the convexity, or quasi–convexity or the three jet condition. In particular we will use the Pöschel version given in [**56**].

4.4.1. Nekhoroshev's theorem. Let us consider the Hamiltonian given by

$$H = h_0(J) + h_\varepsilon(J, \phi) \ , \tag{4.24}$$

(compare it with equation (4.18)), where h_0 is the integrable part, h_ε is the perturbation depending on a small parameter $\varepsilon \in \mathbb{R}$ and $J \subseteq U \subset \mathbb{R}^2$. Let us define the norm $|u|_s$ of a function u with Fourier expansion $\sum\limits_{k \in \mathbb{Z}^2} u_k(J) \exp\{ik\theta\}$ as

$$|u|_s = \sup_{J \in U} \sum_{k \in \mathbb{Z}^2} |u_k(J)| \cdot \exp\{|k|s\} \ ,$$

for some $s \in \mathbb{R}_+$, where $|k| = |k_1| + |k_2|$. Let $\omega(J) = \partial_J h_0(J)$ be the frequency and let $Q(J) = \partial_J^2 h_0(J)$ be the Hessian of the unperturbed part, which is assumed to be uniformly bounded with respect to the operator norm induced by the Euclidian norm. Let M be a bound of the norm of $Q(J)$. We will say that the integrable Hamiltonian h_0 is l, m*–quasi–convex* if there exist constants $l, m > 0$ such that h_0 satisfies at least one of the following conditions in the whole domain of $J \in U$:

$$\begin{aligned} |\langle \omega(J), \xi \rangle| &> l\|\xi\| \\ \langle Q(J)\xi, \xi \rangle &\geq m\|\xi\|^2, \end{aligned} \tag{4.25}$$

for all $\xi \in \mathbb{R}^2$, where $\langle \cdot, \cdot \rangle$ stands for the scalar product. We can now state the Nekhoroshev's theorem as stated by Pöschel [**56**]:

THEOREM 4.1. *Suppose h_0 is l, m–quasi–convex, and*

$$|h_\varepsilon|_s \leq \varepsilon < \varepsilon_0 = \frac{mr_0}{2^{10}A^{2n}} , \tag{4.26}$$

where $r_0 = 4l/m$, $A = 11M/m$, n is the dimension of the system (in our case $n = 2$). Then for every orbit with initial position $(J_0, \phi_0) \in U \times \mathbb{T}^2$ one has

$$\|J(t) - J_0\| \leq R_0\Big(\frac{\varepsilon}{\varepsilon_0}\Big)^a \tag{4.27}$$

for

$$|t| \leq T_0 \exp\left(\frac{s_0}{6}\Big(\frac{\varepsilon_0}{\varepsilon}\Big)^a\right) , \tag{4.28}$$

where $a = 1/2n$, $R_0 = r_0/A$, $T_0 = A^2 s/\Omega_0$,
with $\Omega_0 = \sup_{\|J-J_0\| \leq R_0} \|\omega(J)|$.

Nekhoroshev's theorem is very important because it provides a property of stability for very long times, and it is applicable to real physical systems because sometimes the life–time of the system is shorter than the stability time derived from the theorem.

The theorem in its present form is constructive, meaning that it can be directly used to derive the stability time for a given dynamical system. The parameters l, m and M and the dimension n are given from the unperturbed part of the Hamiltonian. The Nekhoroshev's regime can be derived from the inequality (4.26) together with an upper bound for ε, which is the norm of the perturbing part h_ε. The variation in action space follows from (4.27) and finally the stability time from

(4.28). The free parameter s can be set such that the stability time becomes optimal.

In order to apply this theorem to the Sitnikov's problem, we have to check that the system satisfies the required conditions. Actually, the unperturbed Hamiltonian turns out to be concave, namely the Hessian of h_0 is negative definite. So, the second of condition (4.25), is satisfied for some $m > 0$ provided that we introduce the absolute value, namely

$$|\langle Q(J)\xi, \xi\rangle| \geq m\|\xi\|^2 \ .$$

It can be done because Nekhoroshev's theorem can be proved also in the concave case. It is sufficient to consider the Hamiltonian given by $-h_0 - h_\varepsilon$, whose motions are conjugated to the Hamiltonian $h_0 + h_\varepsilon$ through an inversion of the time [**62**].

Therefore, we can find an explicit stability time for the system through (4.28); moreover, through (4.26), we can provide the conditions that the system has to satisfy in order to apply the theorem. In fact, the size of the remainder provides a value of the perturbation, and it explicitly depends on the two parameters e and η; for any value of them the optimal order of truncation r_{opt} changes and the norm can be computed through an easy algorithm. In particular, we can find a domain of the eccentricity e and the rescaling parameter η for which the condition (4.26) is satisfied.

Figure 4.4 shows the domain of e and η for which condition (4.26) is satisfied. It is a grid of discrete values of e and η; the continuous border of the domain is not easy to compute. Table 1 shows the Nekhoroshev's time corresponding to some values of (e, η) such that condition (4.26) is satisfied.

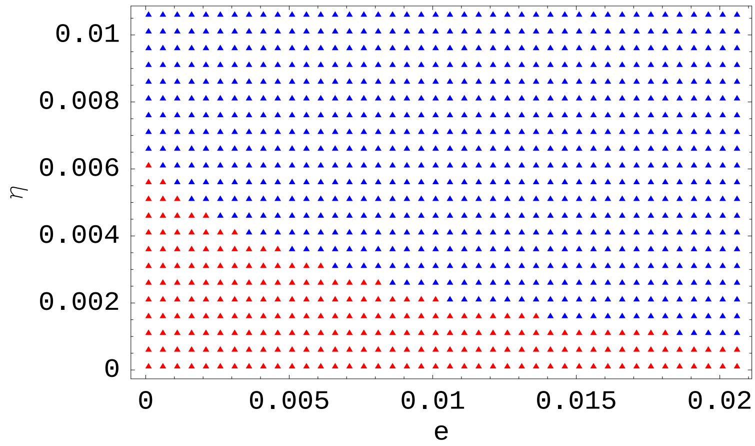

FIGURE 4.4. The Figure shows the domain of e and η: the red triangles define those points (e, η) such that condition (4.26) is satisfied; the blue triangles those points for which the condition is not satisfied.

e	η	time
0.001	0.001	$2.22844 \cdot 10^{41}$
0.001	0.005	$2.53508 \cdot 10^{6}$
0.005	0.002	$1.3257 \cdot 10^{6}$
0.01	0.002	399216
0.015	0.001	136643
0.02	0.001	91556
0.02	0.0001	$4.03721 \cdot 10^{9}$

TABLE 1. The Table shows the Nekhoroshev's stability time using formula (4.28) provided by [**56**] for some values of e and η such that the condition (4.26) is satisfied.

4.5. Parameterization of invariant tori in the Sitnikov's problem

In this Section we want to provide an explicit parameterization of invariant tori for the Sitnikov's problem, which is a nearly–integrable system. Let us consider the normalized Hamiltonian (4.18) truncated up to the optimal order r_{opt}. We want to introduce a new parameter ε being of the same order as the remainder. We rewrite the Hamiltonian omitting the index r to simplify the notation as

$$H(J_1, J_2, \phi_1, \phi_2; e, \eta) = Z(J_1, J_2; e, \eta) + \varepsilon R(J_1, \phi_1, \phi_2; e, \eta) \ . \quad (4.29)$$

Provided that the eccentricity e and the rescaling parameter η are in the Nekhoroshev's domain, the remainder will be small too. We will consider e and η as fixed parameters and we will take as perturbation the size of the remainder (which is exponentially small as we have seen in the previous Section).

In this case the concept of integrability is different from the concept used in classical literature of the Sitnikov's problem; in fact, usually the eccentricity measures the size of the perturbation and the integrable case is considered when the eccentricity is taken equal to zero (see [**48**]). In the Hamiltonian formulation used in our work, the perturbation depends on more parameters and after the normalization, the unperturbed Hamiltonian turns out to be dependent on the eccentricity, so that some values of $e \neq 0$ can be considered to be part of the integrable case. In fact, if the remainder is equal to zero, which is the integrable case, we have $\dot{\phi} = \omega(J; e, \eta)$ (the unperturbed frequency depends on e).

We introduce the following parameterization of the action–angle variables in order to find a representation of an invariant torus for the Sitnikov's problem with frequency $\Omega = (\omega_1, \omega_2)$. Let us write the variables in the following way:

$$\begin{aligned} \phi_1 &= \theta_1 + u_1(\theta_1, \theta_2) \\ \phi_2 &= \theta_2 \\ J_1 &= v_1(\theta_1, \theta_2) \\ J_2 &= v_2(\theta_1, \theta_2) \ , \end{aligned} \tag{4.30}$$

where $\theta_1, \theta_2 \in \mathbb{T}$ and u_1, v_1, v_2 are real, analytical functions. In particular, θ_1, θ_2 are functions of the time and they are such that their derivatives with respect to the time are equal to the frequency of the torus:

$$\begin{cases} \dot{\theta}_1 = \omega_1 \\ \dot{\theta}_2 = \omega_2 \ . \end{cases}$$

From the equations of motion derived from (4.29), we can derive some conditions about the frequency $\Omega = (\omega_1, \omega_2)$. In fact, let us denote by $R_x(x, y)$ the partial derivative of R with respect to the variable x; then if we derive the equations of motion from the Hamiltonian (4.29), we obtain:

$$\begin{cases} \dot{\phi}_1 = \frac{\partial H}{\partial J_1} = \omega(J_1; e, \eta) + \varepsilon R_{J_1}(J_1, \phi_1, \phi_2; e, \eta) \\ \dot{\phi}_2 = \frac{\partial H}{\partial J_2} = 1 \\ \dot{J}_1 = \frac{\partial H}{\partial \phi_1} = -\varepsilon R_{\phi_1}(J_1, \phi_1, \phi_2; e, \eta) \\ \dot{J}_2 = \frac{\partial H}{\partial \phi_2} = -\varepsilon R_{\phi_2}(J_1, \phi_1, \phi_2; e, \eta) \ . \end{cases} \tag{4.31}$$

Let us define the operator D as $D \equiv \omega \frac{\partial}{\partial \theta_1} + \frac{\partial}{\partial \theta_2}$. Then, if we differentiate the parametric equations (4.30) with respect to the time, we obtain

$$\begin{cases} \dot{\phi}_1 = \omega_1 + D u_1(\theta_1, \theta_2) \\ \dot{\phi}_2 = \omega_2 \\ \dot{J}_1 = D v_1(\theta_1, \theta_2) \\ \dot{J}_2 = D v_2(\theta_1, \theta_2) \ . \end{cases} \tag{4.32}$$

If we equate equations (4.31) and (4.32) we obtain the following equalities:

$$\begin{aligned}
\omega_1 + Du_1(\theta_1, \theta_2) &= \omega(J_1; e, \eta) + \varepsilon R_{J_1}(J_1, \phi_1, \phi_2; e, \eta) \\
\omega_2 &= 1 \\
Dv_1(\theta_1, \theta_2) &= -\varepsilon R_{\phi_1}(J_1, \phi_1, \phi_2; e, \eta) \\
Dv_2(\theta_1, \theta_2) &= -\varepsilon R_{\phi_2}(J_1, \phi_1, \phi_2; e, \eta)\ ,
\end{aligned} \tag{4.33}$$

that provide the following relations:

$$\begin{aligned}
\omega_1 &= \omega(J_1; e, \eta) = \frac{\partial Z}{\partial J_1} \\
\omega_2 &= 1 \\
Du_1(\theta_1, \theta_2; e, \eta) &= \varepsilon R_{J_1}(J_1, \phi_1, \phi_2; e, \eta) \\
Dv_1(\theta_1, \theta_2; e, \eta) &= -\varepsilon R_{\phi_1}(J_1, \phi_1, \phi_2; e, \eta) \\
Dv_2(\theta_1, \theta_2; e, \eta) &= -\varepsilon R_{\phi_2}(J_1, \phi_1, \phi_2; e, \eta)\ .
\end{aligned} \tag{4.34}$$

As the reader can see, we have introduced the dependence on e and η in the functions u_1, v_1, v_2 as it comes out from (4.33).

We can use the above equalities in order to find the parameterization of the torus with frequency $(\omega_1, \omega_2) = (\omega, 1)$; we recall that we are in the extended phase–space where the angle variable ϕ_2 is the time t; in fact, from $\omega_2 = 1$ we get $\theta_2 = t$, since $\dot{\theta}_2 = \omega_2 = 1$. Then we note that, in the right hand side of (4.34), if we insert the parameterization (4.30), we obtain some equations in the unknown functions u_1, v_1, v_2 as follows:

$$\begin{aligned}
\omega + Du_1(\theta_1, \theta_2; e, \eta) &= \omega(v_1; e, \eta) + \varepsilon R_{J_1}(v_1, \theta_1 + u_1, \theta_2; e, \eta) \\
Dv_1(\theta_1, \theta_2; e, \eta) &= -\varepsilon R_{\phi_1}(v_1, \theta_1 + u_1, \theta_2; e, \eta) \\
Dv_2(\theta_1, \theta_2; e, \eta) &= -\varepsilon R_{\phi_2}(v_1, \theta_1 + u_1, \theta_2; e, \eta)\ .
\end{aligned} \tag{4.35}$$

We can note that the first and the second equations are uncoupled from the remaining one; therefore, from those we can find the functions u_1 and v_1, and successively from the third equation we can find the solution v_2. In order to find an explicit solution of the system (4.35), we want to expand the function u_1, v_1, v_2 in Taylor series as follows:

$$\begin{aligned} u_1(\theta_1, \theta_2; e, \eta) &= \sum_{j=1}^{+\infty} \varepsilon^j u_{1j}(\theta_1, \theta_2; e, \eta) \\ v_1(\theta_1, \theta_2; e, \eta) &= \sum_{j=0}^{+\infty} \varepsilon^j v_{1j}(\theta_1, \theta_2; e, \eta) \\ v_2(\theta_1, \theta_2; e, \eta) &= \sum_{j=0}^{+\infty} \varepsilon^j v_{2j}(\theta_1, \theta_2; e, \eta) \ , \end{aligned} \tag{4.36}$$

for some real functions u_{1j}, u_{1j}, u_{1j}. In order to have the convergence of the Taylor–series (4.36), we should require some convergence conditions about the Taylor coefficients u_{1j}, v_{1j}, v_{2j}, namely we will require that $\left|\dfrac{u_{1j+1}}{u_{1j}}\right| < 1$, and the same requirement is done for v_{1j} and v_{2j}. Inserting (4.36) in (4.35) we obtain some equations, which allows us to compute explicitly the Taylor coefficients. In fact, if we equate same orders of ε we obtain recursive equations that, step by step (labelled by the index j), provide the solutions u_{1j}, v_{1j}, v_{2j}.

We will show how to compute the Taylor coefficients u_{1j}, v_{1j} explicitly for the first three steps, namely for the orders $j = 0$, 1, 2. Let us consider the first two equations of (4.35); if we insert the Taylor series (4.36) and if we expand the functions R_{J_1} and R_{ϕ_1} around ε, we get the following equations (for easier notations we omit the dependence on θ_1, θ_2, e, η):

$$\begin{aligned}
\omega + \varepsilon Du_{11} + \varepsilon^2 Du_{12} + \cdots &= \omega(v_{10}) + \varepsilon f_1(v_{10}, v_{11}) \\
&\quad + \varepsilon^2 f_2(v_{10}, v_{11}, v_{12}, u_{11}) + \cdots \\
Dv_{10} + \varepsilon Dv_{11} + \varepsilon^2 Dv_{12} + \cdots &= \varepsilon g_1(v_{10}) + \varepsilon^2 g_2(v_{10}, v_{11}, u_{11}) + \cdots
\end{aligned} \tag{4.37}$$

where the functions f_j and g_j are obtained from the expansion of R_{J_1} and R_{ϕ_1}, and the dependence on the v_{1j}s and the u_{1j}s is written explicitly. In the following we will denote by $a)$ the first equation of (4.37) and by $b)$ the second one. We start by equating the order $j = 0$ of (4.37): from $a)$ we get an expression of ω in the unknown v_{10}:

$$\omega = \omega(v_{10}) \ , \tag{4.38}$$

and from $b)$ we get

$$Dv_{10} = \omega \frac{\partial v_{10}}{\partial \theta_1} + \frac{\partial v_{10}}{\partial \theta_2} = 0 \tag{4.39}$$

from which v_{10} turns out to be equal to a constant (for the moment it is unknown).

When we equate terms of order $j = 1$ in (4.37) we get the two following equations in the three unknowns v_{10}, v_{11}, u_{11}:

$$\begin{aligned}
Du_{11} &= \omega \frac{\partial u_{11}}{\partial \theta_1} + \frac{\partial u_{11}}{\partial \theta_2} = f_1(v_{10}, v_{11}) \\
Dv_{11} &= \omega \frac{\partial v_{11}}{\partial \theta_1} + \frac{\partial v_{11}}{\partial \theta_2} = g_1(v_{10})
\end{aligned} \tag{4.40}$$

In order to find a solution we introduce a new notation: we split the function v_{10} (and the same will be done for the other unknown functions) as sum of two parts: one is the average of v_{10}, the other one is the part with zero average of v_{10}. We will denote by $\bar{v}_{10}$ the average and by $\tilde{v}_{10}$ the zero average part. We recall that the average $\bar{h} =< h >$

over $\mathbb{T}^n$ of a function $h(x)$ with $x \in \mathbb{T}^n$ is defined as

$$\bar{h} = \frac{1}{(2\pi)^n} \int_{T^n} h(x) dx \ .$$

Let us consider the equation $Dz = w$ where z and w are smooth functions; in order to guarantee the existence of the solution of such equation, we must require that z is a zero average function (see [**12**]). In this case, from (4.40) we can get two more equations given by

$$\begin{aligned} < f_1(v_{10}, v_{11}) > &= 0 \\ < g_1(v_{10}) > &= 0 \ . \end{aligned} \tag{4.41}$$

If we insert the expression $v_{10} = \bar{v}_{10} + \tilde{v}_{10}$ in the last equation, we see that the constant $\bar{v}_{10}$ disappears, because it multiplies terms with zero average, so that any constant satisfies the equation: we can choose it to be equal to any constant. On the contrary, $\bar{v}_{11}$ does not disappear from the equation and it turns out to be equal to zero.

Remark 4.1. *From equation* (4.38)*, if we fix* $\bar{v}_{10} = const$*, we are fixing the frequency of the torus we are looking for.*

Now we insert $v_{10} = const$ in (4.40) b) and we write $v_{11} = \bar{v}_{11} + \tilde{v}_{11}$; then, equation (4.40) b) depends only on $\tilde{v}_{11}$ so that, from it, we can determine explicitly $\tilde{v}_{11}$ (it turns out to be different from zero). Then, we insert v_{11} in (4.40) a) in order to obtain an explicit expression for $\tilde{u}_{11}$. So, at the end of the order $j = 1$, we have the explicit form of v_{10}, v_{11}, $\tilde{u}_{11}$.

We can proceed to the second step, namely equating terms of order $j = 2$ in (4.37). We have the following equations

$$\begin{aligned} Du_{12} &= \omega \frac{\partial u_{12}}{\partial \theta_1} + \frac{\partial u_{12}}{\partial \theta_2} = f_2(v_{10}, v_{11}, v_{12}, u_{11}) \\ Dv_{12} &= \omega \frac{\partial v_{12}}{\partial \theta_1} + \frac{\partial v_{12}}{\partial \theta_2} = g_2(v_{10}, v_{11}, u_{11}) \ , \end{aligned} \tag{4.42}$$

and

$$
\begin{aligned}
< f_2(v_{10}, v_{11}, v_{12}, u_{11}) > &= 0 \\
< g_2(v_{10}, v_{11}, u_{11}) > &= 0 \ .
\end{aligned}
\tag{4.43}
$$

From the last equation, in which the only unknown is $\bar{u}_{11}$, we get again that $\bar{u}_{11}$ disappears, so that we choose, for example, $\bar{u}_{11} = 0$. Then, coming back to equation (4.42) b), we can easily see that it depends only on $\tilde{v}_{12}$ which we can explicitly determine. Successively, we consider the first equation of (4.43) that depends only on $\bar{v}_{12}$, so that it can be explicitly determined.

To summarize the recursive algorithm, at each step we have four equations given by

$$
\begin{array}{l}
Du_{1j} = \omega \frac{\partial u_{1j}}{\partial \theta_1} + \frac{\partial u_{1j}}{\partial \theta_2} = f_j(v_{10}, \cdots, v_{1j}, u_{11}, \cdots, u_{1(j-1)}) \\
Dv_{1j} = \omega \frac{\partial v_{1j}}{\partial \theta_1} + \frac{\partial v_{1j}}{\partial \theta_2} = g_j(v_{10}, \cdots, v_{1(j-1)}, u_{11}, \cdots, u_{1(j-1)}) \\
< f_j(v_{10}, \cdots, v_{1j}, u_{11}, \cdots, u_{1(j-1)}) >= 0 \\
< g_j(v_{10}, \cdots, v_{1(j-1)}, u_{11}, \cdots, u_{1(j-1)}) >= 0 \ ,
\end{array}
\tag{4.44}
$$

and four unknowns, namely $\bar{u}_{1(j-1)}$, $\tilde{u}_{1j}$, $\bar{v}_{1j}$, $\tilde{v}_{1j}$, so that we are able to determine explicitly all of them.

REMARK 4.2. *i*) *At any order the term $\bar{u}_{1j}$ disappears from the equations, so that the constant can be arbitrarily chosen, and it will be taken always equal to zero (while it does not happen for $\bar{v}_{1j}$ that, as we can see in the following, it can turn out to be different from zero).*
ii) *The functions Du_{1j} and Dv_{1j} always depend, respectively, on $\tilde{u}_{1j}$ and $\tilde{v}_{1j}$, being $\bar{u}_{1j}$ and $\bar{v}_{1j}$ constants, and therefore, such that their derivatives with respect to θ_1 and θ_2 are equal to zero.*

We want to show some real calculations of the functions u_{1j} and v_{1j} for $j = 0, 1, 2$. To make easier and, above all, faster the computations we do not take the normalized Hamiltonian up to the optimal order of truncation, but we consider the normalized Hamiltonian up to the order 10. From the previous Remark, we consider the functions $\bar{u}_{11}$ and $\bar{u}_{12}$ equal to zero from the beginning (always to make more clear the notations of the formulae).

We start by equating the order $j = 0$; from (4.37) b), we get

$$\omega \frac{\partial \tilde{v}_{10}}{\partial \theta_1}(\theta_1, \theta_2) + \frac{\partial \tilde{v}_{10}}{\partial \theta_2}(\theta_1, \theta_2) = 0 \ ,$$

that says to us that the function $\tilde{v}_{10}$ must be equal to zero. From (4.37) a) we can fix the frequency ω as

$$\omega = \frac{1}{2}\Big(4\sqrt{2} + 3\sqrt{2}e^2 - 9\eta\Big) \ . \tag{4.45}$$

At this step, actually, the frequency depends on $\bar{v}_{10}$, which is equal to a constant. It can be chosen equal to one in order to obtain the action J_1 of the order unity.

Remark 4.3. *We must guarantee that the frequency written in* (4.45) *is a diophantine number. Let us show the following argument: we consider ω as a continuous function of e, i.e. $\omega = \omega(e)$ with $e \in [0, e_0]$ for some e_0. We know that there exists a set of full measure of diophantine numbers ω; it implies that there exists a subset $E \subset [0, e_0]$ of full measure, such that for any $e \in E$, $\omega(e)$ is diophantine. Now we can fix e such that $\omega(e)$ is a diophantine number. We also note that if we consider the Hamiltonian* (4.29) *truncated to another order, we obtain different dependence on e. In particular, if we consider the Hamiltonian truncated to a higher order, we get an expression of ω in which more terms in e appear, but they turn out to be of higher order of e. Therefore, when we fix an order of truncation of the Hamiltonian, we can consider the frequency ω we find, as a truncation of the frequency given by considering the Hamiltonian truncated up to the optimal order* [**63**].

Then, we can proceed with the order $j=1$; equating the first order of ε of equation (4.37) we get the following:

$$
\begin{aligned}
\omega\frac{\partial\tilde{u}_{11}}{\partial\theta_1}+\frac{\partial\tilde{u}_{11}}{\partial\theta_2} &= \cos\theta_2 a_{0,1}+\cos 3\theta_2 a_{0,3}+\cos(2\theta_1-3\theta_2)a_{2,-3}\\
&+\cos(2\theta_1-\theta_2)a_{2,-1}+\cos(2\theta_1+\theta_2)a_{2,1}\\
&+\cos(2\theta_1+3\theta_2)a_{2,3}+\cos(4\theta_1-\theta_2)a_{4,-1}\\
&+\cos(4\theta_1+\theta_2)a_{4,1}+\frac{9}{2}\eta\bar{v}_{11}\\
\omega\frac{\partial\tilde{v}_{11}}{\partial\theta_1}+\frac{\partial\tilde{v}_{11}}{\partial\theta_2} &= \sin(2\theta_1-3\theta_2)b_{2,-3}+\sin(2\theta_1-\theta_2)b_{2,-1}\\
&+\sin(\theta_1+\theta_2)b_{2,1}+\sin(2\theta_1+3\theta_2)b_{2,3}\\
&+\sin(4\theta_1-\theta_2)b_{4,-1}+\sin(4\theta_1+\theta_2)b_{4,1}\ , \qquad (4.46)
\end{aligned}
$$

where the terms $a_{i,j}$ and $b_{i,j}$ (related to the coefficients i and j of sin and cos) are known polynomials in the variables e and η. We recall that we have to solve equations (4.44), namely we have to equate to zero the average of the right hand side of the previous equations; when we solve them, we obtain that $\bar{v}_{11}$ must be equal to zero.Furthermore, we obtain the following expression for $\tilde{u}_{11}$ and $\tilde{v}_{11}$:

$$
\begin{aligned}
\tilde{u}_{11}(\theta_1,\theta_2) &= \sin(\theta_2)+\sin 3(\theta_2)c_{0,3}+\sin(2\theta_1-3\theta_2)c_{2,-3}+\\
&\sin(2\theta_1-\theta_2)c_{2,-1}+\sin(2\theta_1+\theta_2)c_{2,1}+\sin(2\theta_1+3\theta_2)c_{2,3}\\
&+\sin(4\theta_1-\theta_2)c_{4,-1}+\sin(4\theta_1+\theta_2)c_{4,1}\\
\tilde{v}_{11}(\theta_1,\theta_2) &= \cos(2\theta_1-\theta_2)d_{2,-3}+\cos(2\theta_1-\theta_2)d_{2,-1}\\
&+\cos(2\theta_1+\theta_2)d_{2,1}+\cos(2\theta_1+3\theta_2)d_{2,3}\\
&+\cos(4\theta_1-\theta_2)d_{4,-1}+\cos(4\theta_1+\theta_2)d_{4,1}\ . \qquad (4.47)
\end{aligned}
$$

Then, equating terms of order $j = 2$ we obtain the equations of the form:

$$\begin{aligned}\omega\frac{\partial\tilde{u}_{12}}{\partial\theta_1}+\frac{\partial\tilde{u}_{12}}{\partial\theta_2} &= \sum_{(k_1,k_2)\in\mathcal{K}}\Big(p(e,\eta)\cos(k_1\theta_1+k_2\theta_2) \\ &\quad +q(e,\eta)\sin(k_1\theta_1+k_2\theta_2)\Big)+r(e,\eta)\ , \quad (4.48)\end{aligned}$$

$$\omega\frac{\partial\tilde{v}_{12}}{\partial\theta_1}+\frac{\partial\tilde{v}_{12}}{\partial\theta_2}=\sum_{(k_1,k_2)\in\mathcal{K}}\Big(s(e,\eta)\cos(k_1\theta_1+k_2\theta_2)+t(e,\eta)\sin(k_1\theta_1+k_2\theta_2)\Big)\ , \quad (4.49)$$

where $\mathcal{K}\subset\mathbb{Z}^2\setminus\{0\}$, p, q, r, s, t are suitable polynomials in e and η. Let us point out something about these equations. If we focus on the right hand side of (4.48), we can see that some constant terms given by $r(e,\eta)$ appear so that, setting the average of the right hand side equal to zero, we obtain a solution of $\bar{v}_{12}$ different from zero; in particular we get:

$$\begin{aligned}\bar{v}_{12} &= \frac{1}{72\eta}\Big(120e\eta a_{2,-1}+120e\eta a_{2,1}-30e\eta a_{4,-1}-30e\eta a_{4,1} \\ &\quad +53\sqrt{2}e^3b_{2,-3}+27\sqrt{2}e^3b_{2,-1}-240e\eta b_{2,-1}+27\sqrt{2}e^3b_{2,1} \\ &\quad -240e\eta b_{2,1}+53\sqrt{2}e^3b_{2,3}+120e\eta b_{4,-1}+120e\eta b_{4,1}\Big)\ , \quad (4.50)\end{aligned}$$

where a_{ij}, b_{ij} are again polynomials in e and η. Moreover we are able to compute explicitly $\tilde{u}_{12}$ and $\tilde{v}_{12}$ that we can write as:

$$\begin{aligned}\tilde{u}_{12}(\theta_1,\theta_2) &= \sum_{(k_1,k_2)\in\mathcal{K}}\Big(\frac{p(e,\eta)}{\omega k_1+k_2}\sin(k_1\theta_1+k_2\theta_2) \\ &\quad +\frac{q(e,\eta)}{\omega k_1+k_2}\cos(k_1\theta_1+k_2\theta_2)\Big)\ , \quad (4.51)\end{aligned}$$

$$\begin{aligned}\tilde{v}_{12}(\theta_1,\theta_2) &= \sum_{(k_1,k_2)\in\mathcal{K}}\Big(\frac{s(e,\eta)}{\omega k_1+k_2}\sin(k_1\theta_1+k_2\theta_2) \\ &\quad +\frac{t(e,\eta)}{\omega k_1+k_2}\cos(k_1\theta_1+k_2\theta_2)\Big)\ . \quad (4.52)\end{aligned}$$

We remark that we are far from the resonances so that, the denominators turn out to be different from zero.

Formally, we could go on to any order, but the computations become more and more difficult. Furthermore, we need to check the the series that we are constructing converge and it can be proved that there exists a domain of e and η such that the series converge.

The outlook is to improve the estimates of the previous Section, (namely extend the estimates to larger values of the parameters) by expanding the Hamiltonian around one of the invariant tori and performing the normalization to higher orders.

Conclusions and perspective

The study of the problems treated in this thesis can provide many information about real phenomena observed in our Solar System. For example, the analysis of the dissipative standard map provides interesting results concerning the spin–orbit resonances; further studies on these models could enlighten us on the evolutional history of the rotation of Solar System bodies. The results obtained for the dissipative standard map can be generalized for the corresponding continuous spin–orbit problem. In order to obtain new information it would be interesting to extend the results to higher dimensional models.

A further step would be to prove the existence of cantori for the dissipative standard map by using the Aubry–Mather theory for dissipative twist maps and to use the parameterization to construct a cantorus with an irrational frequency ω as limit of periodic orbits of period p_n/q_n.

Concerning the Sitnikov's problem, it would be very interesting to improve the estimates provided by applying the Nekhoroshev's theorem in a neighborhood of a KAM torus. Moreover, it could be interesting to extend the problem to the case in which the third body is not constrained to be on a straight line, but it can move in the whole space, or to the case in which the third body has non–negligible mass, so that it perturbs the motion of the primaries. Furthermore, we can add some kinds of dissipation as, for example, a linear drag or a Poynting–Robertson drag or a loss of mass of the third body.

Bibliography

[1] D. K. Arrowsmith, C.M. Place, *An introduction to Dynamical Systems.* Cambridge University Press, 1990.

[2] C. Beaugé, S. Ferraz-Mello, *Capture in exterior mean-motion resonance due to Poynting-Robertson drag*, Icarus **110**, 239–260, 1994.

[3] C. Beaugé, S. Ferraz-Mello, *Resonance Trapping in The Primordial Solar Nebula: The case of a Stokes Drag Dissipation*, Icarus **103**, 301–318, 1993.

[4] G. Benettin, L. Galgani, A. Giorgilli, *A proof of Nekhoroshev's theorem for the stability times in nearly integrable Hamiltonian systems*, Cel. Mech. **37**, 1-25, 1985.

[5] G. D. Birkhoff, *Sur quelques courbes fermée remarkables.* Bull. Soc. Math. de France,**60**, 1–26, 1932.

[6] H. W. Broer, C. Simó, J. C. Tatjer, *Towards global models near homoclinic tangencies of dissipative diffeomorphisms*, Nonlinearity **11**, 667–770, 1998.

[7] D. Brouwer, G. M. Clemence, *Methods of Celestial Mechanics*, Academic Press, New York, 1961.

[8] R. Calleja, A. Celletti, *Breakdown of invariant attractors for the dissipative standard map*, CHAOS, vol. **20**, 2010.

[9] M. Casdagli, *Periodic orbits for dissipative twist maps.* Ergod. Th. and Dynam. Sys. **7**, 165–173, 1987.

[10] A. Celletti, *Analysis of resonances in the spin-orbit problem in Celestial Mechanics: The synchronous resonance (Part I),* Journal of Applied Mathematics and Physics (ZAMP), **41**, 174–204, 1990.

[11] A. Celletti, *Stability and Chaos in Celestial Mechanics,* Praxis Springer, 2010.

[12] A. Celletti, L. Chierchia, *A constructive theory of Lagrangian tori and computer–assisted applications*, Dynamics Reported, New Series, Springer-Verlag, **4**, 60-129,1995.

[13] A. Celletti, L. Chierchia, *Construction of stable periodic orbits for the spin-orbit problem of Celestial Mechanics*, Reg. Chaotic Dyn. **3**, 107–121, 1998.

[14] A. Celletti, L. Chierchia, *Quasi-periodic attractors in Celestial Mechanics*, Archive for Rational Mechanics and Analysis, **191**, no. 2, 311–345, 2009.

[15] A. Celletti, S. Di Ruzza, *Periodic and quasi–periodic orbits of the dissipative standard map*, Preprint 2010.

[16] A. Celletti, S. Di Ruzza, *Resonances in the solar system*, Preprint 2009.

[17] A. Celletti, C. Falcolini, *Singularities of periodic orbits near invariant curves*, Physica D **170**, no. 2, 87–102, 2002.

[18] A. Celletti, C. Froeschlé, E. Lega, *Dynamics of the conservative and dissipative spin–orbit problem*, Planetary and Space Science, **55**, 889–899, 2007.

[19] A. Celletti, M. Guzzo, *Cantori of the dissipative sawtooth map*, Chaos **19**, 013140, pp.6, 2009.

[20] A. Celletti, R.S. MacKay, *Regions of non–existence of invariant tori for a spin–orbit model*, Chaos **17**, 043119, pp. 12, 2007.

[21] A. Chenciner, *Sur un énoncé dissipatif du théorème géometrique de Poicaré-Birkhoff.* C.R. Acad.Sc. Paris, **294**,(série I) 243-245, 1982.

[22] A. Chenciner, *Orbites périodiques et ensembles de Cantor invarints d'Aubry-Mather au voisinage d'une bifurcation de Hopf dégénéré de difféomorphismes de* $\mathbb{R}^2$. C.R. Acad.Sc. Paris, **297**,(série I) 465–467, 1983.

[23] A. Chenciner, *La dynamique au voisinage d'un point fixe elliptique conservatif: de Poicaré et Birkhoff à Aubry et Mather.* Séminaire Bourbaki, **622**, 121–122, 1985.

[24] A. Chenciner, *Bifurcations de points fixes elliptiques. II Orbites periodiques et ensembles de Cantor invariants.* Invent. math. **80**, 81–106, 1985.

[25] B.V. Chirikov, *A universal instability of many dimensional oscillator systems*, Physics Reports **52**, 264–379, 1979.

[26] G. Colombo, *Rotational Period of the Planet Mercury,* Nature **208**, 575, 1965.

[27] G. Colombo, I.I. Shapiro, *The Rotation of the Planet Mercury,* Astroph. J. **145**, 296–307, 1966.

[28] G. Contopoulos, *Resonance Phenomena and the Non–Applicability of the "Third" Integral*, Bull. Astron. 3^{rd} Ser. **2**, Fasc. 1, 223, 1967.

[29] S. Di Ruzza, C. Lhotka, *Nekhoroshev's estimates near Kolmogorov tori in the Sitnikov problem*, Preprint 2010.

[30] R. Dvorak, *Numerical results to the Sitnikov problem*, Celest. Mech. Dynam. Astron. **56**, 71-80, 1993.

[31] R. Dvorak, F. Freistetter, J. Kurths, *Chaos and stability in planetary systems*, Lect. Notes Phys. **683**, Springer, Berlin Heidelberg, 2005.

[32] R. Dvorak, Y. S. Sun, *The phase space structure of the extended Sitnikov–problem*, Celestial Mechanics and Dynamical Astronomy **67**, 87–106, 1997.

[33] C. Efthymiopoulos, *On the connection between the Nekhoroshev theorem and Arnold diffusion*, Celestial Mechanics and Dynamical Astronomy, **102**, 49–68, 2008.

[34] A. Giorgilli, Notes on exponential stability of Hamiltonian systems, in Dynamical Systems. Part I: Hamiltonian Systems and Celestial Mechanics, Pubblicazioni della Classe di Scienze, Scuola Normale Superiore, Pisa. Centro di Ricerca Matematica "Ennio De Giorgi": Proceedings; published by the Scuola Normale Superiore in Pisa.

[35] A. Giorgilli, E. Zehnder, *Exponential stability for time dependent potentials*, ZAMP **43**, 1992.

[36] F. Fassò, M. Guzzo, G. Benettin, *Nekhoroshev–Stability of Elliptic Equilibria of Hamiltonian Systems*, Commun. Math. Phys. **197**, 347–360, 1998.

[37] S. B. Faruque,*Solution of the Sitnikov problem*, Celest. Mech. Dynam. Astron. **87**, 353–369, 2003.

[38] C. Golé, *Symplectic Twist Maps.* Advanced series in nonlinear dynamics, Volume 18, World Scientific, 2001.

[39] J. M. Green, *A method for determining a stochastic transition*, J. Math. Phys. **20**, 1979.

[40] J. Hagel, *An analytical approach to small amplitude solutions of the extended nearly circular Sitnikov problem*, Celestial Mechanics and Dynamical Astronomy, **103**, 251-266, 2009.

[41] J. Hagel, *A new analytic approach to the Sitnikov Problem.* Celestial Mechanics and Dynamical Astronomy, **53**, 267-292, 1992.

[42] J. Hagel, C. Lhotka *A high order perturbation analysis of the Sitnikov Problem.* Celestial Mechanics and Dynamical Astronomy, **93**, 201–228, 2005.

[43] G.R. Hall, *A topological version of a theorem of Mather on twist maps.* Ergod. Th. and Dynam. Sys. (1984) **2**, 585-603.

[44] A. Katok, *Some remarks on Birkhoff and Mather twist map theorems.* Ergod. Th. and Dynam. Sys. **2**, 185–194, 1982.

[45] J. J. Klavetter, *Rotation of Hyperion. I. Observations,* Astron. J. **97**, 570–579, 1989.

[46] P. Le Calvez, *Existence d'orbites quasi-periodiques dans les attracteurs de Birkhoff.* Commun. Math. Phys. **106**, 383–394, 1986.

[47] J. Liu and Y. S. Sun, *On the Sitnikov problem*, Celes. Mech. **49**, 285-302, 1990.

[48] W. D. MacMillan, *An Integrable Case In The Restricted Problem Of Three Bodies*, The Astronomical Journal, No **27**, pp. 11–13.

[49] J. N. Mather, *Existence of quasi-periodic orbits for twist homeomorfisms of the annulus.* Topology Vol. **21**, No. 4, pp. 457-467, 1982.

[50] K. R. Meyer, G. R. Hall *Introduction To Hamiltonian Dynamical Systems And The N–Body*, Springer-Verlag Berlin, 1992.

[51] J. Moser, *Stable and Random Motions in Dynamical Systems*, Princeton University Press, Princeton, 1973.

[52] P. Murdin (Editor), *Encyclopedia of Astronomy and Astrophysics,* Nature Publishing Group, 2001.

[53] C. D. Murray, S. F. Dermott, *Solar System Dynamics,* Cambridge University Press, 1999.

[54] N. Nekhoroshev, *An exponential estimate of the time of stability of nearly integrable Hamiltonian systems* Russ. Math. Surveys **32**, 1-65, 1977.

[55] Z. Nitecki, *Differentiable Dynamics: an Introduction to the Orbit Structure of Diffeomorphisms*, The MIT Press, Cambridge, 1971.

[56] J. Pöschel, *Nekhoroshev estimates for quasi–convex Hamiltonian systems*, Math. Z. **213**, 187216, 1993.

[57] K. A. Sitnikov, *Existence of oscillatory motion for the three–body problem*, Dokl. Akad. Nauk. USSR 133, No. **2**, 303-306, 1960.

[58] P. Soulis, T. Bountis, R. Dvorak, *Stability of motion in the Sitnikov 3–body problem*, Celestial Mechanics and Dynamical Astronomy, **99**, no. 2, 129–148, 2007.

[59] W. Wenzel, O. Biham, C. Jayaprakash, *Periodic orbits in the dissipative standard map*, Phys. Rev. A **43**, no. 12, 6550–6557, 1991.

[60] J. Wisdom, *Chaotic behavior and the origin of the* $3/1$ *Kirkwood gap* , Icarus, vol. **56**, pp. 51–74, 1983.

[61] J. Wisdom, S. J. Peale, F. Mignard, *The chaotic rotation of Hyperion,* Icarus **58**, 137-152 1984.

[62] Private communication with M. Guzzo.

[63] Private communication with P. Negrini.